Pacific Northwest
NATIONAL LABORATORY

PNNL-31161

FAST-1.0.1: Integral Assessment

Developed under NQA-1-2017

April 2021

KJ Geelhood, PNNL
TJ Zipperer, PNNL
CE Goodson, PNNL
D Richmond, PNNL
WG Luscher, PNNL
J Corson, NRC
DV Colameco, PNNL
L Kyriazidis, NRC

Prepared for the U.S. Nuclear Regulatory Commission
Office of Nuclear Regulatory Research
Under contract DE-AC05-76RL01830
Interagency Agreement 31310019N0001
Task Order Number: 31310019F0047

DISCLAIMER

This report was prepared as an account of work sponsored by an agency of the United States Government. Neither the United States Government nor any agency thereof, nor Battelle Memorial Institute, nor any of their employees, makes **any warranty, express or implied, or assumes any legal liability or responsibility for the accuracy, completeness, or usefulness of any information, apparatus, product, or process disclosed, or represents that its use would not infringe privately owned rights.** Reference herein to any specific commercial product, process, or service by trade name, trademark, manufacturer, or otherwise does not necessarily constitute or imply its endorsement, recommendation, or favoring by the United States Government or any agency thereof, or Battelle Memorial Institute. The views and opinions of authors expressed herein do not necessarily state or reflect those of the United States Government or any agency thereof.

PACIFIC NORTHWEST NATIONAL LABORATORY
operated by
BATTELLE
for the
UNITED STATES DEPARTMENT OF ENERGY
under Contract DE-AC05-76RL01830

Printed in the United States of America

Available to DOE and DOE contractors from the
Office of Scientific and Technical Information,
P.O. Box 62, Oak Ridge, TN 37831-0062;
ph: (865) 576-8401
fax: (865) 576-5728
email: reports@adonis.osti.gov

Available to the public from the National Technical Information Service
5301 Shawnee Rd., Alexandria, VA 22312
ph: (800) 553-NTIS (6847)
email: orders@ntis.gov <https://www.ntis.gov/about>
Online ordering: http://www.ntis.gov

PNNL-31161

FAST-1.0.1: Integral Assessment

Developed under NQA-1-2017

April 2021

KJ Geelhood, PNNL
DV Colameco, PNNL
WG Luscher, PNNL
CE Goodson, PNNL
D Richmond, PNNL
TJ Zipperer, PNNL
L Kyriazidis, NRC
J Corson, NRC

Prepared for the U.S. Nuclear Regulatory Commission
Office of Nuclear Regulatory Research
Under Contract DE-AC05-76RL01830
Interagency Agreement 31310019N0001
Task Order Number: 31310019F0047

Pacific Northwest National Laboratory
Richland, Washington 99352

Project Summary and Document Characteristics

Project Name	FAST Fuel Performance Code Development and Assessment
Project No.	75197 Task 3130019F0047
Product Management Office No. / Organization	PM053 / Nuclear Science and Legacy Waste

Approvals

Role	Name	Signature	Date
Project Manager	Tara O'Neill	Tara K O'Neil Digitally signed by Tara K O'Neil Date: 2021.04.14 14:59:14 -07'00'	
Lead Software Developer	Ken Geelhood	Kenneth J (Ken) Geelhood Digitally signed by Kenneth J (Ken) Geelhood Date: 2021.04.14 10:51:00 -07'00'	
Code Custodian	David Colameco	David V Colameco Digitally signed by David V Colameco Date: 2021.04.14 09:54:48 -07'00'	

Revision History

Revision	Date	Comments
0	April 2021	Initial Release

Abstract

An integral assessment has been performed to quantify the predictive capabilities of FAST, a thermal-mechanical nuclear fuel performance code designed to analyze fuel behavior from beginning of life to burnup levels allowed by the U.S. Nuclear Regulatory Commission (NRC). FAST code calculations are shown to compare satisfactorily to a preselected set of experimental data with both steady-state and anticipated operating occurrence (AOO) conditions.

This document describes the assessment of FAST-1.0.1, the latest version of FAST, released April 2021.

This page intentionally blank.

Foreword

The ability to accurately calculate the performance of light water reactor (LWR) fuel rods under high burnup conditions is a major objective of the reactor safety research program being conducted by the U.S. Nuclear Regulatory Commission (NRC). To achieve this objective, the NRC has sponsored an extensive program of analytical computer code development. One product of this program is NRC's FAST code, which provides the ability to accurately calculate the high burnup response of LWR fuel rods.

The NRC also continues to sponsor both in-pile and out-of-pile experiments to benchmark and assess the analytical code capabilities. Over 100 new assessment cases were recently added to the integral assessment database, bringing the database total to 137 assessment cases. The new assessment cases use data from recent integral irradiation experiments and post-irradiation examination (PIE) programs which provided valuable information on modern cladding materials and high burnup fuel behavior.

This report documents an integral assessment performed using the latest version of FAST, FAST-1.0, to demonstrate the code's ability to accurately calculate the performance of newer fuel designs and operating conditions.

This page intentionally blank.

Executive Summary

This document is Volume 2 of a three volume series that describes the FAST code and its assessment. Volume 1 [Geelhood et al., 2021b] describes the FAST code along with input instructions. Volume 2 (this document) describes the integral code assessment, done by comparing the code predictions for fuel temperatures, fission gas release (FGR), rod internal void volume, fuel swelling, cladding creep/growth, cladding corrosion, and hoop strain to data from integral irradiation experiments and post-irradiation examination (PIE) programs. Volume 3 [Geelhood et al., 2021a] describes the Material Library used by FAST. The cases used for code assessment were selected based on the following criteria:

- Well-characterized design and operational data were provided.
- The reported results spanned ranges of interest for both design and operating parameters.

Thus, the fuel rod cases were selected to represent both boiling water reactor (BWR) and pressurized water reactor (PWR) fuel types, with pellet-to-cladding gap sizes within, above, and below the normal range for power reactor rods. The fill gas is pure helium in most cases, but cases are included for which helium-xenon fill gas mixtures were used to assess the gap conductance model. The linear heat generation rates at beginning of life (BOL) range up to 60 [kW/m] (18 [kW/ft]), and during end of life (EOL) power ramps, they range up to 47 [kW/m] (14 [kW/ft]). The rod-average fuel burnups range up to 99 [GWd/MTU], but only up to 76 [GWd/MTU] for power ramp cases. However, the code is only considered validated to rod-average burnup of 62 [GWd/MTU]. The EOL FGR ranges from less than 1% to greater than 50% of the produced quantity.

The primary code assessment database (used also for benchmarking the thermal and FGR models) consists of 137 well-characterized fuel rods. These include 45 test rods that experienced EOL power ramps (used for FGR and cladding hoop strain) and 92 “steady-state” cases including uranium dioxide (UO_2), mixed oxide (MOX) fuel, and urania-gadolinia (UO_2-Gd_2O_3) Halden rods used for fuel temperatures, and UO_2, MOX, and UO_2-Gd_2O_3 rods used for FGR.

Five rods from the primary set were used to assess FAST predictions of EOL void volume. The cases selected include full-length power reactor rods and shorter test reactor rods. A mix of test reactor and power reactor rods was also used to assess the fuel volume change due to densification and swelling.

The FAST model for cladding waterside oxidation was evaluated against BWR Zircaloy-2 and PWR Zircaloy-4, ZIRLO®, and M5™ rod data.

The FAST predictions of cladding hoop strain were assessed against 27 BWR and PWR rods that were power ramped in various test reactors.

The following conclusions about FAST were made as a result of this assessment:

- Thermal: Comparisons were made for BOL UO_2 temperature measurements and UO_2, MOX, and UO_2-Gd_2O_3 temperature measurements as a function of burnup. Overall, FAST gave rea-

sonable predictions of fuel centerline temperature for fuel rods with UO_2, MOX, and UO_2-Gd_2O_3 fuel (standard deviation of less than 5%).

- Fission Gas Release: Comparisons were made for the UO_2 and MOX FGR measurements for rods with widely varying power levels and burnups. Overall, FAST gave reasonable predictions (within 5% FGR absolute) of fission gas release for fuel rods with UO_2 and MOX fuel.

- Internal Void Volume: Comparisons were made to data from two commercial reactor and three test reactor fuel rods. The code predicted the two commercial rods well but overpredicted the BR-3 test rod data by approximately 20% (relative) on average.

- Cladding Corrosion: Comparisons were made to data from two commercial BWR rods with Zircaloy-2 cladding, two commercial PWR rods with Zircaloy-4 cladding, two commercial PWR rods with ZIRLO® cladding, and one commercial PWR rod with M5™ cladding. The oxide corrosion predictions were very good and tend to bracket the data.

- Cladding Hoop Strain: The original hoop strain assessment cases that were available up to a burnup of around 45 $[GWd/MTU]$ demonstrated that, on average, FAST slightly overpredicts cladding hoop strain by 0.1% strain. FAST overpredicted all the short hold times cases. Despite this overprediction, FAST provides reasonable hoop strain predictions up to 62 $[GWd/MTU]$.

Acronyms and Abbreviations

ADU	Ammonium diuranate
AOO	Anticipated operating occurrence
ATR	Advanced Test Reactor
AUC	Ammonium uranyl carbonate
BNFL	British Nuclear Fuels, Ltd.
BOL	Beginning of life
BWR	Boiling water reactor
DNB	Departure from nucleate boiling
EOL	End of life
FGR	Fission gas release
GNF	Global Nuclear Fuel
HBEP	High Burnup Effects Program
HBWR	Heavy boiling water reactor
HUHB	Halden Ultra High Burnup
LHGR	Linear heat generation rate
LOCA	Loss-of-coolant accident
LWR	Light water reactor
MIMAS	Micronized master blend
NRC	U.S. Nuclear Regulatory Commission
PCMI	Pellet/Cladding Mechanical Interaction
PIE	Post-irradiation examination
PNNL	Pacific Northwest National Laboratory
PWR	Pressurized water reactor
SBR	Short binderless route
SCIP	Studsvik Cladding Integrity Program
SPND	Self-powered neutron detector
TCD	Thermal conductivity degradation
TD	Theoretical density

This page intentionally blank.

Contents

Figures

This page intentionally blank.

Tables

This page intentionally blank.

1.0 Introduction

This report is Volume 2 of a two volume series that describes the FAST code and its assessment. Volume 1 [Geelhood et al., 2021b] describes the FAST code. This document describes the assessment of the integral performance of FAST.

This report provides the results of the assessment of the integral code predictions to measured data for fuel temperatures, fission gas release (FGR), internal void volume, cladding deformation, oxidation, and hydriding. The benchmark datasets are described in Section 2.0. Appendix A describes each set of benchmark data and gives the code input for each data comparison. The benchmark data are drawn from a wide range of burnup levels and operating conditions that are relevant to commercial operations. Experimental fuel rods with linear heat generation rates (LHGRs) at or near the maxima for commercial fuel operations were selected because the U.S. Nuclear Regulatory Commission (NRC) licenses fuel to the most limiting rod in the core. Not all the data selected are at limiting conditions. Some of the cases involve commercial fuel rods that operated at normal commercial operating conditions, which are significantly less than the limiting conditions. Also, it is noted that most of the thermal and FGR benchmark cases are drawn from experimental programs that involved numerous fuel rods, of which only a few were selected as benchmark cases. This was either because the rods in a given group were all irradiated under similar conditions and had similar FGR or because only rods with design parameters and operating conditions similar to current commercial practice were selected.

The integral code assessments include comparisons to fuel temperature data in Chapter 3.0 and FGR data in Section 4.0. Comparisons of code predictions to internal void volume, cladding corrosion and hydriding, and hoop strain data are given in Chapters 5.0, 6.0, and 7.0 respectively. A summary and conclusions are found in Chapter 8.0.

This page intentionally blank.

2.0 Assessment Data Description

A total of 137 benchmark cases (fuel rods) that have post-irradiation examination (PIE) were selected for the integral assessment of the FAST code. These include 92 fuel rods with steady-state power operation covering a wide range of burnup and 45 fuel rods with steady-state irradiations followed by an end of life (EOL) power ramp. The purpose of the code assessment was to assess the code against a limited set of well-qualified data that span the range of limiting operational conditions for commercial light water reactors (LWRs) to verify that the code adequately predicts the integral data. The integral data of interest were fuel temperatures, FGR, corrosion, void volumes, and cladding deformation. The cases in this relatively limited group were selected using criteria regarding the completeness and the quality of the rod performance data, as follows:

- The cases should all provide pre-irradiation characterization with well-qualified fuel rod powers, and some data should include PIE data of interest (e.g., FGR, cladding dimensional changes).
- Cases for temperature assessment should provide well-qualified fuel centerline temperature data as a function of time or burnup to verify fuel temperature predictions.
- Cases ranging from low to high fuel burnup, as well as low to high (limiting) LHGR, should be provided to cover the operating ranges for LWR operation for each fuel performance issue of interest (e.g., fuel temperature, FGR, deformation).
- Cases should provide cladding oxidation, hydriding, and deformation under prototypic pressurized water reactor (PWR) and boiling water reactor (BWR) conditions.
- Cases should demonstrate the effects (FGR and cladding deformation) of normal operational transients, and overpower transients including anticipated operational occurrences (AOOs) at low and high burnup.

The selected cases fulfill the above criteria, and they provide a mix of well-qualified test reactor data and less qualified (fuel rod power uncertainties are generally greater) commercial power reactor rod data.

Figures 2-1, 2-2, and 2-3 show the rod-average LHGRs as a function of rod-average burnup (from full power histories of all the rods) for the rods in the temperature, FGR, and hoop strain assessment databases, respectively. These figures demonstrate the range of burnup and LHGRs to which the FAST predictions have been qualified for each of these integral code predictions. For the code prediction of cladding corrosion, the predictions are a function of time, power level, and coolant temperature. FAST has been qualified to predict cladding corrosion of Zircaloy-2 under BWR conditions beyond a rod-average burnup of 62 [GWd/MTU], and Zircaloy-4, ZIRLO®, and M5™ under PWR conditions beyond a rod-average burnup of 70 [GWd/MTU] for 12 [ft] cores. The outlet temperature of 14 [ft] reactor cores may be higher than has been assessed for FAST, and the corrosion predictions at these temperatures have not been assessed.

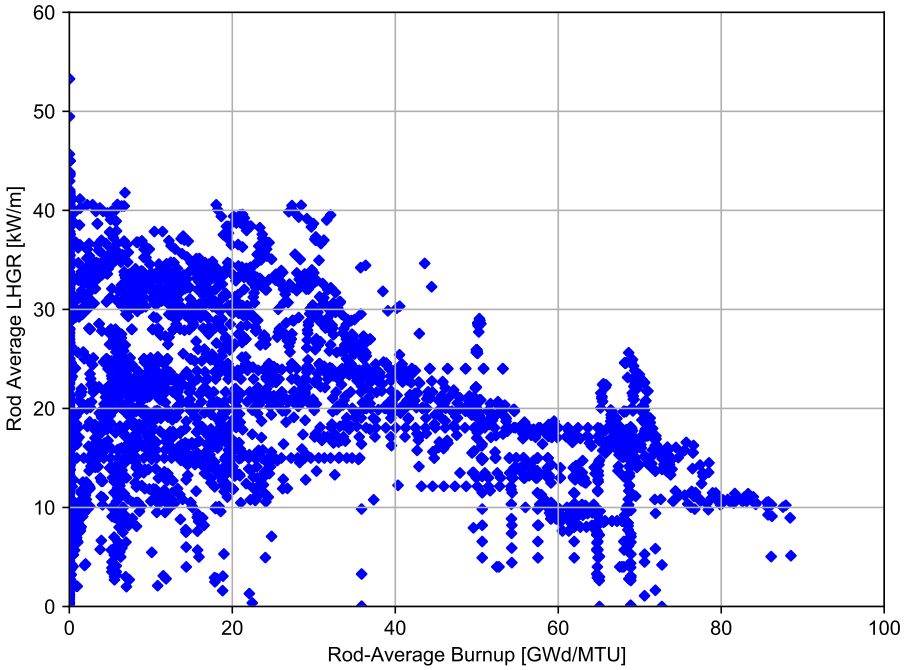

Figure 2-1. Rod-average LHGR vs. rod-average burnup for temperature assessment cases

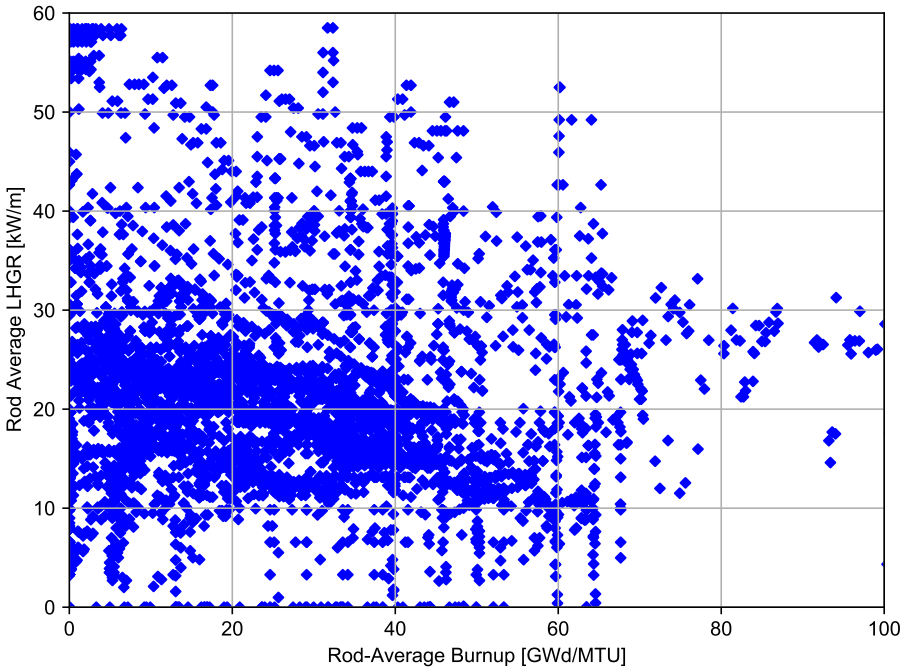

Figure 2-2. Rod-average LHGR vs. rod-average burnup for fission gas release assessment cases

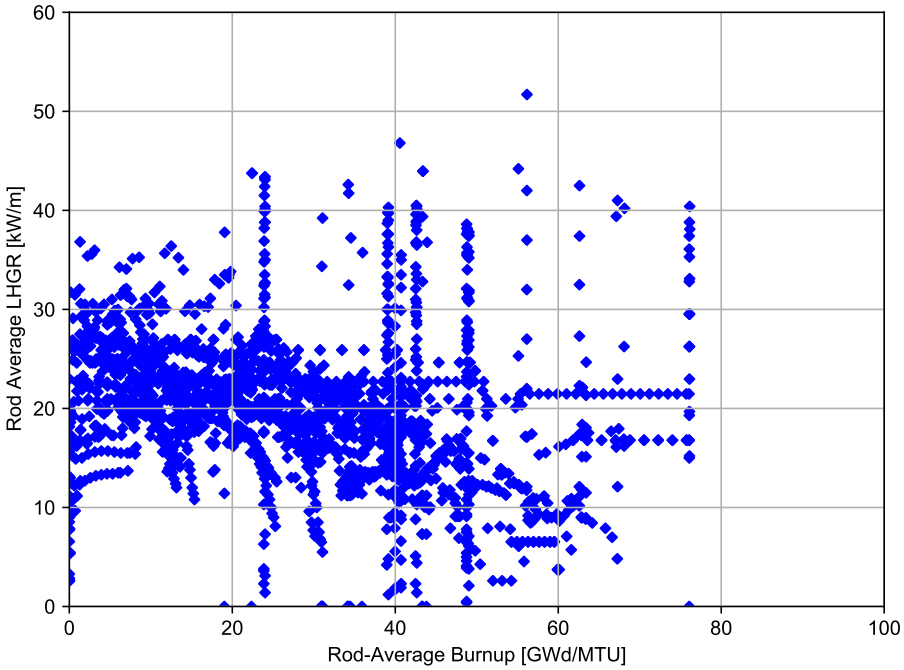

Figure 2-3. Rod-average LHGR vs. rod-average burnup for hoop strain assessment cases

2.1 Description of the Steady-State Cases

The steady-state assessment cases are listed in Table 2-1 and the EOL burnup and fuel type are given for each case. This table presents the steady-state fuel behavior phenomena that are assessed in this report and indicates which cases are used for that assessment. An “X” in a table cell indicates that the corresponding data comparison was performed for a particular case to assess code predictions.

Detailed information and FAST input files for each case are found in Appendix A.1.

Table 2-1. Steady-state fuel rod data cases used for FAST integral assessment

Reactor	Reference	Rod	Fuel Type	Rod-Average Burnup [GWd/MTU]	Thermal vs. Burnup	BOL Thermal	FGR	Void Volume	Corrosion
Halden HBWR	[Lanning, 1986]	IFA-432r1	UO_2	45	X	X	–	–	–
		IFA-432r2	UO_2	30	–	X	–	–	–
		IFA-432r3	UO_2	45	X	X	–	–	–
Halden HBWR	[Bradley et al., 1981]	IFA-513r1	UO_2	12	X	X	–	–	–
		IFA-513r6	UO_2	12	X	X	–	–	–
Halden HBWR	[Rø and Rossiter, 2005]	IFA-633r1	UO_2	40	–	X	–	–	–
		IFA-633r3	UO_2	40	–	X	–	–	–
		IFA-633r5	UO_2	40	–	X	–	–	–
Halden HBWR	[Thérache, 2005] [Jošek, 2008a]	IFA-677.1r2	UO_2	32	X	X	–	–	–
		IFA-677.1r3	UO_2	6	–	X	–	–	–
		IFA-677.1r4	UO_2	6	–	X	–	–	–
		IFA-677.1r6	UO_2	7	–	X	–	–	–
Halden HBWR	[Wiesenack, 1992]	IFA-562r18	UO_2	76	X	–	–	–	–
Halden HBWR	[Matsson and Turnbull, 1998]	IFA-597r8	UO_2	71	X	–	X	–	–
Halden HBWR	[Tvergerg and Amaya, 2001]	IFA-515.10rA1	UO_2	80	X	–	–	–	–
		IFA-515.10rA2	UO_2-Gd_2O_3	80	X	–	–	–	–
		IFA-515.10rB1	UO_2	80	X	–	–	–	–
		IFA-515.10rB2	UO_2-Gd_2O_3	80	X	–	–	–	–

Table 2-1. Steady-state fuel rod data cases used for FAST integral assessment (continued)

Reactor	Reference	Rod	Fuel Type	Rod-Average Burnup [GWd/MTU]	Thermal vs. Burnup	BOL Thermal	FGR	Void Volume	Corrosion
Halden HBWR	[Klecha, 2006]	IFA-681r1	UO_2	33	X	X	–	–	–
		IFA-681r2	UO_2-Gd_2O_3	23	X	–	–	–	–
		IFA-681r3	UO_2-Gd_2O_3	12	X	–	–	–	–
		IFA-681r4	UO_2-Gd_2O_3	22	X	–	–	–	–
		IFA-681r5	UO_2	32	X	–	–	–	–
		IFA-681r6	UO_2-Gd_2O_3	13	X	–	–	–	–
Halden HBWR	[Turnbull and White, 2002]	IFA-558r6	UO_2	41	X	–	–	–	–
Halden HBWR	[White, 1999]	IFA-629-1r1	MOX	33	X	–	–	–	–
		IFA-629-1r2	MOX	29 (FGR) 40 (Thermal)	X	–	X	–	–
Halden HBWR	[Beguin, 1999] [Fujii and Claudel, 2001]	IFA-610.2	MOX	56	X	–	–	–	–
		IFA-610.4	MOX	57	X	–	–	–	–
Halden HBWR	[Claudel and Huet, 2001]	IFA-648.1r1	MOX	62	X	–	–	–	–
		IFA-648.1r2	MOX	62	X	–	–	–	–
Halden HBWR	[Petiprez, 2002]	IFA-629.3r5	MOX	72	X	–	X	–	–
		IFA-629.3r6	MOX	68	X	–	X	–	–
Halden HBWR	[Mertens et al., 1998] [Mertens and Lippens, 2001]	IFA-606 Phase 2	MOX	49	X	–	X	–	–

Table 2-1. Steady-state fuel rod data cases used for FAST integral assessment (continued)

Reactor	Reference	Rod	Fuel Type	Rod-Average Burnup [GWd/MTU]	Thermal vs. Burnup	BOL Thermal	FGR	Void Volume	Corrosion
Halden HBWR	[Tverberg et al., 2005]	IFA-636r2	UO_2-Gd_2O_3	25	X	–	–	–	–
		IFA-636r4	UO_2-Gd_2O_3	25	X	–	–	–	–
BR-3 PWR	[Balfour, 1982] [Balfour et al., 1982]	24i6	UO_2	60.1	–	–	X	X	–
		36i8	UO_2	61.5	–	–	X	X	–
		111i5	UO_2	48.6	–	–	X	X	–
		28i6	UO_2	53.3	–	–	X	–	–
		30i8	UO_2	57.85	–	–	X	–	–
DR-3 PWR	[Bagger et al., 1978]	m2-2c	UO_2	43.75	–	–	X	–	–
		pa29-4	UO_2	47.39	–	–	X	–	–
BR-3 PWR	[Lanning et al., 1987]	HBEP BNFL5-DH	UO_2	42	–	–	X	–	–
BR-3 PWR	[Barner et al., 1990]	HBEP BNFL-DE	UO_2	33.9	–	–	X	–	–
NRX PWR	[de Meulemeester et al., 1973]	EPL-4	UO_2	10.4	–	–	X	–	–
NRX PWR	[Notley et al., 1967] [Notley and MacEwan, 1965]	CBR	UO_2	2.7	–	–	X	–	–
		CBY	UO_2	2.65	–	–	X	–	–
		LFF	UO_2	3.29	–	–	X	–	–
		CBP	UO_2	2.61	–	–	X	–	–

Table 2-1. Steady-state fuel rod data cases used for FAST integral assessment (continued)

Reactor	Reference	Rod	Fuel Type	Rod-Average Burnup [GWd/MTU]	Thermal vs. Burnup	BOL Thermal	FGR	Void Volume	Corrosion
EL-3 PWR	[Janvier et al., 1967]	4110-ae2	UO_2	6.2	–	–	X	–	–
		4110-be2	UO_2	6.6	–	–	X	–	–
Zorita PWR	[Balfour et al., 1982]	332	UO_2	56.8	–	–	X	–	–
Halden HBWR	[Chantoin et al., 1997]	FUMEX 6f	UO_2	55.45	–	–	X	–	–
		FUMEX 6s	UO_2	55.45	–	–	X	–	–
Halden HBWR	[Turnbull, 2001]	IFA429DH	UO_2	98.9	–	–	X	–	–
ANO-2 PWR	[Smith et al., 1994]	TSQ002	UO_2	53.2	–	–	X	X	X
Oconee PWR	[Newman, 1986]	15309	UO_2	50	–	–	X	X	X
Halden HBWR	[Blair and Wright, 2004]	IFA-651.1r1	MOX	22.41	X	–	X	–	–
		IFA-651.1r3	MOX	21.73	X	–	X	–	–
		IFA-651.1r6	MOX	20.27	X	–	X	–	–
ATR	[Morris et al., 2000] [Morris et al., 2001] [Morris et al., 2005] [Hodge et al., 2002] [Hodge et al., 2003]	PII C2 P5	MOX	21	–	–	X	–	–
		PIII C3 P6	MOX	30	–	–	X	–	–
		PIII C10 P13	MOX	30	–	–	X	–	–
		PIV C4 P7	MOX	40	–	–	X	–	–
		PIV C5 P8	MOX	50	–	–	X	–	–
		PIV C6 P9	MOX	50	–	–	X	–	–
		PIV C12 P15	MOX	50	–	–	X	–	–

Table 2-1. Steady-state fuel rod data cases used for FAST integral assessment (continued)

Reactor	Reference	Rod	Fuel Type	Rod-Average Burnup [GWd/MTU]	Thermal vs. Burnup	BOL Thermal	FGR	Void Volume	Corrosion
Gravelines-4 PWR	[Beguin, 1999] [Fujii and Claudel, 2001] [Claudel and Huet, 2001] [Petiprez, 2002]	N06	MOX	48	–	–	X	–	–
		N12	MOX	57	–	–	X	–	–
		P16	MOX	53	–	–	X	–	–
Halden HBWR	[Wright, 2004]	IFA 633.1r6	MOX	32	X	–	X	–	–
Beznau-1	[Cook et al., 2003] [Cook et al., 2004]	M504 H8	MOX	37.5	–	–	X	–	–
		M504 I2	MOX	43	–	–	X	–	–
		M504 K9	MOX	42.5	–	–	X	–	–
		M504 M9	MOX	44.2	–	–	X	–	–
Beznau-1	[Boulanger et al., 2004]	M308 Segment 2	MOX	57.5	–	–	X	–	–
Halden HBWR	[Koike, 2004]	IFA-597.4/ .5/ .6/ .7r10	MOX	35.7	X	–	X	–	–
		IFA-597.4/ .5/ .6/ .7r11	MOX	36.8	X	–	X	–	–
Fugen HBWR	[Ozawa, 2004]	E09 Rods Inner	MOX	29.6	–	–	X	–	–
		E09 Rods Intermediate	MOX	39.3	–	–	X	–	–
		E09 Rods Outer	MOX	42	–	–	X	–	–
Monticello BWR	[Baumgartner, 1984]	MTB99 Rod A1	UO_2	45	–	–	–	–	X

Table 2-1. Steady-state fuel rod data cases used for FAST integral assessment (continued)

Reactor	Reference	Rod	Fuel Type	Rod-Average Burnup [GWd/MTU]	Thermal vs. Burnup	BOL Thermal	FGR	Void Volume	Corrosion
TVO-1 BWR	[Barner et al., 1990]	HBEP H8/36-6	UO_2	51.4	–	–	–	–	X
Vandellos PWR	[CSN and ENUSA, 2002]	A06	UO_2	68	–	–	–	–	X
		A12	UO_2	68	–	–	–	–	X
Vandellos PWR	[Segura and Bernaudat, 2002]	N05	UO_2	70	–	–	–	–	X
BR-3/BR-2	[Hoffmann and Kraus, 1984] [Manley et al., 1989] [Reindl et al., 1991]	GAIN Rod 301	UO_2-Gd_2O_3	38.8	–	–	X	–	–
		GAIN Rod 302	UO_2-Gd_2O_3	37.79	–	–	X	–	–
		GAIN Rod 701	UO_2-Gd_2O_3	38.9	–	–	X	–	–
		GAIN Rod 702	UO_2-Gd_2O_3	38.9	–	–	X	–	–
Ringhals 3	[Schrire, 2018]	R3-2AH3-D12	UO_2	33.3	–	–	–	X	–
		R3-0AH5-E14	UO_2	57.82	–	–	–	X	–
		R3-2AH3-D15	UO_2	34.1	–	–	–	X	–
Ringhals 2	[Schrire, 2018]	R2-AL06-D6	UO_2	27.97	–	–	–	X	–
		R2-AD23-D5	UO_2	62.95	–	–	–	X	–
		07R2D5	UO_2	62.0	–	–	–	X	–

2.2 Description of the Power-Ramp Cases

The power-ramp assessment cases are listed in Table 2-2, and the EOL burnup, fuel type, ramp terminal power level, and hold time are given for each case. This table presents the power-ramp fuel behavior phenomena that are assessed in this report and indicates which cases are used for that assessment. An “X” in a table cell indicates that the corresponding data comparison was performed for a particular case to assess code predictions.

Detailed information and FAST input files for each case is found in Appendix A.2.

Table 2-2. Power-ramped fuel rod data cases used for FAST integral assessment

Base Irradtion/Ramp Testing	Reference	Rod	Fuel Type	Rod-Average Burnup [GWd/MTU]	Ramp Terminal Level [kW/m]	Ramp Hold Time	FGR	Hoop Strain
Obringheim/Petten	[Barner et al., 1990]	HBEP D200	UO_2	25	45.3	2.4 days	X	–
		HBEP D226	UO_2	44	45.0	2.6 days	X	–
Obringheim/Petten	[Djurle, 1985]	PK1/1	UO_2	35.4	37.2	12 hr	–	X
		PK1/3	UO_2	35.2	42.6	12 hr	–	X
		PK2/1	UO_2	45.2	36.8	12 hr	–	X
		PK2/3	UO_2	44.6	44.0	12 hr	–	X
		PK2-S	UO_2	43.4	44.0	12 hr	–	X
		PK4/1	UO_2	33.7	34.3	12 hr	–	X
		PK4/2	UO_2	33.8	39.2	12 hr	–	X
		PK6/1	UO_2	36.7	43.7	1 hr	–	X
		PK6/2	UO_2	36.8	35.7	12 hr	X	X
		PK6/3	UO_2	36.5	43.3	12 hr	X	–
		PK6/S	UO_2	35.9	41.0	12 hr	X	–
Studsvik/Studsvik	[Mogard et al., 1979] [Lysell and Birath, 1979]	Inter-Ramp Rod 16	UO_2	21	43.8	24 hr	X	X
		Inter-Ramp Rod 18	UO_2	18	37.79	24 hr	X	X
Halden/DR-2	[Knudsen et al., 1983]	RISØF14-6	UO_2	27	28.7	3 days	X	–
		RISØF7-3	UO_2	35	30.2	17 hr	X	–
		RISØF9-3	UO_2	33	29.7	30 hr	X	–
Quad Cities 1 / DR3	[Chantoin et al., 1997]	ge2	UO_2	41.9	41.9	38 hr	X	X

Table 2-2. Power-ramped fuel rod data cases used for FAST integral assessment (continued)

Base Irradtion/Ramp Testing	Reference	Rod	Fuel Type	Rod-Average Burnup [GWd/MTU]	Ramp Terminal Level [kW/m]	Ramp Hold Time	FGR	Hoop Strain
		ge4	UO_2	24.0	24.0	34 hr	X	X
		ge6	UO_2	42.3	38.1	5 days	X	X
		ge7	UO_2	41	35.5	4 hr	X	X
ANO-1/Studsvik	[Wesley et al., 1994]	BW stud R1	UO_2	62.3	22.1	12 hr	X	X
		BW stud R3	UO_2	62.1	24.7	12 hr	X	X
Biblis A /DR3	[Chantoin et al., 1997]	RISØAN1	UO_2	41.3	40.3	3 days	X	X
		RISØAN8	UO_2	40.3	30.1	12 hr	X	X
Gravelines-5/Siloe	[Struzik, 2004]	regate	UO_2	50.2	38.5	1.5 hr	X	–
Beznau-1/Petten	[White et al., 2001] [Cook et al., 2000] [Cook et al., 2003] [Cook et al., 2004]	M501 HR-1	MOX	37	38.1	12 hr	X	
		M501 HR-2	MOX	37	35.7	12 hr	X	–
		M501 HR-3	MOX	37	46.2	12 hr	X	–
		M501 HR-4	MOX	36	47.0	12 hr	X	–
		M501 MR-1	MOX	34	38.1	12 hr	X	–
		M501 MR-2	MOX	34	41.9	12 hr	X	–
		M501 MR-3	MOX	34	40.5	12 hr	X	–
		M501 MR-4	MOX	33	41.7	20 min	X	–

Table 2-2. Power-ramped fuel rod data cases used for FAST integral assessment (continued)

Base Irradtion/Ramp Testing	Reference	Rod	Fuel Type	Rod-Average Burnup [GWd/MTU]	Ramp Terminal Level [kW/m]	Ramp Hold Time	FGR	Hoop Strain
Leibstadt/Studsvik	[Kallstrom, 2005]	KKL-1	UO_2	63	42.5	40 min	X	–
		KKL-2	UO_2	67	41	30 s	–	X
		KKL-3	UO_2	56	52	12 hr	–	X
Ringhals/Studsvik		KKL-4	UO_2	40	45	5 s	–	X
		M5-H1	UO_2	67	40	5 s	–	X
Oskarshamn/Studsvik		M5-H2	UO_2	68	40	12 hr	–	X
Vandellos/Studsvik		O2	UO_2	55	40	30 s	–	X
		Z-2	UO_2	76	40	6 hr	–	X
		Z-3	UO_2	76	40	$< 1s^*$	–	X
		Z-4	UO_2	76	38	6 hr	–	X

This page intentionally blank.

3.0 Thermal Behavior Assessment

Thermal predictions are important for calculating initial fuel stored energy, which is used as input to loss-of-coolant accident (LOCA) analyses. The fuel temperatures are also used to calculate FGRs and EOL rod pressures and to verify no fuel has melted. In general, PWR LOCA and fuel melt analyses are calculated with FAST to be more limiting at burnups between 25 and 35 [GWd/MTU], while the same analyses for BWRs are generally more limiting at burnups between 15 and 25 [GWd/MTU].

Comparisons of predicted and measured fuel centerline temperatures from instrumented Halden reactor test assemblies have been used to evaluate the code's ability to predict BOL temperatures and through-life temperature histories (i.e., rod power vs. burnup). The BOL and through-life temperature comparisons are separated because they have different biases and uncertainties (based on standard deviation) in the code thermal predictions. The through-life temperature history comparisons will be used to bound the uncertainties on PWR and BWR LOCA initialization and fuel melting analyses. The BOL temperature database includes not only rods with helium-filled gaps, but also rods with xenon- and xenon-helium-filled gaps and rods with pellet/cladding gap sizes both larger and smaller than typically used in commercial fuel designs. These variations in gap size and fill gas indicate that the code can properly account for the thermal resistance across the fuel cladding gap as a function of gap size and gas composition and is not just tuned to provide good results for typical LWR commercial fuel designs.

The comparisons of measured and predicted through-life fuel center temperature histories were done with two goals in mind. The first was to determine if the code properly accounts for the fuel thermal conductivity degradation (TCD) with burnup. The second goal was to determine if the code properly predicts the effect of thermal feedback on fuel temperature caused by gas release and consequent contamination of the initial helium fill gas with lower conductivity fission gas.

The BOL and through-life code-to-data comparisons are discussed separately in the following sections.

3.1 Temperature Predictions

The BOL fuel centerline temperature predictions are assessed against centerline temperature measurements taken during the first ramp to power. This power ramp occurs during the first 1 to 2 days of operation. Because of this, the initial fuel rod dimensions apply and there is no time for phenomena such as FGR, fuel densification and swelling, cladding creep, or cladding corrosion.

3.1.1 UO_2 Temperature Predictions

FAST was assessed against BOL temperature measurements taken during the first ramp to power. Thirteen rods are used to assess the performance of FAST at BOL: IFA-432 rod 1, IFA-432 rod 2, IFA-432 rod 3, IFA-513 rod 1, IFA-513 rod 6, IFA-681 rod 1, IFA-633 rod 1, IFA-633 rod 3, IFA-633 rod 5, IFA-677.1 rod 2, IFA-677.1 rod 3, IFA-677.1 rod 4, and IFA-677.1 rod 6. Figure 3-1 shows the predicted vs. measured temperature for the BOL ramp up to power for the 13 assessment cases.

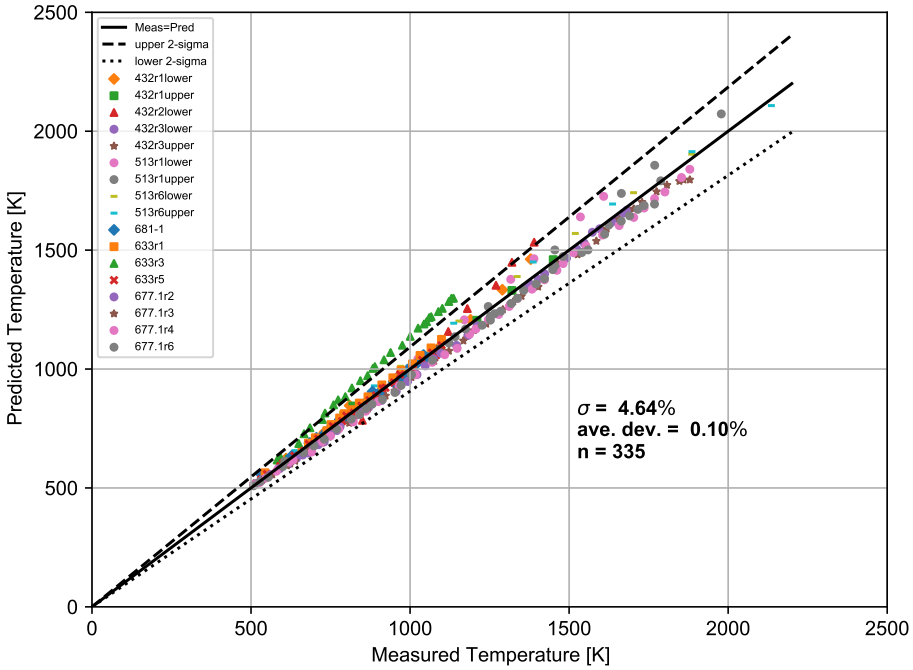

Figure 3-1. Measured and predicted centerline temperature for the first ramp to power for 13 assessment cases

This figure shows that FAST predicts these centerline temperatures within a standard error of 4.6% of the measured centerline temperature and no bias (and an average deviation $\frac{\sum(P-M)/M}{n}$ of +0.03%). A standard error of 4.6% is reasonable given the uncertainty in the thermocouple data and the calculated rod power. The BOL fuel temperature assessment is an improvement over the FAST predictions due to the incorporation of a new fuel relocation model in FAST.

3.2 Assessment of Temperature Predictions as a Function of Burnup

3.2.1 UO_2 Centerline Temperature Predictions as a Function of Burnup

The assessment of FAST UO_2 temperature predictions was performed using the same cases that were used for the BOL assessment, with the following differences.

1. IFA-432 rod 2 has been removed as an assessment of FAST as a function of burnup, as the test is not prototypic of current fuel designs due to its large gap, and a small overprediction in FGR can result in a large temperature overprediction.

2. IFA-633 rods 1, 3, and 5 and IFA-677.1 rods 3, 4, and 6 originally only had BOL temperature reported and only recently had measured temperature as a function of burnup reported. Therefore, these rods are not included in this assessment.

3. IFA-562 rod 18, IFA-597 rod 8, IFA-515.10 rods A1 and B1, IFA-681 rod 5, and IFA-558 rod 6 have been added in addition to the BOL assessment cases.

The following figures show measured and predicted fuel centerline temperatures from rods with centerline temperature measurements. Individual rod predictions may demonstrate a systematic error (bias) that may be due to thermocouple decalibration or a systematic error in the power history or axial power shape (power at thermocouple location) provided due to decalibration in or with the neutron detectors. However, when all the comparisons are examined, it is found that there is no overall systematic error (bias) in the prediction of UO_2 fuel temperature throughout life, as can be seen in Figure 3-2. For all the cases, a standard error of 6.0% on the centerline temperature was calculated.

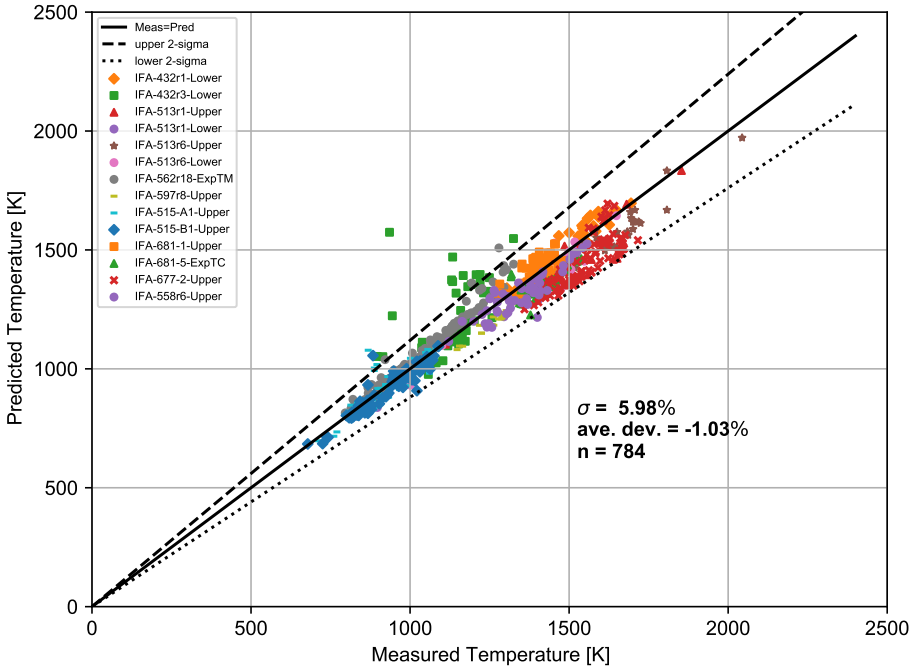

Figure 3-2. Measured and predicted centerline temperature for the UO_2 assessment cases throughout life

These data are also shown in terms of relative bias in Figure 3-3 as a function of burnup. There appears to be an underpredictive bias of 4.0% on average early in life between 2 and 16 [GWd/MTU]. However, there appears to be no systematic bias in the predictions with increasing burnup.

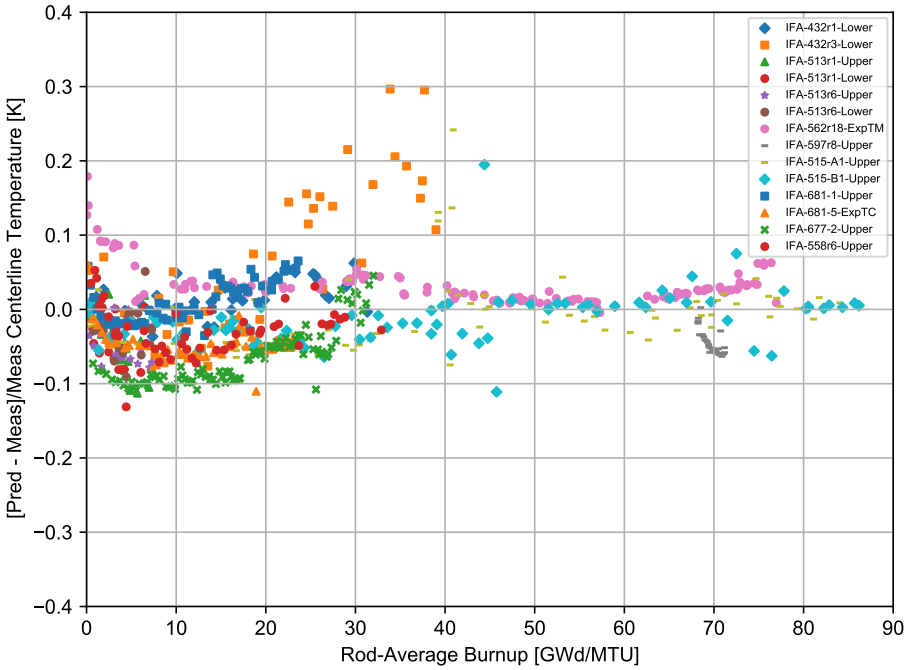

Figure 3-3. Predicted minus measured divided by measured centerline temperature for the UO_2 assessment cases as a function of burnup

Figue 3-4 shows the measured and predicted centerline temperature for IFA-432r1. This figure contains data from the lower thermocouple. This rod also contained an upper thermocouple, but it failed after 150 days. The comparisons to the upper thermocouple data are similar to the lower thermocouple. This figure shows excellent agreement between the FAST predictions and the data.

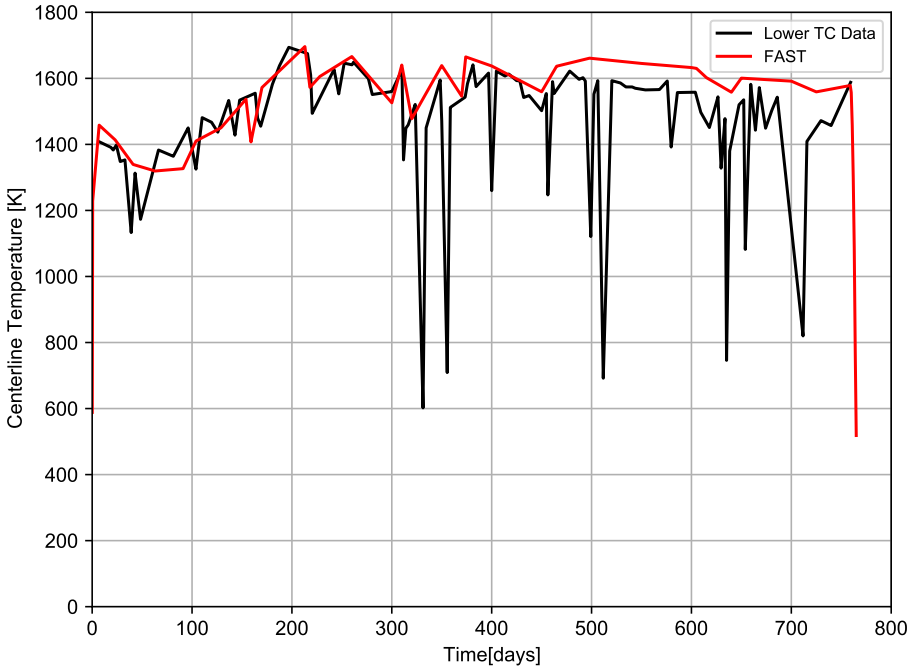

Figure 3-4. Measured and predicted centerline temperature for IFA-432 rod 1 UO_2 lower thermocouple (burnup = 45 [GWd/MTU], as-fabricated radial gap = 114 [μm])

Figure 3-5 shows the measured and predicted centerline temperature for IFA-432r3. This figure contains data from the lower thermocouple. This rod also contained an upper thermocouple, but it failed after 550 days. The comparisons to the upper thermocouple data are similar to the lower thermocouple. This figure shows excellent agreement between the FAST predictions and the data at BOL, and an overprediction of about 100 [K] (7% relative) at EOL. This overprediction may be due to FAST overpredicting the gas release, leading to higher predicted temperatures. As noted earlier, overprediction of gas release leads to lower gap conductivity and results in higher fuel temperature predictions. It should also be noted that some of the helium fill and fission gases were found to have leaked out of these IFA-432 rods based on rod puncture data (i.e., the leak was theorized to have occurred around the thermocouple penetrations through the end caps).

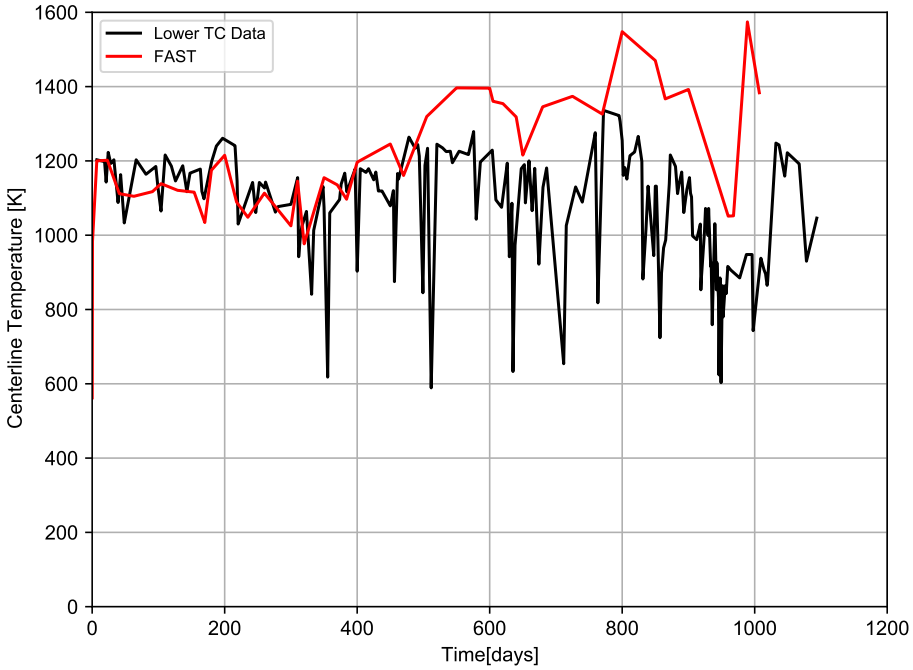

Figure 3-5. Measured and predicted centerline temperature for IFA-432 rod 3 UO_2 lower thermocouple (burnup = 45 [GWd/MTU], as-fabricated radial gap = 38 [μm])

Figures 3-6 and 3-7 show the measured and predicted centerline temperature for IFA-513r1. These figures contain data from the upper and lower thermocouples and show reasonable agreement between the FAST predictions and the data.

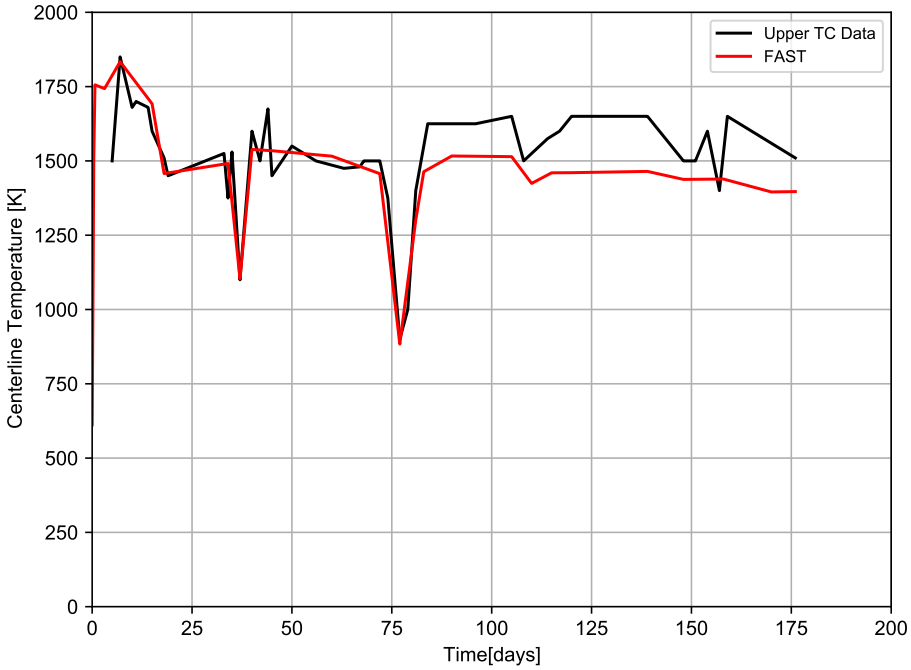

Figure 3-6. Measured and predicted centerline temperature for IFA-513 rod 1 UO_2 upper thermocouple (burnup=10 [GWd/MTU], as-fabricated radial gap=108 [μm])

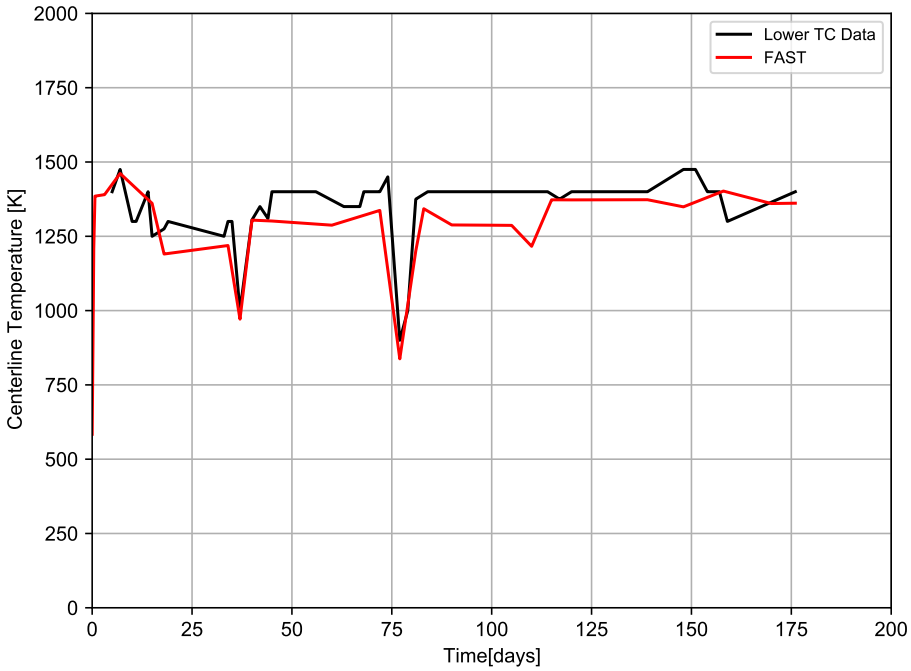

Figure 3-7. Measured and predicted centerline temperature for IFA-513 rod 1 UO_2 lower thermocouple (burnup=10 [GWd/MTU], as-fabricated radial gap=108 [μm])

Figures 3-9 and 3-8 show the measured and predicted centerline temperature for IFA-513r6. These

figures contain data from the upper and lower thermocouples and show reasonable agreement between the FAST predictions and the data.

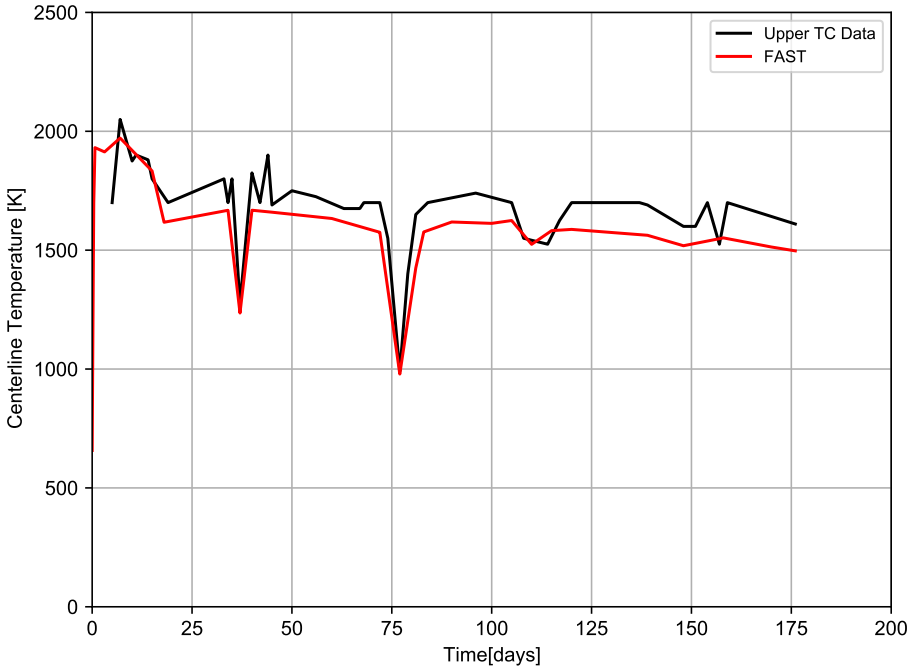

Figure 3-8. Measured and predicted centerline temperature for IFA-513 rod 6 UO_2 upper thermocouple (burnup=10 [GWd/MTU], as-fabricated radial gap=108 [μm])

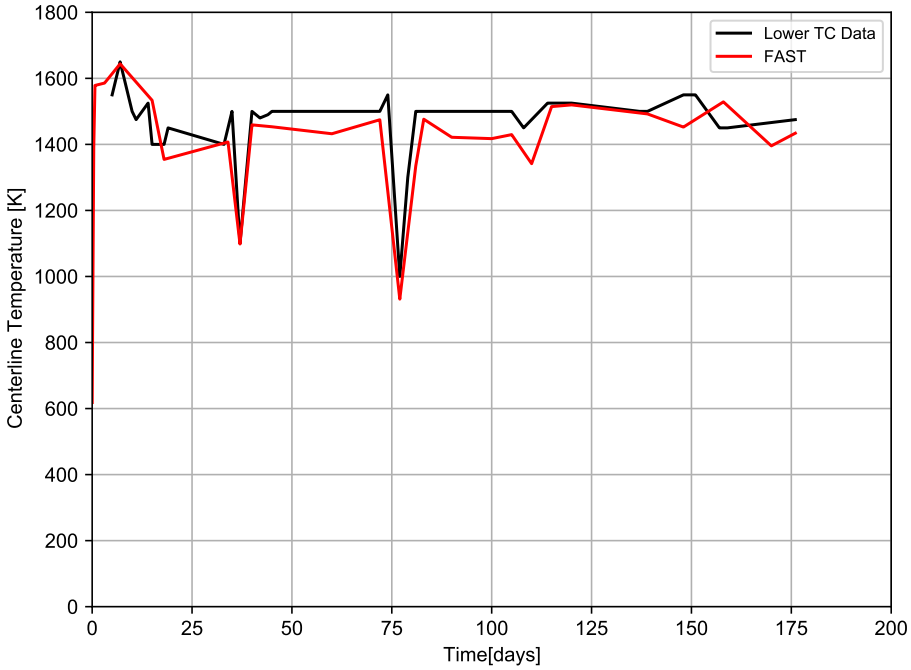

Figure 3-9. Measured and predicted centerline temperature for IFA-513 rod 6 UO_2 lower thermocouple (burnup=10 [GWd/MTU], as-fabricated radial gap=108 [μm])

Figure 3-10 shows the measured and predicted centerline temperature for IFA-562r18. This figure contains rod axial-averaged temperature data from the expansion thermometer. This figure shows excellent agreement between the FAST predictions and the data.

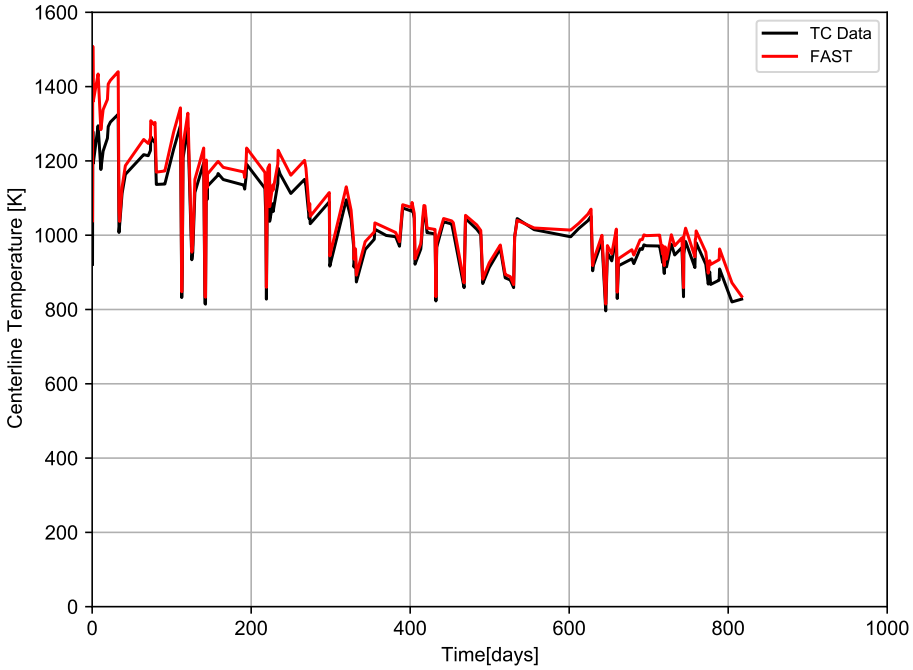

Figure 3-10. Measured and predicted rod-average centerline temperature for IFA-562 rod 18 UO_2 (burnup = 76 [GWd/MTU], as-fabricated radial gap = 50 [μm])

Figure 3-11 shows the measured and predicted centerline temperature for IFA-597r8. This rod was refabricated from a commercial rod that was irradiated to 68 [GWd/MTU]. This figure contains upper thermocouple data and shows reasonable agreement between the FAST predictions and the data ($\pm$75 [K], 6% relative).

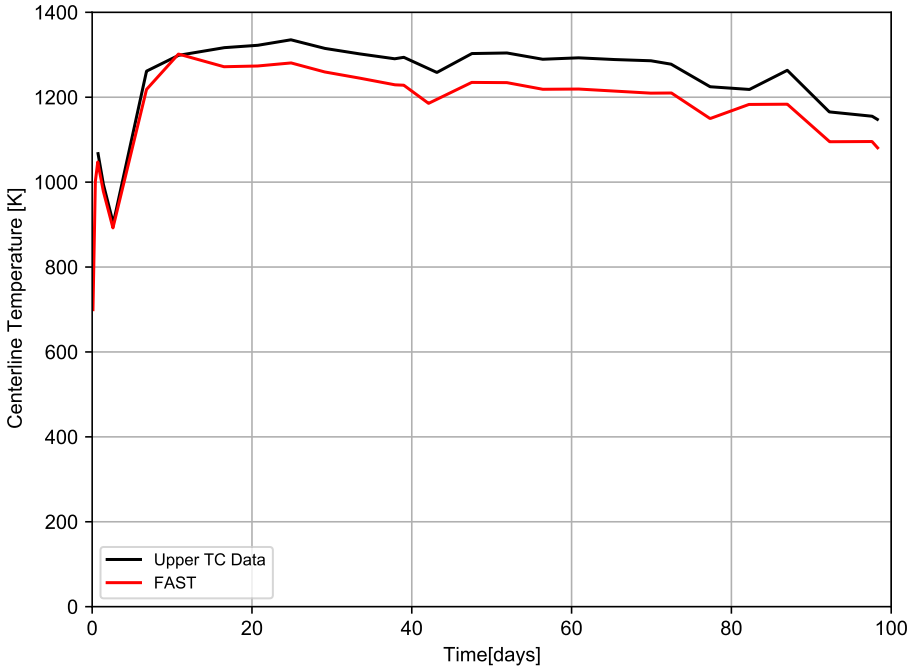

Figure 3-11. Measured and predicted centerline temperature for IFA-597 rod 8 (starting burnup = 68 [GWd/MTU], ending burnup=71 [GWd/MTU], as-fabricated radial gap=105 [μm])

Figures 3-12 and 3-13 show the measured and predicted centerline temperature for IFA-515.10 rods A1 and B1. These figures contain upper thermocouple data and show reasonable agreement between the FAST predictions and the data ($\pm$50 [K], 6% relative).

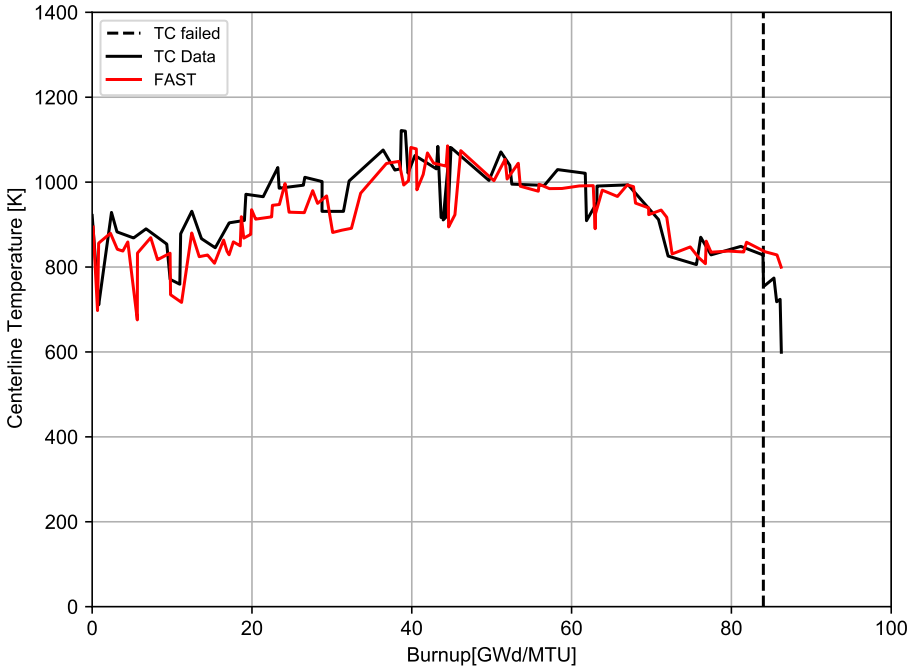

Figure 3-12. Measured and predicted centerline temperature for IFA-515.10 rod A1 (UO_2) (burnup = 80 [GWd/MTU], as-fabricated radial gap=25 [μm])

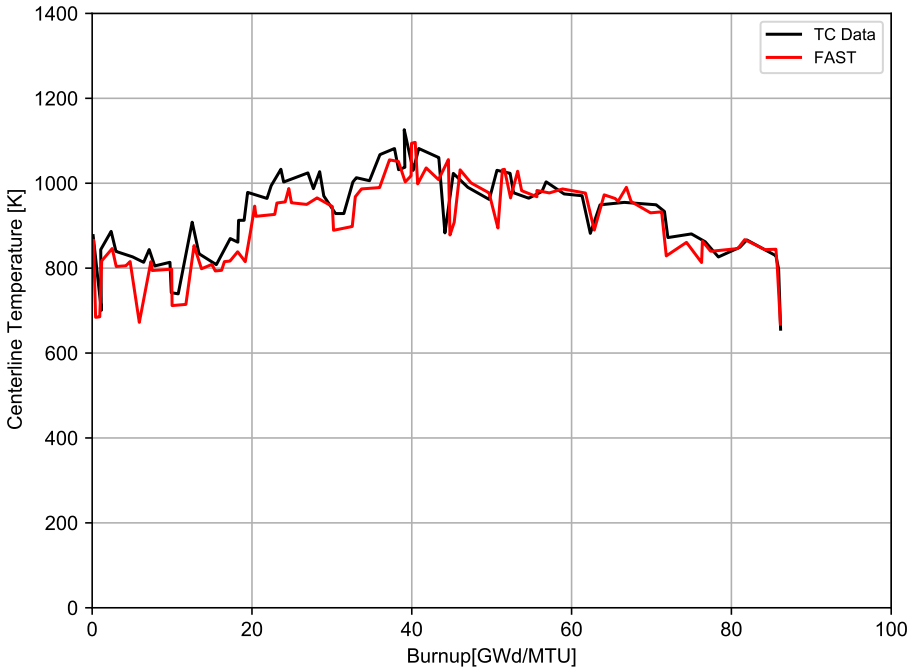

Figure 3-13. Measured and predicted centerline temperature for IFA-515.10 rod B1 (UO_2) (burnup = 80 [GWd/MTU], as-fabricated radial gap = 25 [μm])

Figures 3-14 and 3-15 show the measured and predicted centerline temperature for IFA-681 rods

1 and 5. These figures contain upper thermocouple data (rod 1) and expansion thermometer data (rod 5). These figures show reasonable agreement between the FAST predictions and the data ($\pm$30 [K], 2% relative).

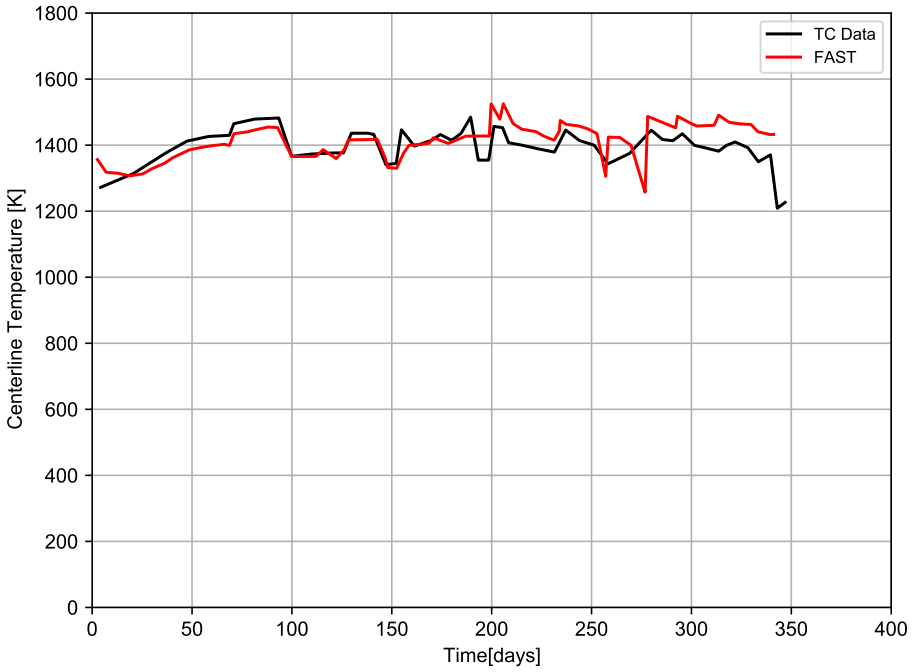

Figure 3-14. Measured and predicted centerline temperature for IFA-681 rod 1 UO_2 (burnup = 33 [GWd/MTU], as-fabricated radial gap = 85 [μm])

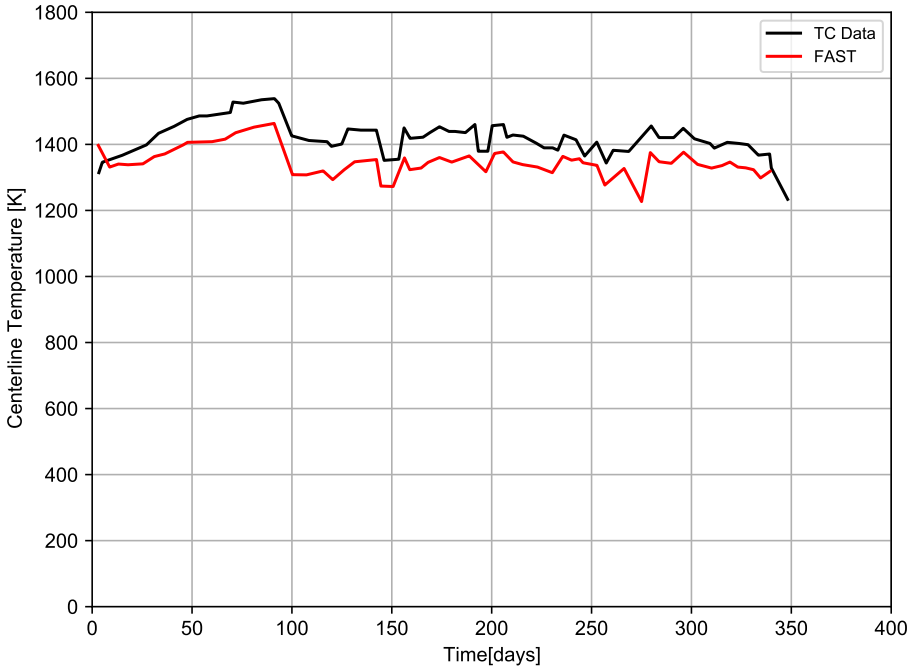

Figure 3-15. Measured and predicted centerline temperature for IFA-681 rod 5 UO_2 (burnup = 32 [GWd/MTU], as-fabricated radial gap = 85 [μm])

Figure 3-16 shows the measured and predicted centerline temperature for IFA-677 rod 2. This figure contains upper thermocouple data and shows significant underprediction of the FAST predictions relative to the data at BOL of up to 150 [K] (11% relative). However, by 300 days, the underprediction has been reduced to a more reasonable level of 75 [K] (5% relative) or less. This rod (Figure 3-16) had similar LHGR and burnup and the same gap size as IFA-681 rod 5 (Figure 3-15) but significantly higher fuel centerline temperatures ($\sim$130 [°C], 10% relative) at low burnups.

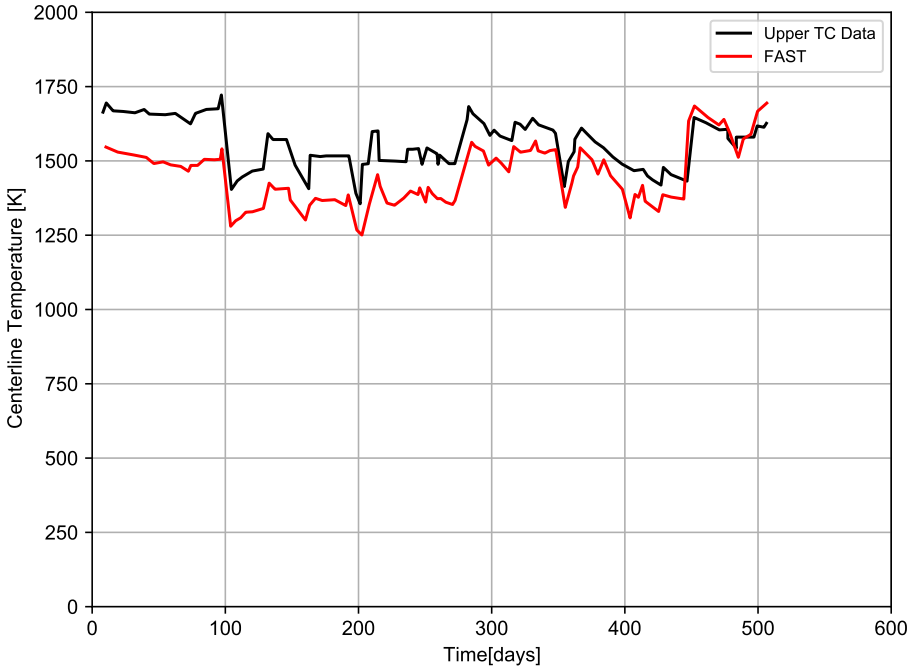

Figure 3-16. Measured and predicted centerline temperature for IFA-677.1 rod 2 UO_2 (burnup = 32 [GWd/MTU], as-fabricated radial gap = 85 [μm])

Figure 3-17 shows the measured and predicted centerline temperature for IFA-558 rod 6. This figure contains upper thermocouple data and shows reasonable agreement between the FAST predictions and the data ($\pm$50-75 [K], 4-6% relative), except at burnups between 25.5 and 28 [GWd/MTU], where temperatures are underpredicted by up to 120 [K] (10% relative) but then start to provide good agreement at 29 [GWd/MTU].

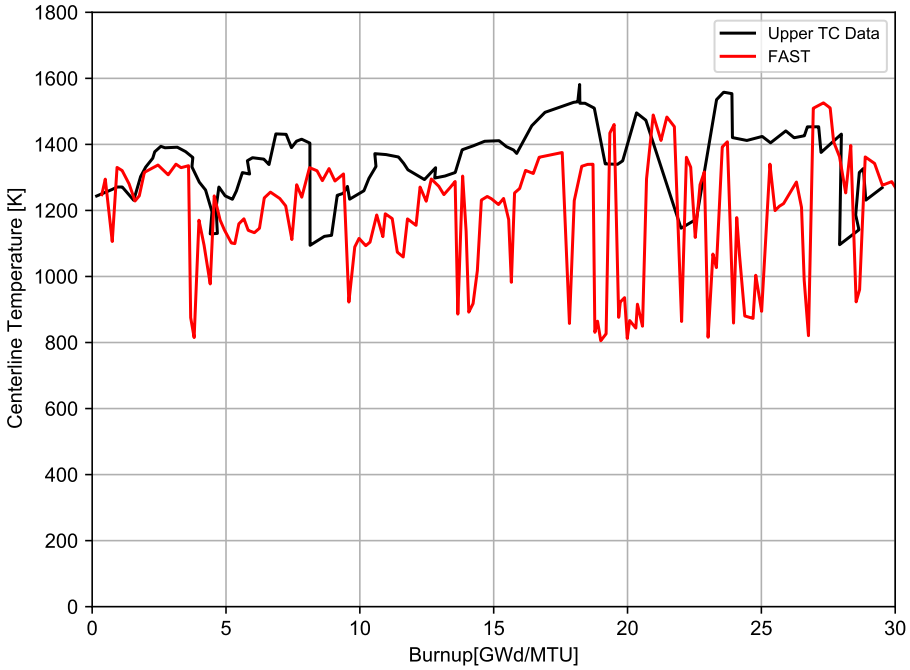

Figure 3-17. Measured and predicted centerline temperature for IFA-558 rod 6 UO_2 (burnup = 41 [GWd/MTU], as-fabricated radial gap = 95 [μm])

This section demonstrates that FAST continues to provide a best-estimate prediction of centerline temperature for UO_2 rods to within a standard error of 4.7% for recent experimental data (see Figure 3-2). The largest deviation was for IFA-677 rod 2 (Figure 3-16), which shows a 150 [K] (11% relative) underprediction at BOL that decreases to less than 75 [K] (6% relative) by 300 days. All the IFA-677 rods were also slightly underpredicted in the BOL temperature section, perhaps demonstrating a bias in this data, particularly compared with rods of similar power, burnup levels, and gap size that demonstrate better agreement with the code.

It is noted that in some of these cases the temperatures are predicted well throughout life, while in other cases there is a deviation with time, and in others there is a consistent bias throughout life. The cases with a deviation with time are likely due to a small difference in FGR predictions that affect the calculated centerline temperature or a drift in neutron detectors with time that affects measured rod powers. In some cases, the neutron detectors are recalibrated between reactor cycles such that at a given burnup or time the predicted and measured temperatures begin to agree better or deviate. The cases with a constant bias throughout life are likely due to a bias in the predictions, the reported rod power, or the measured temperature.

3.2.2 MOX Centerline Temperature Predictions as a Function of Burnup

FAST predictions have been benchmarked against centerline temperatures taken from eight Halden tests with instrumented fuel assemblies containing 15 MOX fuel rods. The results of these comparisons are provided in this section.

The following figures show measured and predicted fuel centerline temperatures from rods with

centerline temperature measurements. Individual rod predictions may demonstrate a systematic error (bias) that may be due to thermocouple decalibration or a systematic error in the power history or axial power shape (power at thermocouple location) provided due to decalibration in or with the neutron detectors. However, when all the comparisons are examined, no overall systematic error (bias) is found in the prediction of MOX fuel temperature, as can be seen in Figure 3-18. For all the cases, a standard error of 5.0% on the centerline temperature was calculated.

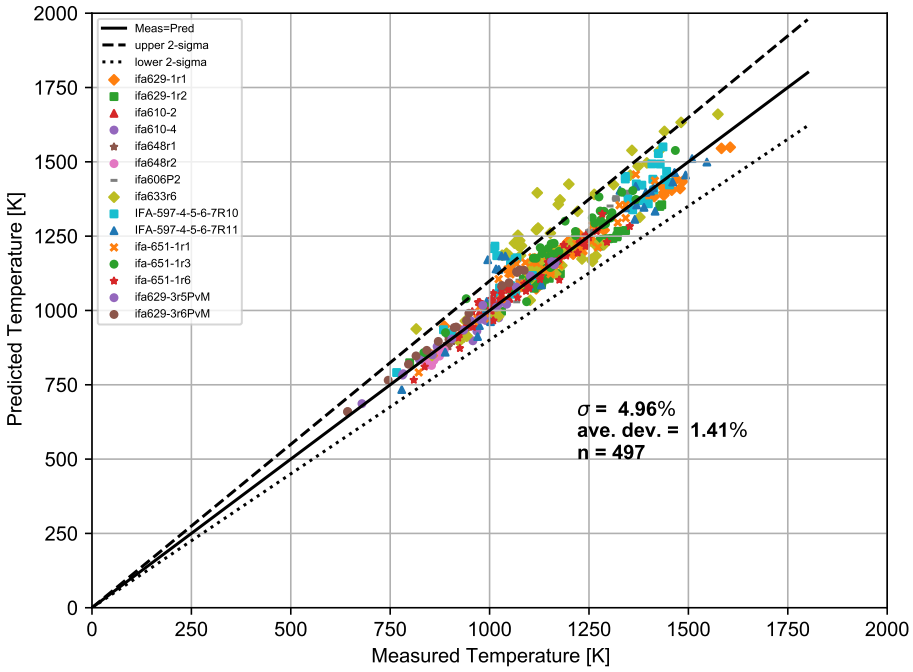

Figure 3-18. Measured and predicted centerline temperature for the MOX assessment cases throughout life

These data are also shown in terms of relative bias in Figure 3-19 as a function of burnup. There appears to be no systematic bias in the predictions with increasing burnup.

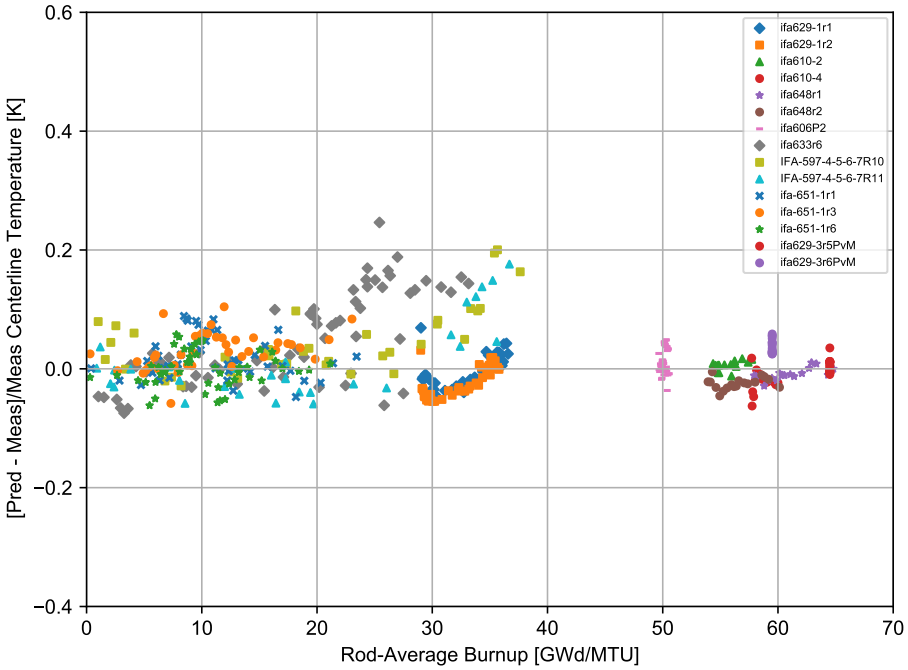

Figure 3-19. Predicted minus measured divided by measured centerline temperature for the MOX assessment cases as a function of burnup

Figures 3-20 and 3-21 show the measured and predicted centerline temperatures for IFA-629.1 rods 1 and 2. These figures show good agreement between the FAST predictions and the data. The slight offset during parts of the irradiation could be due to power or thermocouple calibration changes at the end of each cycle.

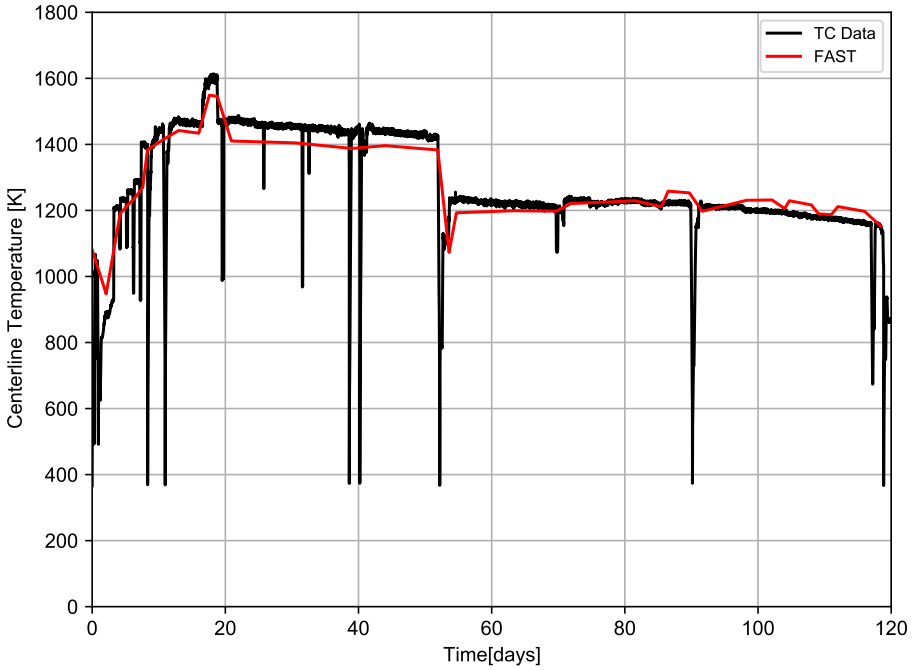

Figure 3-20. Measured and predicted centerline temperature for IFA-629.1 rod 1 (MOX) (starting burnup = 27 [GWd/MTU], ending burnup=33 [GWd/MTU], as□fabricated radial gap = 84 [μm])

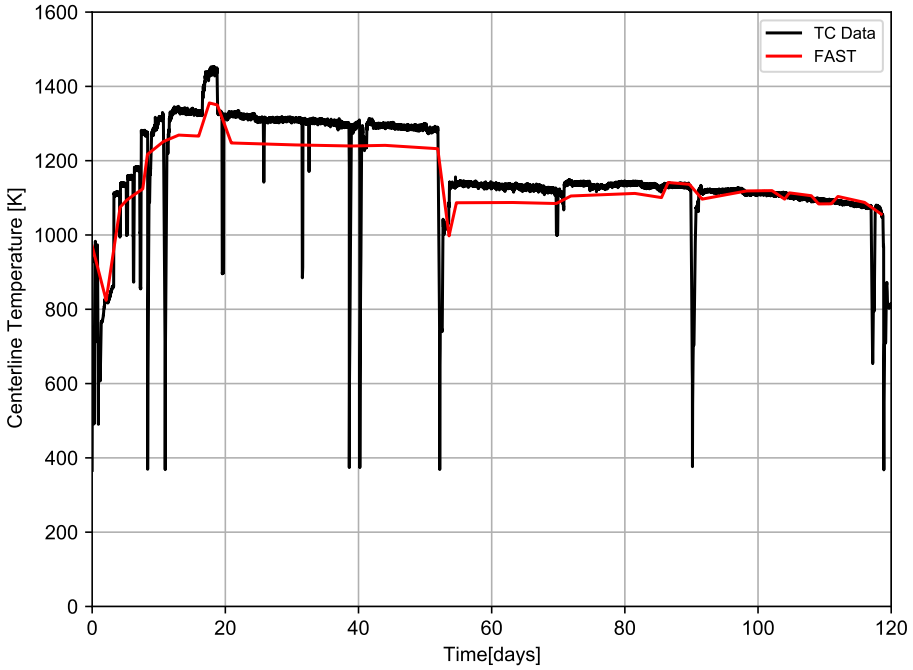

Figure 3-21. Measured and predicted centerline temperature for IFA-629.1 rod 2 (starting burnup = 29 [GWd/MTU], ending burnup = 40 [GWd/MTU], as-fabricated radial gap = 84 [μm])

Figures 3-22 and 3-23 show the measured and predicted centerline temperature for IFA-610.2 and IFA-610.4. These figures show excellent agreement between the FAST predictions and the data.

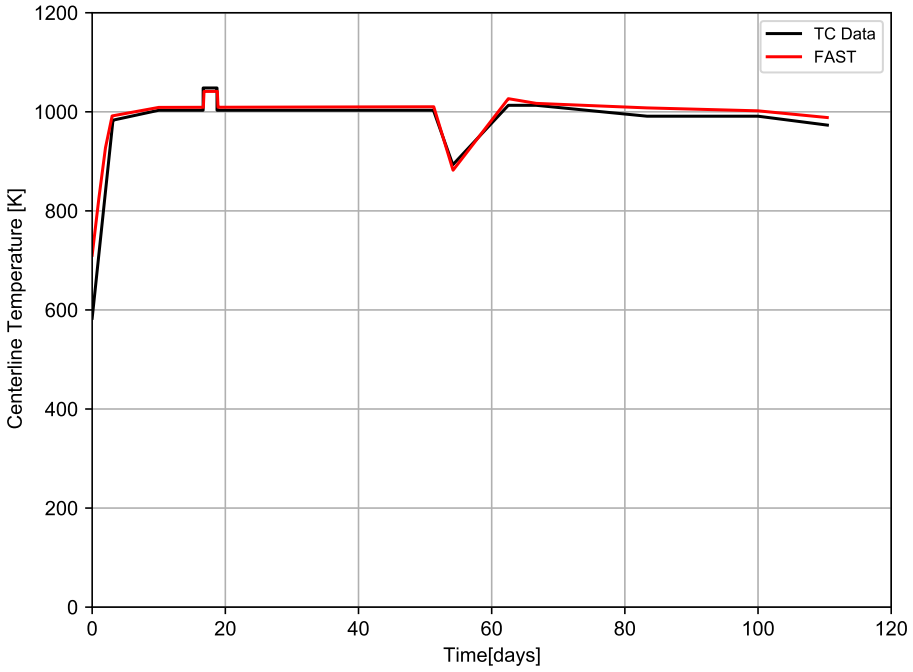

Figure 3-22. Measured and predicted centerline temperature for IFA-610.2 (MOX) (starting burnup = 55 [GWd/MTU], ending burnup = 56 [GWd/MTU], as-fabricated radial gap = 84 [μm])

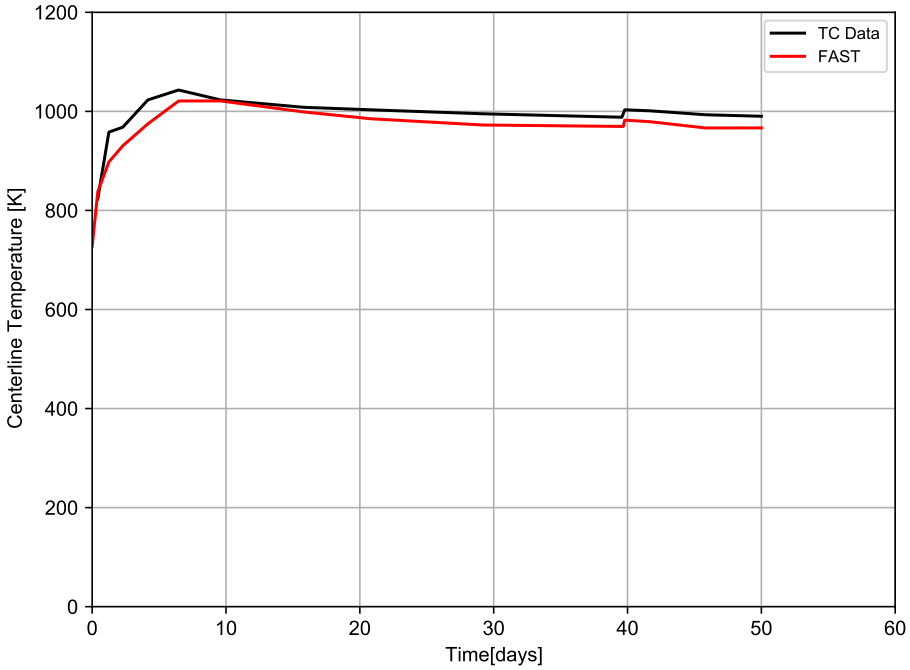

Figure 3-23. Measured and predicted centerline temperature for IFA-610.4 (MOX) (starting burnup = 56 [GWd/MTU], ending burnup = 57 [GWd/MTU], as-fabricated radial gap = 84 [μm])

Figures 3-24 and 3-25 show the measured and predicted centerline temperature for IFA-648.1 rods 1 and 2. These figures show excellent agreement between the FAST predictions and the data.

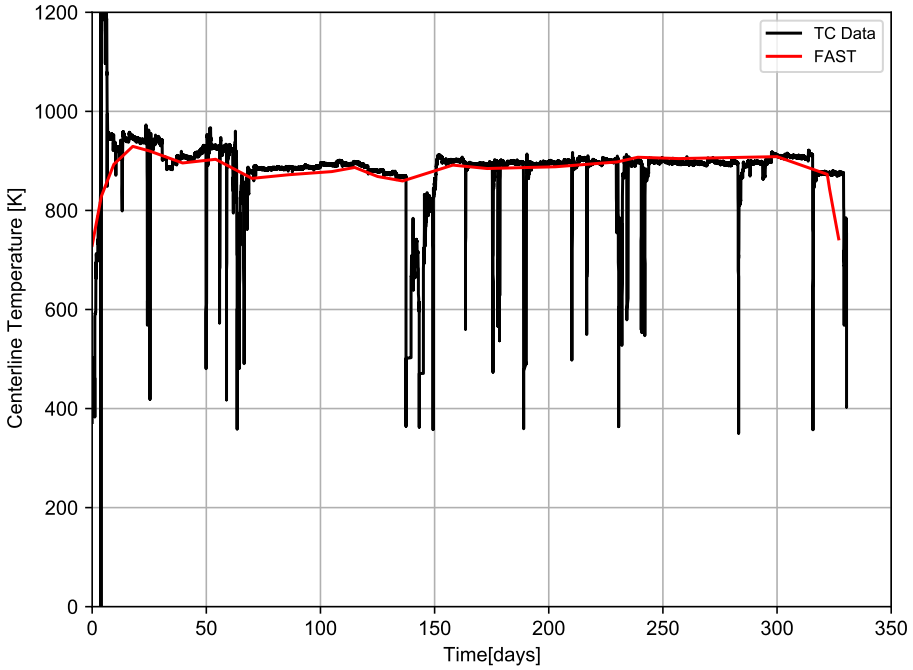

Figure 3-24. Measured and predicted centerline temperature for IFA-648.1 rod 1 (MOX) (starting burnup = 55 [GWd/MTU], ending burnup = 62 [GWd/MTU], as-fabricated radial gap = 84 [μm])

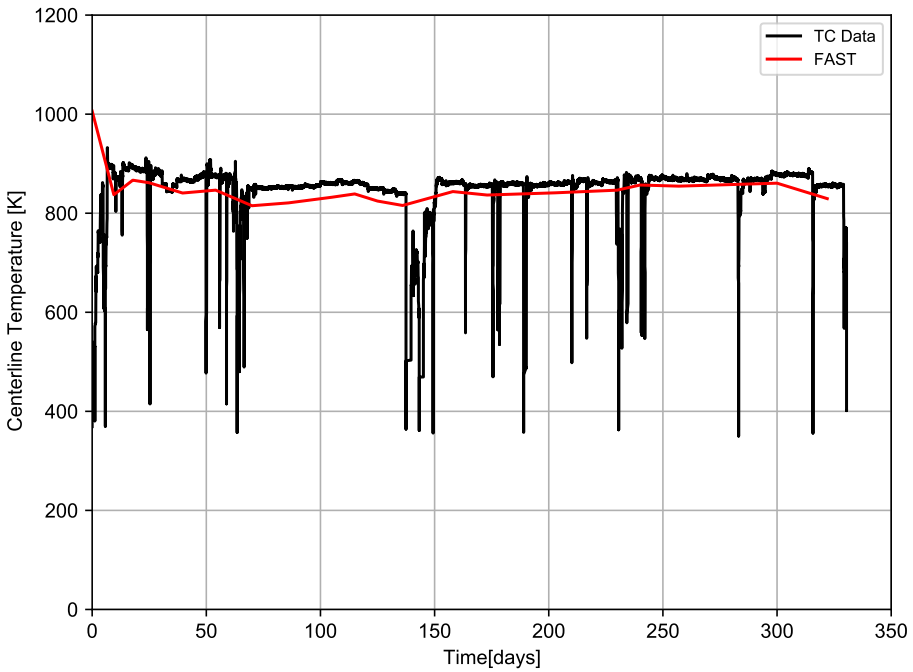

Figure 3-25. Measured and predicted centerline temperature for IFA-648.1 rod 2 (MOX) (starting burnup = 55 [GWd/MTU], ending burnup = 62 [GWd/MTU], as-fabricated radial gap = 84 [μm])

Figures 3-26 and 3-27 show the measured and predicted centerline temperature for IFA-629.3 rods 5 and 6. These figures show excellent agreement between the FAST predictions and the data.

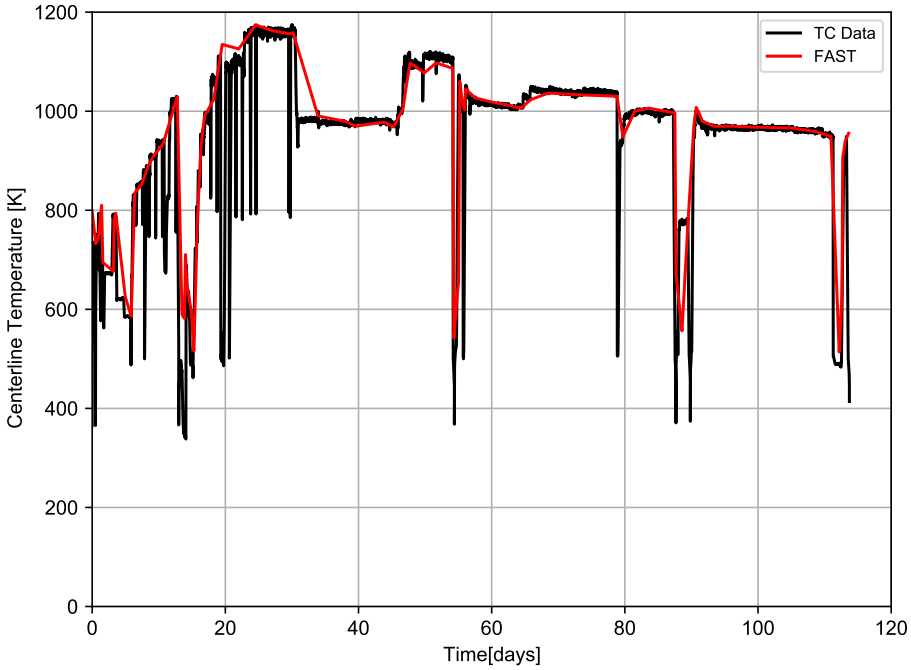

Figure 3-26. Measured and predicted centerline temperature for IFA-629.3 rod 5 (MOX) (starting burnup = 62 [GWd/MTU], ending burnup = 72 [GWd/MTU], as-fabricated radial gap = 84 [μm])

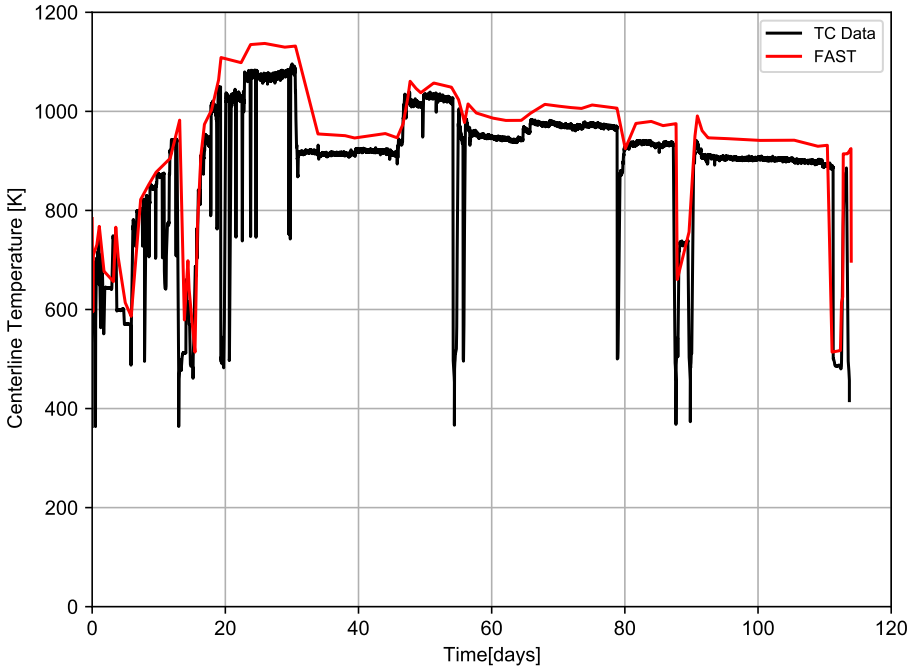

Figure 3-27. Measured and predicted centerline temperature for IFA-629.3 rod 6 (MOX) (starting burnup = 62 [GWd/MTU], ending burnup = 68 [GWd/MTU], as-fabricated radial gap = 84 [μm])

Figure 3-28 shows the measured and predicted centerline temperature for IFA-606 Phase 2. This figure shows reasonable agreement between the FAST predictions and the data (within $\pm$75 [K], 7% relative).

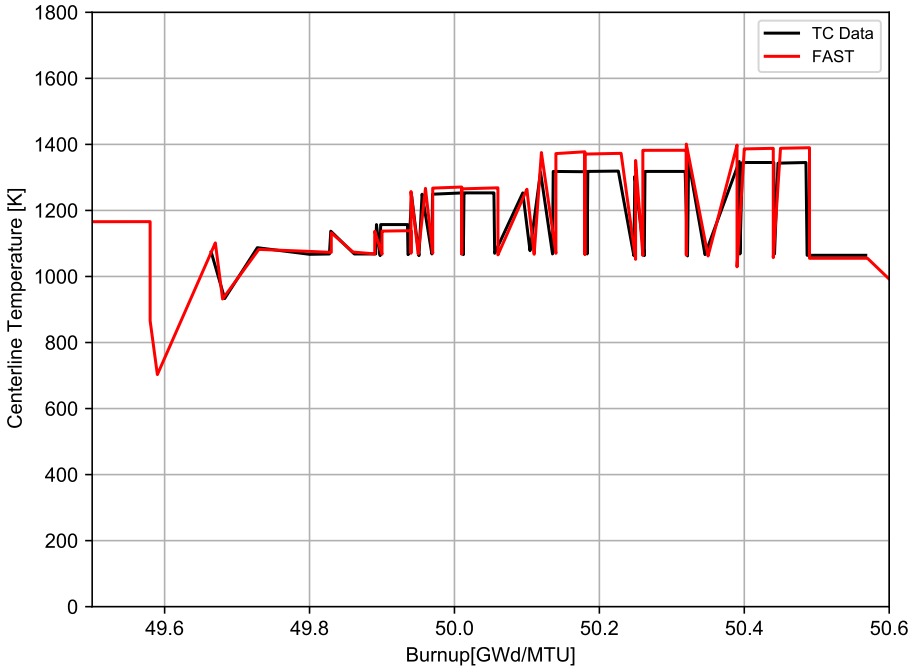

Figure 3-28. Measured and predicted centerline temperature for IFA-606 Phase 2 (MOX) (starting burnup = 49 [GWd/MTU], as-fabricated radial gap = 94 [μm])

Figure 3-29 shows the measured and predicted centerline temperature for IFA-633-1 rod 6. This figure shows reasonable agreement between the FAST predictions and the data (within $\pm$75 [K], 5% relative) until about 26 [GWd/MTU], when FAST overpredicts the data by about 125 to 150K (13% relative). This may be because FAST overpredicts the FGR (measured FGR=6% , predicted=13%) for this rod, which will lead to increased fuel ratures.

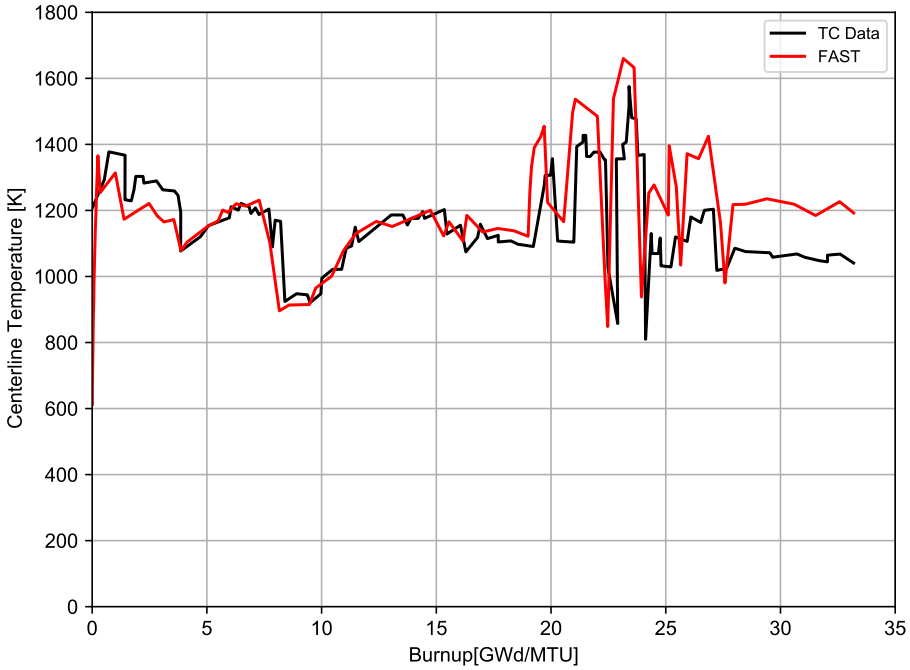

Figure 3-29. Measured and predicted centerline temperature for IFA-633-1 rod 6 (MOX) (burnup = 32 [GWd/MTU], as-fabricated radial gap= 104 [μm])

Figures 3-30 and 3-31 show the measured and predicted centerline temperature for IFA-597.4, .5, .6, .7 rods 10 and 11. These figures show excellent agreement between the FAST predictions and the data up to 25 [GWd/MTU], when the code begins to overpredict the data by up to 100 [K] (7% relative).

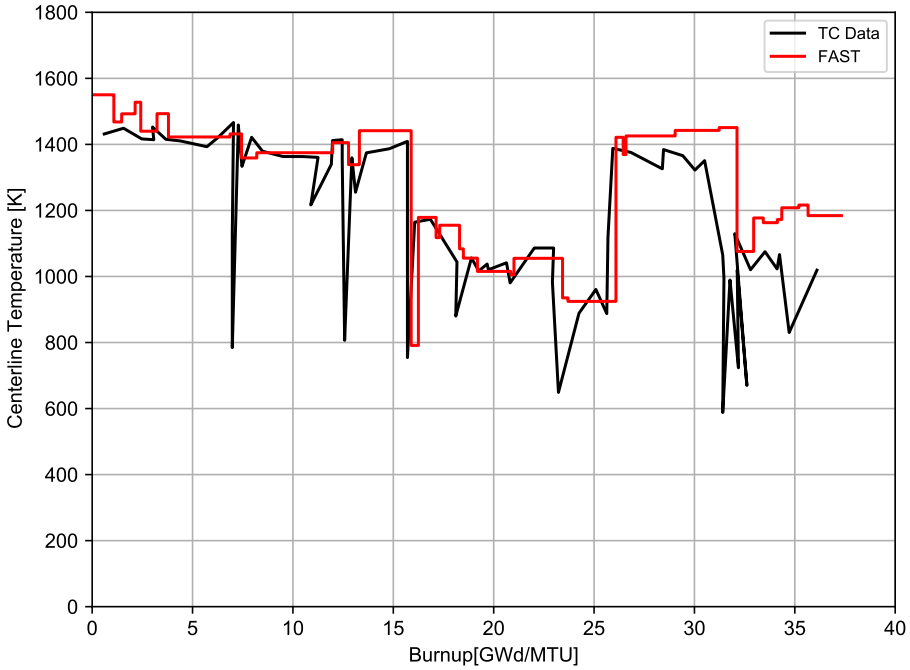

Figure 3-30. Measured and predicted centerline temperature for IFA-597.4, .5, .6, .7 rod 10 (MOX) (burnup = 36 [GWd/MTU] as-fabricated radial gap = 95 [μm])

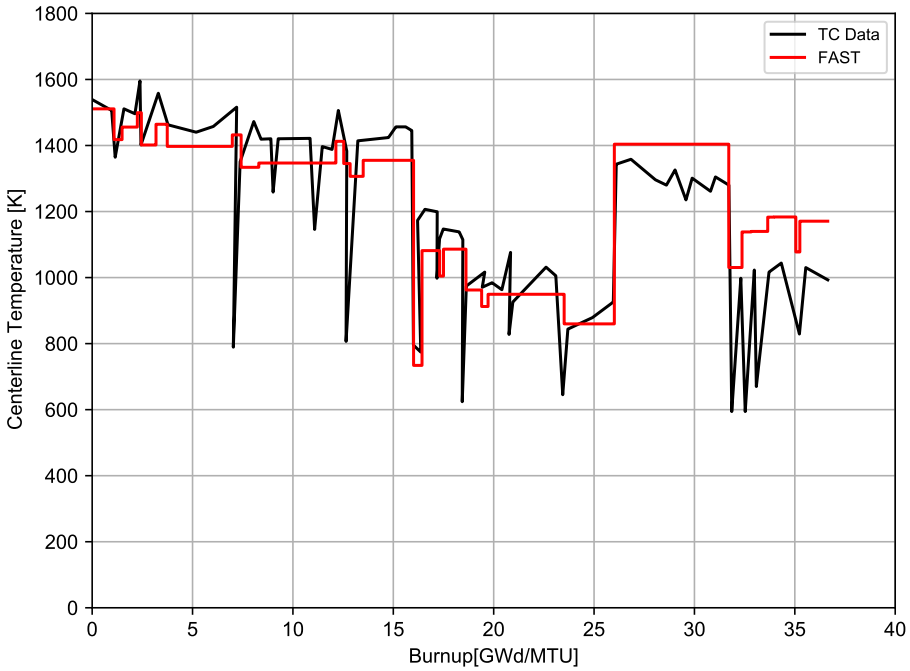

Figure 3-31. Measured and predicted centerline temperature for IFA-597.4, .5, .6, .7 rod 11 (MOX) (burnup = 37 [GWd/MTU] as-fabricated radial gap = 95 [μm])

Figures 3-32, 3-33, and 3-34 show the measured and predicted centerline temperature for IFA-

651.1 rods 1, 3, and 6. These figures show excellent agreement between the FAST predictions and the data from rods 1 and 6 that were instrumented with centerline thermocouple, and reasonable agreement ($\pm$50 [K], 5% relative) with the data from rod 3 that was instrumented with an expansion thermometer.

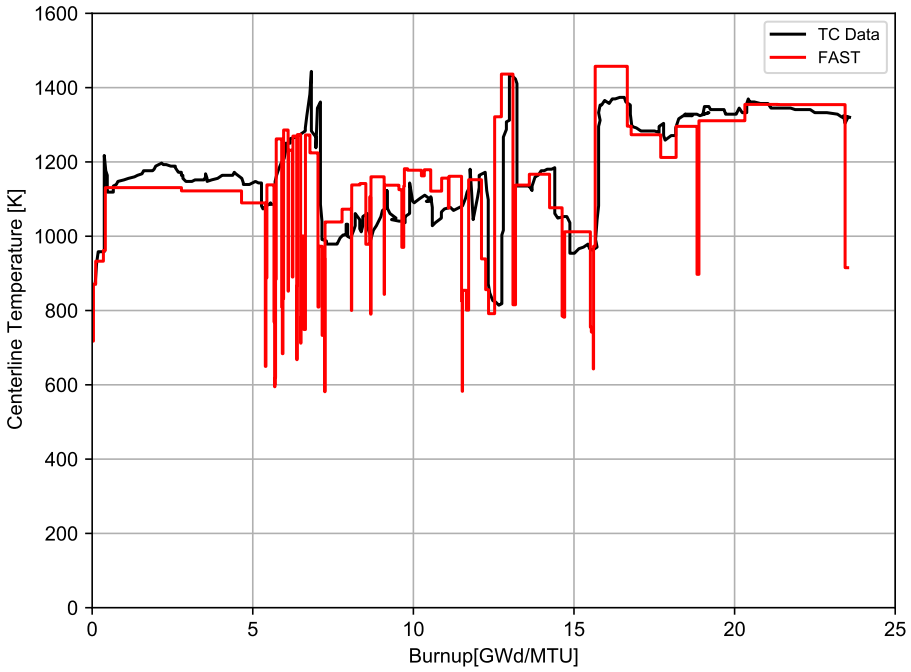

Figure 3-32. Measured and predicted centerline temperature for IFA-651.1 rod 1 (MOX) (burnup = 22 [GWd/MTU] as-fabricated radial gap = 79 [μm])

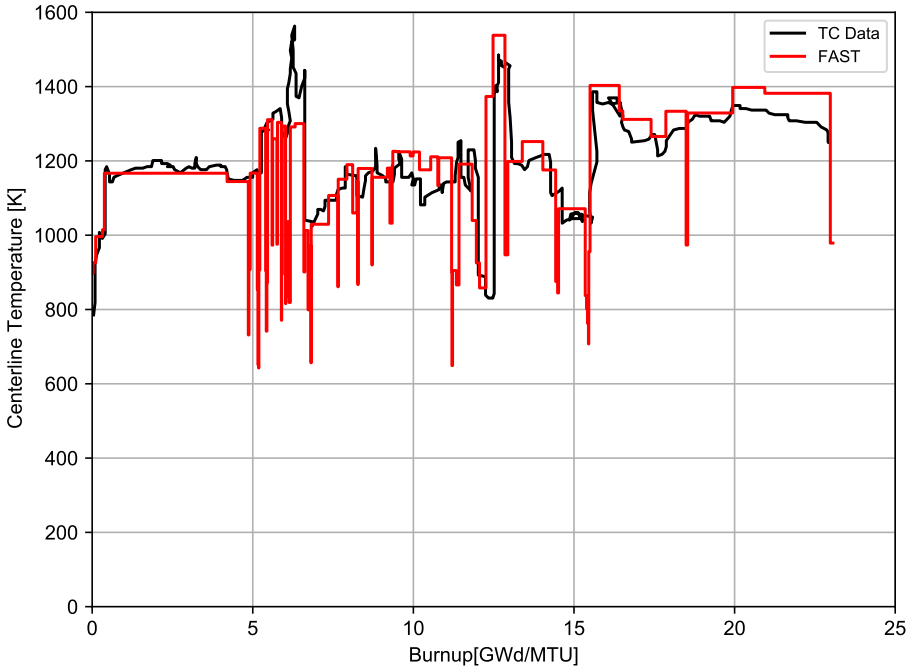

Figure 3-33. Measured and predicted centerline temperature for IFA-651.1 rod 3 (MOX) (burnup = 22 [GWd/MTU] as-fabricated radial gap = 79 [μm])

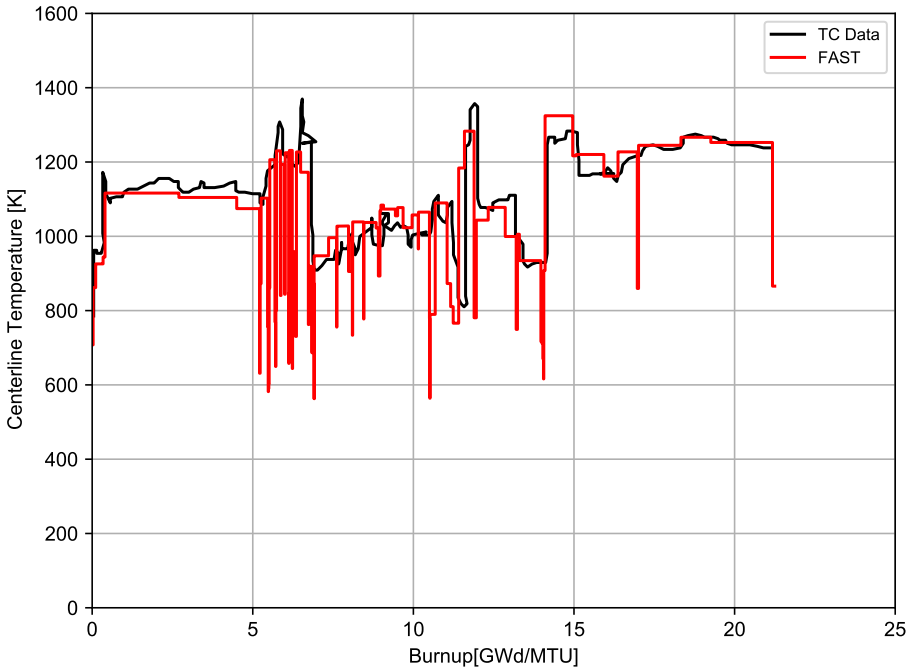

Figure 3-34. Measured and predicted centerline temperature for IFA-651.1 rod 6 (MOX) (burnup = 20 [GWd/MTU] as-fabricated radial gap = 81 [μm])

This section demonstrates that FAST continues to provide a best-estimate prediction of centerline

temperature for MOX rods to within a standard error of 4.9% . The largest deviation was for IFA-633.1 rod 6 (Figure 3-29), which shows up to a 150 [K] (13% relative) overprediction at higher burnup. This may be due to overpredicting the FGR for this rod.

3.2.3 UO_2-Gd_2O_3 Centerline Temperature Predictions as a Function of Burnup

The adjustment for gadolinia in the thermal conductivity model has been assessed against centerline temperature predictions from three instrumented fuel assemblies irradiated at the Halden reactor. The results of these comparisons are provided in this section.

The following figures show measured and predicted fuel centerline temperatures from rods with centerline temperature measurements. Individual rod predictions may demonstrate a systematic error (bias) that may be due to thermocouple decalibration or a systematic error in the power history or axial power shape (power at thermocouple location) provided due to decalibration in or with the neutron detectors with time. However, when all the comparisons are examined, no overall systematic error (bias) is found in the prediction of UO_2-Gd_2O_3 temperature throughout life, as can be seen in Figure 3-35. For all the cases, a standard error of 4.8% on the centerline temperature was calculated.

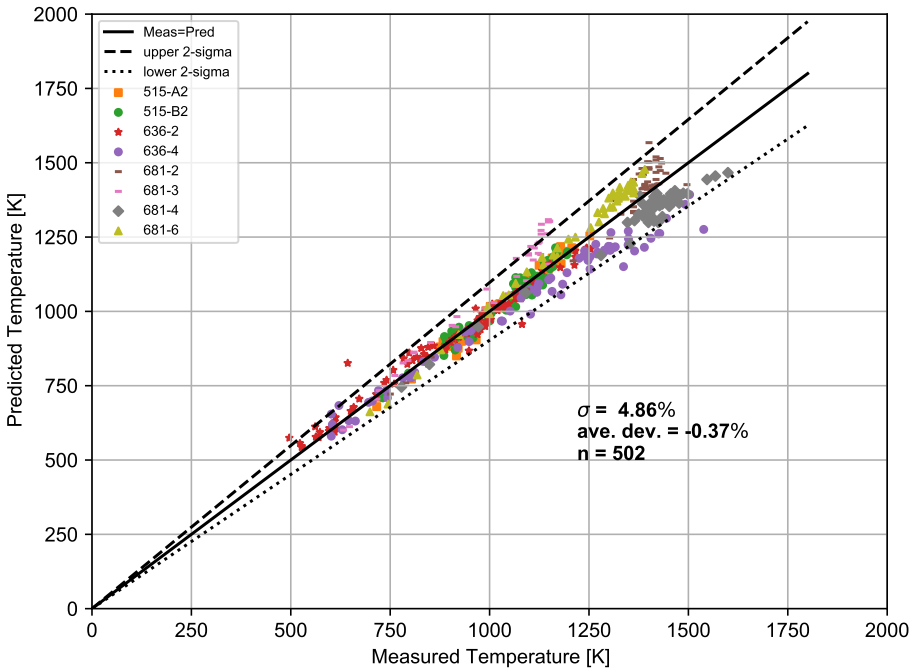

Figure 3-35. Measured and predicted centerline temperature for the UO_2-Gd_2O_3 assessment cases throughout Life

These data are also shown in terms of relative bias in Figure 3-36 as a function of burnup. It can be seen that there appears to be no systematic bias in the predictions with increasing burnup.

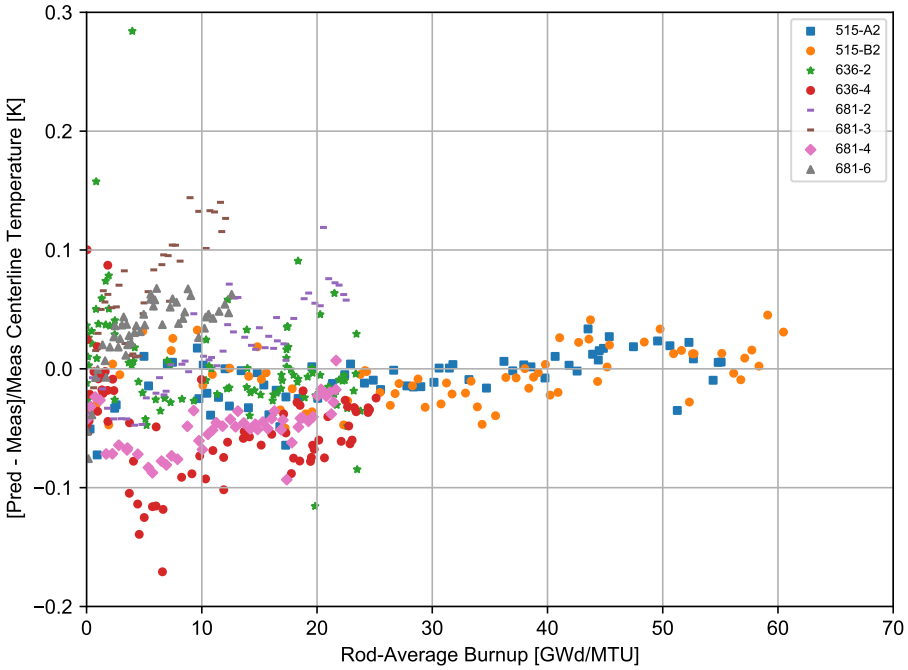

Figure 3-36. Predicted minus measured divided by measured centerline temperature for the $UO_2Gd_2O_3$ assessment cases as a function of burnup

Figures 3-37 and 3-38 show the measured and predicted centerline temperature for IFA-515.10 rods A1, A2, B1, and B2. Rods A1 and B1 (Figures 37(a) and 38(a)) are UO_2 rods and rods A2 and B2 (Figures 37(b) and 38(b)) are UO_2-Gd_2O_3 rods with depleted gadolinium that did not contain any ^{155}Gd or ^{157}Gd. There are two factors that influence the centerline temperature for UO_2-Gd_2O_3 rods relative to UO_2 rods: 1) TCD due to Gd addition and 2) radial power profile due to the neutron absorption of ^{155}Gd and ^{157}Gd. These rods were meant to show the difference only due to the TCD from gadolinia (Gd_2O_3), not due to the difference in radial power profile. A modified version of FAST that uses the UO_2 radial power profile model (TUBRNP) for UO_2-Gd_2O_3 rods (A2 and B2) was used to perform these calculations. These figures show that FAST predicts the centerline temperatures for UO_2-Gd_2O_3 rods as well as for UO_2 rods. In these figures, the vertical line denotes where the thermocouple failed. Although data were reported after this point, it is not valid.

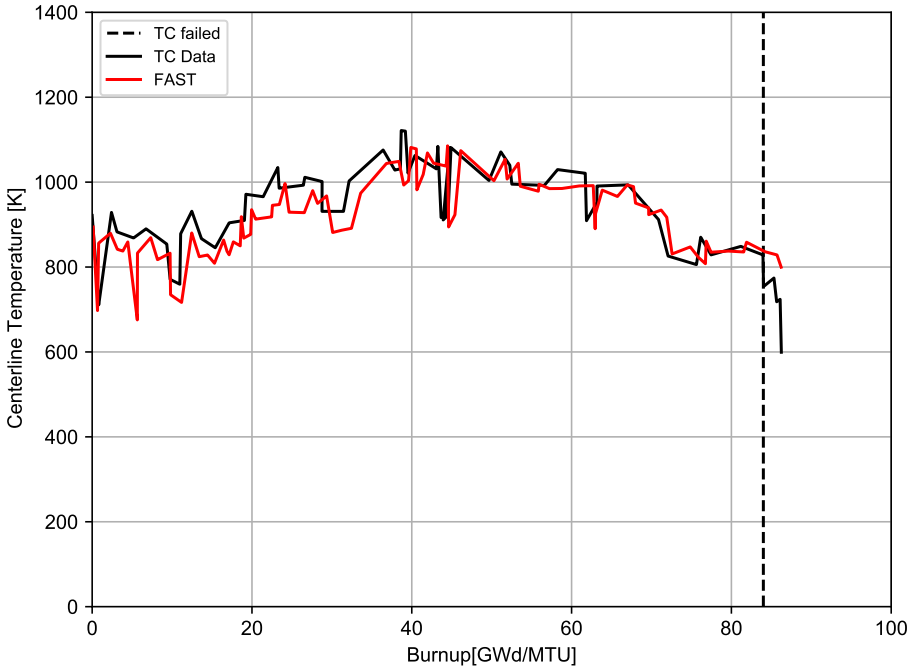

(a) Rod A1

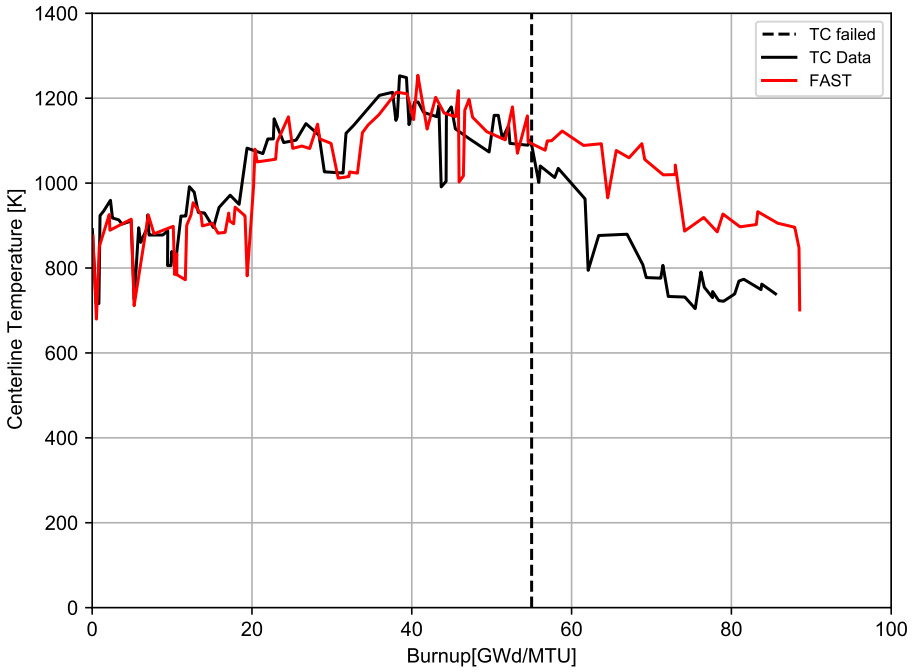

(b) Rod A2

Figure 3-37. Measured and predicted centerline temperature for IFA-515.10 rods A1 (UO_2) and A2 (UO_2-8% Gd_2O_3) (burnup=80 [GWd/MTU], as-fabricated radial gap=25 [μm])

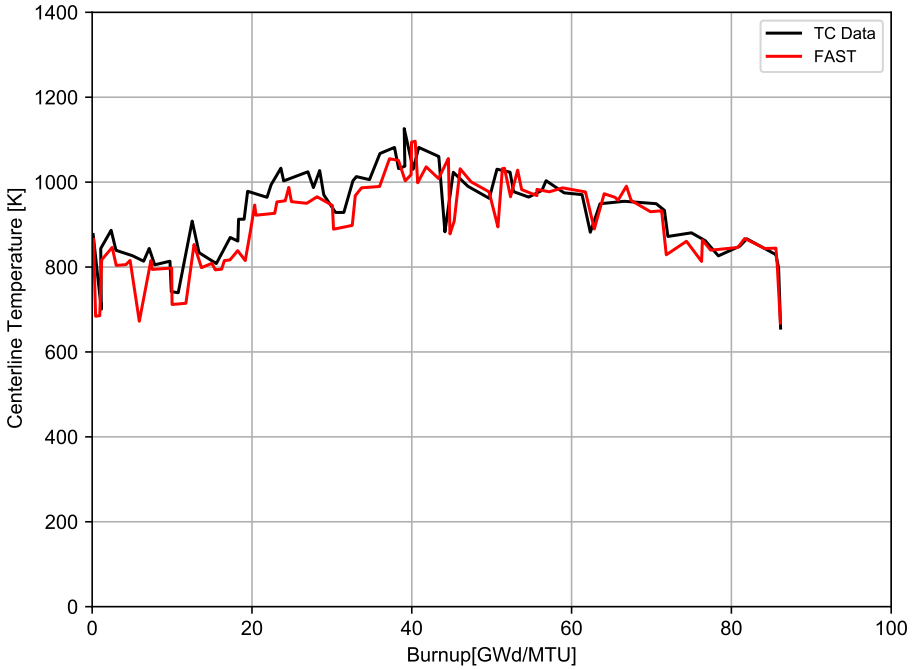

(a) Rod B1

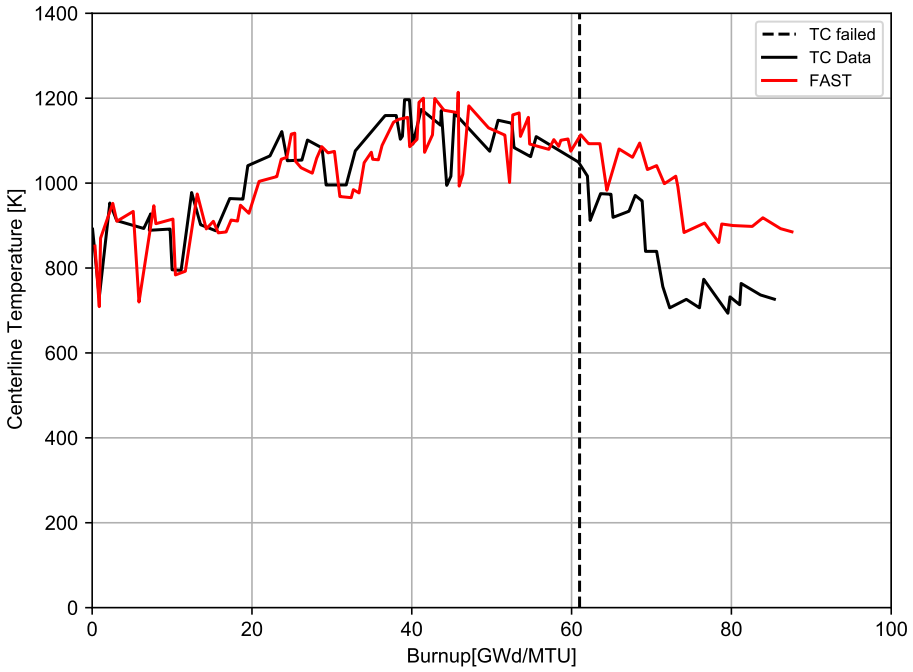

(b) Rod B2

Figure 3-38. Measured and predicted centerline temperature for IFA-515.10 rods B1 (UO_2) and B2 (UO_2-8% Gd_2O_3) (burnup=80 [GWd/MTU], as-fabricated radial gap=25 [μm])

Figures 3-39 and 3-40 show the measured and predicted centerline temperature for IFA-636 rods 2 and 4. These rods contain standard Gd (no Gd depletion like IFA-515.10), so the release version

of FAST could be used. Rod 2 was equipped with a centerline thermocouple, and the data from this thermocouple is shown in Figure 3-39. Rod 4 contains solid pellets, and the data is shown in Figure 3-40 is estimated from rod 2. Because rod 4 does not have a direct measurement of temperature (no thermocouple), there is more uncertainty in the data because this is estimated by Halden using the rod 2 temperature data and correcting for no thermocouple hole. In addition, as the Gd is burning out during the first rise to power, there is a high level of uncertainty on the reported rod power. Because of this, FAST may not predict the centerline temperature well during this period. These figures show excellent agreement between the FAST predictions and the data for rod 2 and significant underprediction (175 [K], 15% relative) between 4 and 10 [GWd/MTU] and reasonable agreement above 10 [GWd/MTU] for rod 4, which has greater uncertainty.

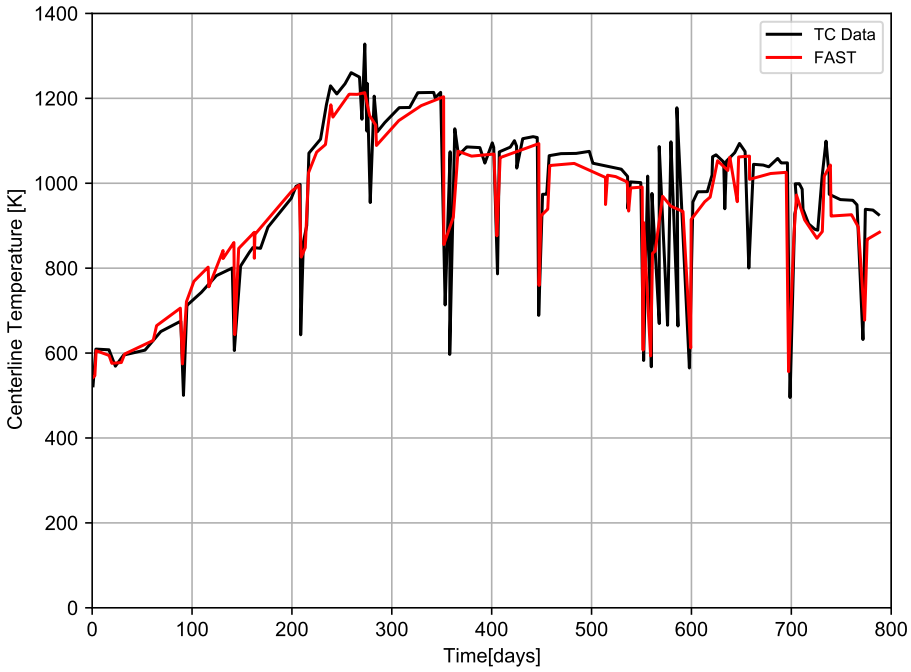

Figure 3-39. Measured and predicted centerline temperature for IFA-636 rod 2 (UO_2-8% Gd_2O_3) (burnup=25 [GWd/MTU], as-fabricated radial gap=77 [μm])

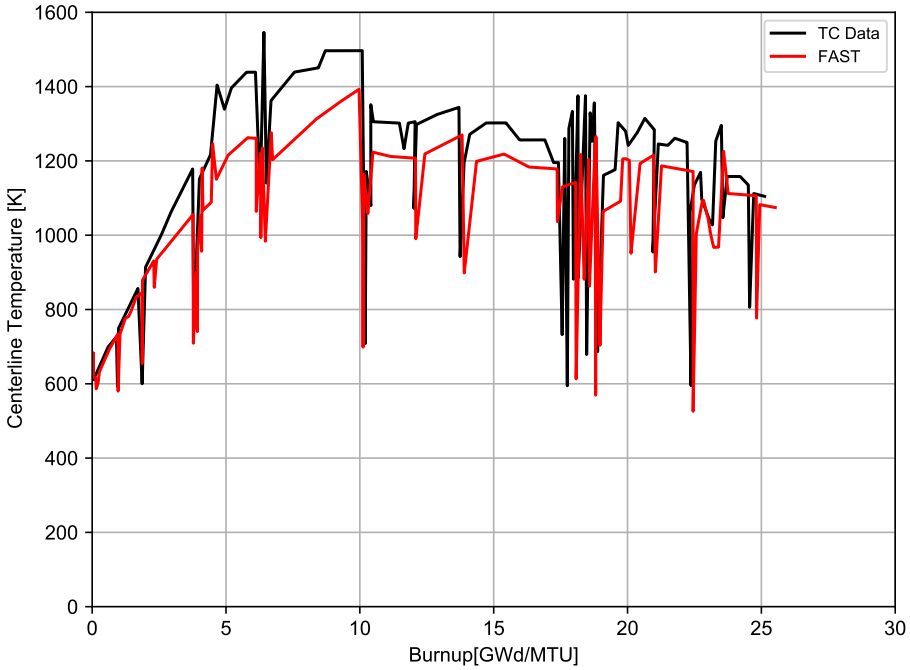

Figure 3-40. Measured and predicted centerline temperature for IFA-636 rod 4 (UO_2-8% Gd_2O_3) (burnup = 25 [GWd/MTU], as-fabricated radial gap = 77 [μm])

Figures 3-41 through 3-46 show the measured and predicted centerline temperature for IFA-681 rods 1, 2, and 3 with centerline thermocouples and rods 4, 5, and 6 with hollow pellets and expansion thermometers. Rods 1 and 5 are UO_2 rods; rods 2 and 4 contain standard Gd with 2 wt% Gd_2O_3; rods 3 and 6 contain standard Gd with 8 wt% Gd_2O_3. Since these rods contain standard Gd, the release version of FAST could be used. During the first rise to power, as the Gd is burning out, there is a high level of uncertainty on the reported rod power. Because of this, FAST may not predict the centerline temperature well during this period. This does not significantly affect future predictions because power levels while the Gd is burning out are low and will not cause significant FGR that will affect future temperature predictions.

These figures show excellent agreement between the FAST predictions and the data for rod 1 (UO_2, Figure 3-41) and 2 (2 wt% Gd_2O_3, Figure 3-42). For rod 3 (8 wt% Gd_2O_3, Figure 3-43), the FAST predictions are in excellent agreement with the data for the first 200 days. After this, FAST overpredicts the data by up to 120 [K] (13% relative). The reason for this is not clear, as both the power and the FAST temperature prediction increase during this time period, but the measured temperature does not increase with increasing power. For the hollow pellet rods, the 2 wt% Gd_2O_3 rods (IFA-681 rod 4 in Figure 3-44 and rod 5 in Figure 3-45) is uniformly underpredicted by about 50-90 [K] (4-7% relative) while the 8 wt% Gd_2O_3 rod (IFA-681 rod 6, Figure 3-46) is predicted well. These differences are well within the uncertainty of temperature measurement and power levels.

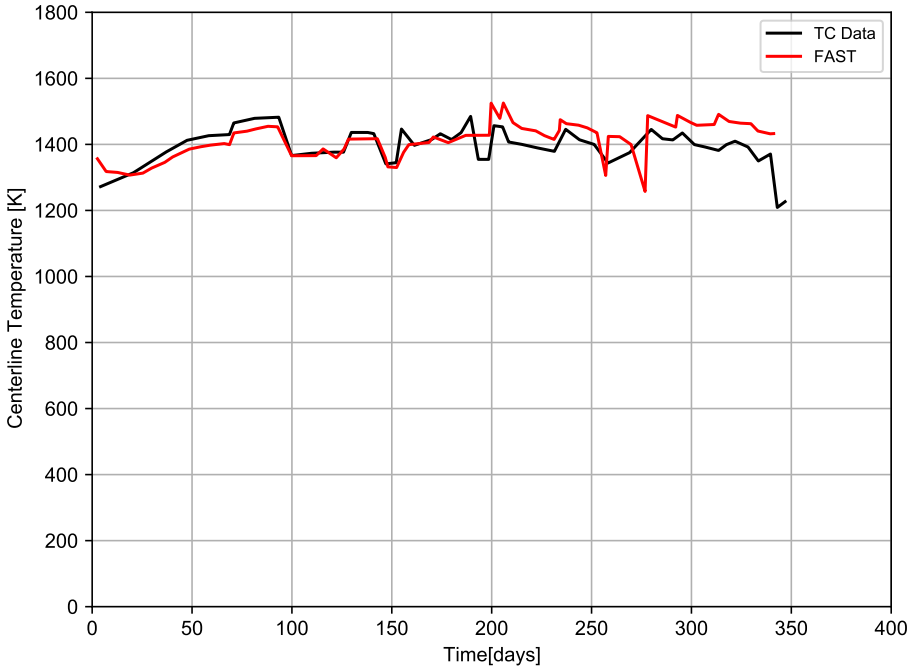

Figure 3-41. Measured and predicted centerline temperature for IFA-681 rod 1 (UO_2) (burnup = 24 [GWd/MTU], as-fabricated radial gap = 85 [μm])

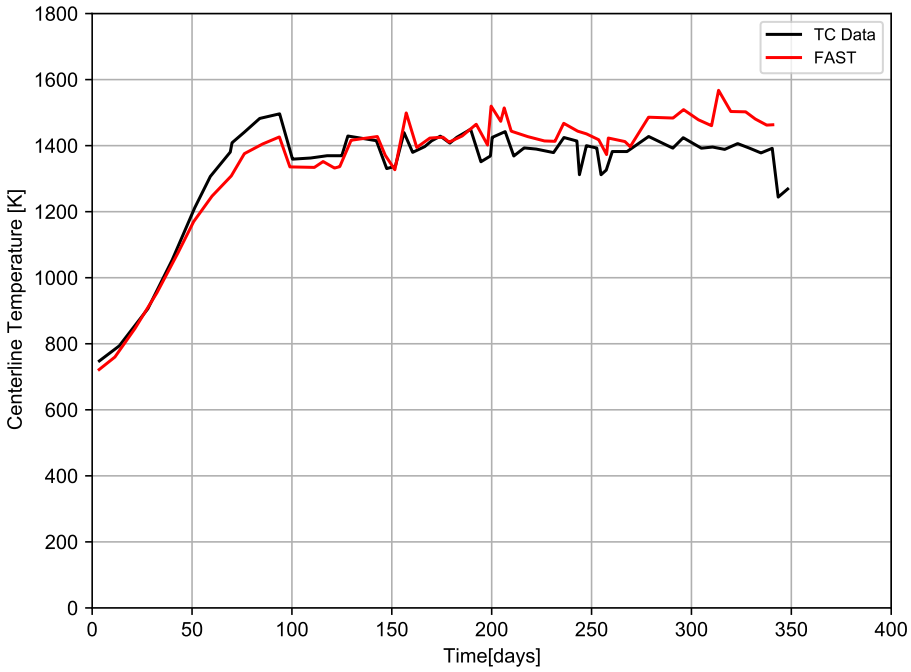

Figure 3-42. Measured and predicted centerline temperature for IFA-681 rod 2 (UO_2-2% Gd_2O_3) (burnup = 23 [GWd/MTU], as-fabricated radial gap = 85 [μm])

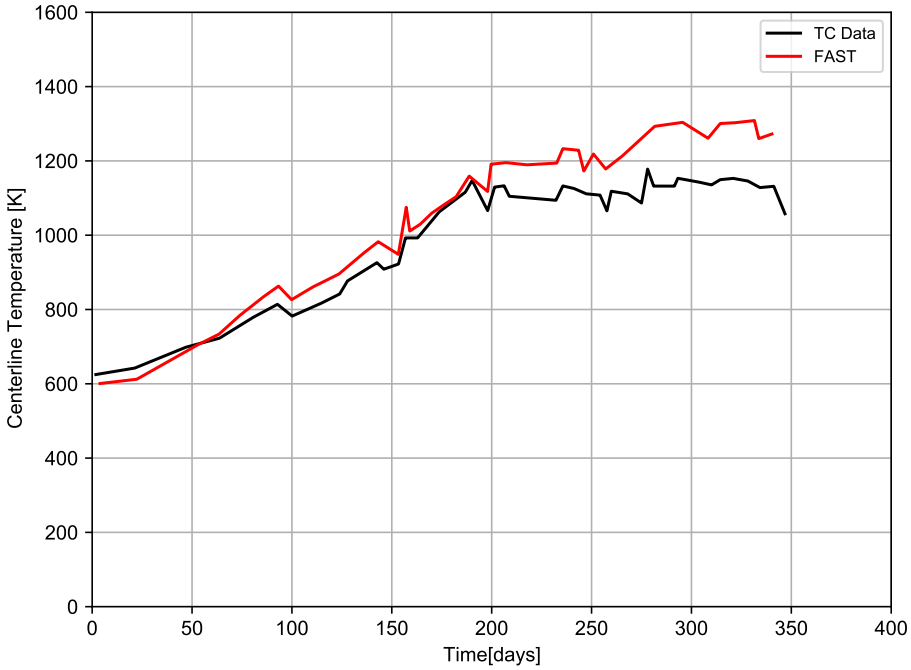

Figure 3-43. Measured and predicted centerline temperature for IFA-681 rod 3 (UO_2-8% Gd_2O_3) (burnup = 12 [GWd/MTU], as-fabricated radial gap=85 [μm])

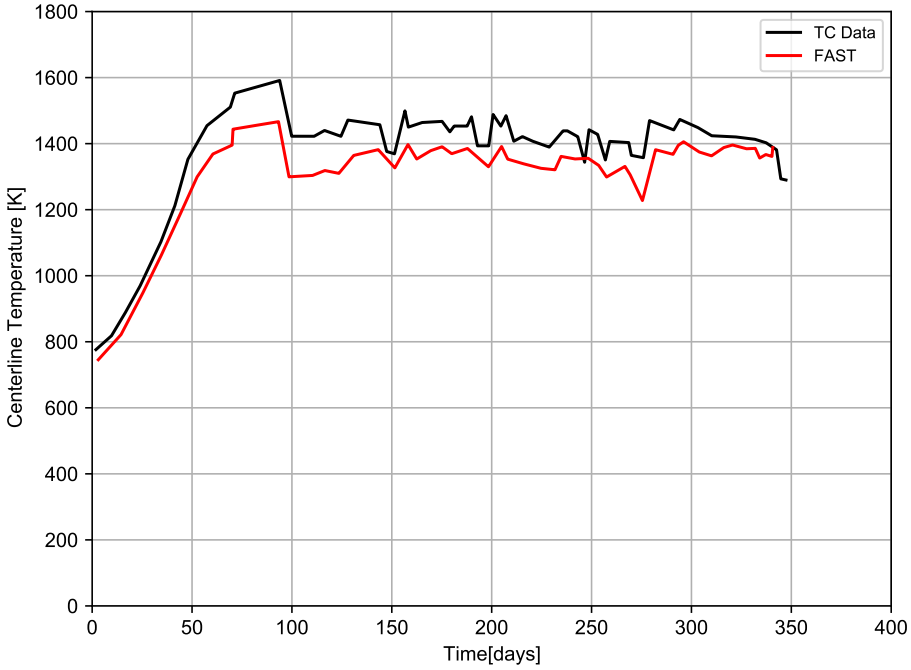

Figure 3-44. Measured and predicted centerline temperature for IFA-681 rod 4 (UO_2-2% Gd_2O_3) (burnup = 22 [GWd/MTU], as-fabricated radial gap = 85 [μm])

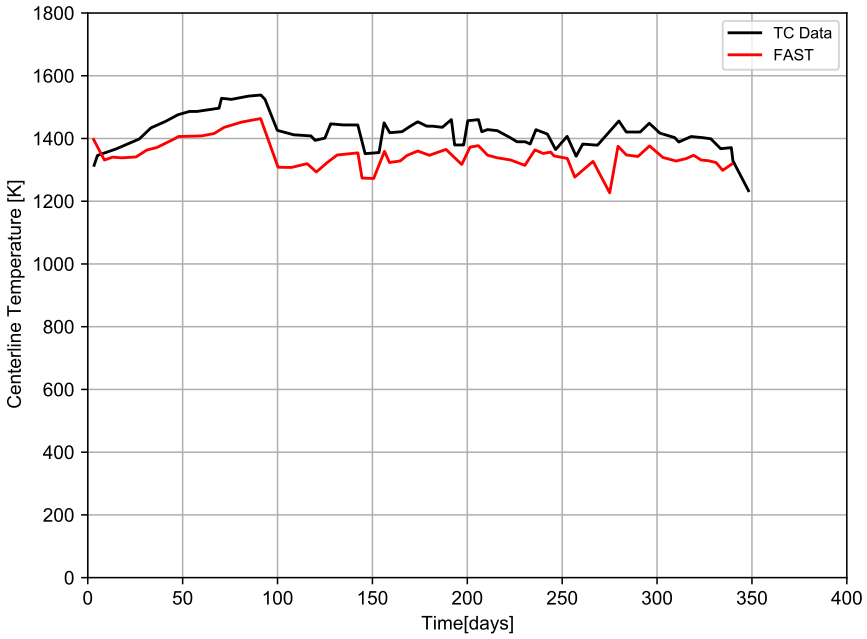

Figure 3-45. Measured and predicted centerline temperature for IFA-681 rod 5 (UO_2) (burnup = 23 [GWd/MTU], as-fabricated radial gap = 85 [μm])

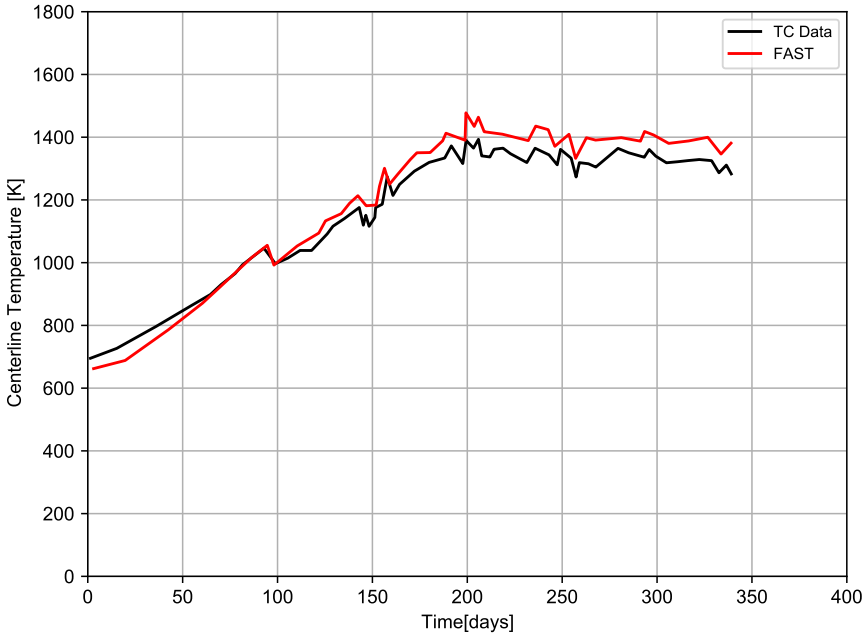

Figure 3-46. Measured and predicted centerline temperature for IFA-681 rod 6 (UO_2-8% Gd_2O_3) (burnup = 13 [GWd/MTU], as-fabricated radial gap = 85 [μm])

This section demonstrates that FAST continues to provide a best-estimate prediction of centerline temperature for UO_2-Gd_2O_3 rods to within a standard error of 4.8% for recent experimental data.

4.0 Fission Gas Release Assessment

4.1 Assessment of Steady-State FGR Predictions

An accurate prediction of FGR is important for two reasons: 1) it has a significant impact on the prediction of gap conductance and, therefore, fuel temperatures (e.g., as demonstrated in Section 3.2, an overprediction of FGR can result in an overprediction of fuel temperatures, and the converse is also true), and 2) it is necessary for the calculation of rod internal pressures that affect LOCA analyses and EOL rod pressures. In many cases, for current operating plants, the limits on and analyses of EOL rod pressures determine the LHGR limits for commercial fuel at burnups greater than 30 [GWd/MTU]. In addition, the NRC requires that these EOL rod pressure analyses include bounding normal operation transients (e.g., xenon transients lasting several hours) and AOOs (e.g., overpower transients lasting several minutes to hours). Therefore, the accurate prediction of transient FGR under conditions of power increases above steady-state operation is important for licensing analyses.

The code's ability to predict FGR in UO_2 fuel has been assessed based on comparisons to FGR data from 23 UO_2 fuel rods with power histories that are relatively steady-state through the rod's irradiation life and 19 UO_2 rods with power bumping (increase in rod power) at EOL to simulate an overpower AOO or normal operational transients. The code's ability to predict FGR in MOX fuel has been assessed based on comparisons to FGR data from 34 MOX fuel rods with power histories that are relatively steady-state through the rod's irradiation life and 8 MOX rods with power bumping (increase in rod power) at EOL to simulate an overpower AOO or normal operational transients. The fuel rods with greater than 5% FGR were selected because the limiting rods in terms of EOL rod pressure in today's plants (particularly for power uprated plants) have releases above 10% FGR.

Four fuel rods with UO_2-Gd_2O_3 fuel were available for assessment of the code's ability to predict FGR in UO_2-Gd_2O_3 fuel. This is not a large database, but these comparisons seem to indicate that FAST will predict FGR from UO_2-Gd_2O_3 fuel well. This is consistent with the observation that the measured FGR from UO_2-Gd_2O_3 rods is similar to the FGR from UO_2 rods with the same power history [Hirai et al., 1995].

The assessment in this section has used the default FGR model in the MASSIH subroutine in the code that is based on a modified release model proposed by [Forsberg and Massih, 1985]. This release model is described in Volume 1 of this report [Geelhood et al., 2021b]. The other FGR models in FAST (i.e., ANS-5.4 and FRAPFGR) provide reasonable predictions of FGR for fuel rods with steady-state power histories, but on average underpredicted FGR for fuel rods with power bumping for a few hours duration.

The following discussions are divided into comparisons of the code predictions to steady-state FGR data and to power bumping (transient) FGR data

4.1.1 UO_2 Steady-State FGR Predictions

Figure 4-1 shows the predicted FGR as a function of measured FGR for the steady-state UO_2 rods. Figure 4-2 shows the predicted minus measured FGR as a function of burnup for the steady-state

UO_2 rods.

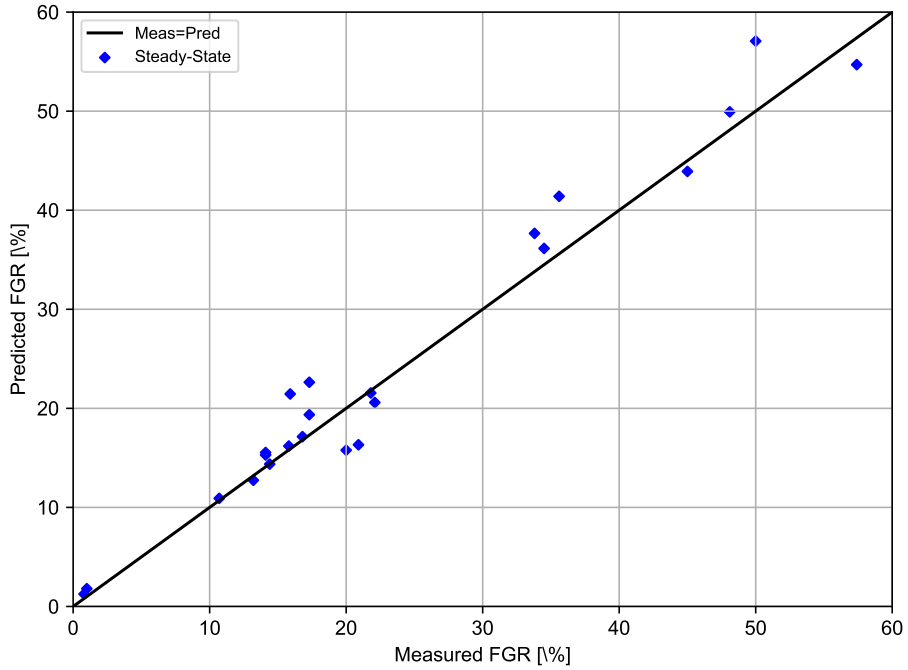

Figure 4-1. Comparison of FAST predictions to measured FGR data for the UO_2 steady-state assessment cases

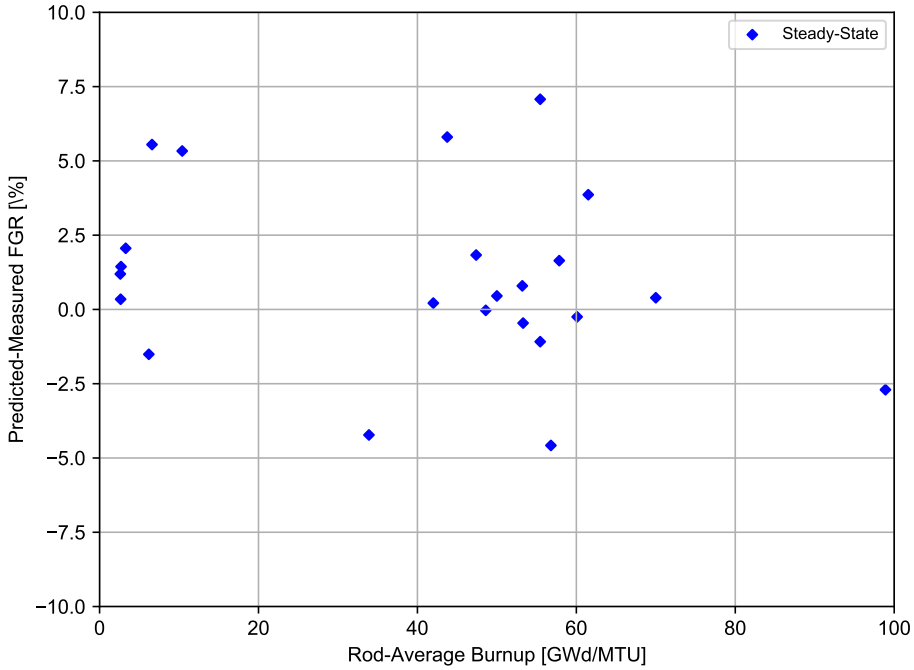

Figure 4-2. Predicted minus measured FGR versus rod-average burnup for the UO_2 steady-state assessment cases

The steady-state UO_2 cases with measured and predicted FGRs are shown in Table 4-1. The standard deviation for the steady-state predictions is 2.6% absolute FGR up to 70 [GWd/MTU]. These figures demonstrate that FAST provides a best-estimate calculation of fission gas over a wide range of gas release levels up to a rod-average burnup of 62 [GWd/MTU]. There are a few cases at higher burnup, but these cases indicated that FAST may begin to underpredict FGR at burnup levels beyond 62 [GWd/MTU] (Figure 4-2).

Table 4-1. Steady-state UO_2 FGR assessment cases

Rod	Rod-Average Burnup [GWd/MTU]	Measured FGR [%]	FAST-1.0.1 Predicted FGR [%]
24i6	60.10	21.80	22.70
36i8	61.50	33.80	38.09
111i5	48.60	14.40	14.79
28i6	53.30	13.20	13.44
HBEP BNFL-DE	42.00	10.70	10.24
LFF	3.29	17.30	19.35
CBP	2.61	14.10	14.51
4110-ae2	6.20	22.10	16.56
4110-be2	6.60	15.90	16.65
332	56.80	20.90	17.24
EPL-4	10.40	17.30	20.72
CBR	2.70	14.10	15.58
CBY	2.65	16.80	16.73
HBEP BNFL5-DH	33.90	20.00	15.73
FUMEX 6f	55.45	45.00±5.00	42.99
FUMEX 6s	55.45	50.00±5.00	56.34
IFA 597.3	70.00	15.80	14.55
IFA429DH	98.90	57.40	54.36
ANO TSQ002	53.20	1.00	1.78
Oconee 15309	50.00	0.80	1.25
30i8	57.85	34.50	36.78
m2-2c	43.75	35.60	41.25
pa29-4	47.39	48.10	45.80

* EOL FGR estimated from rod pressure data (larger error than data from puncture)

4.1.2 MOX Steady-State FGR Predictions

Figure 4-3 shows the predicted FGR as a function of measured FGR for the steady-state MOX rods. Figure4-4 shows the predicted minus measured FGR as a function of burnup for the steady-

state MOX rods.

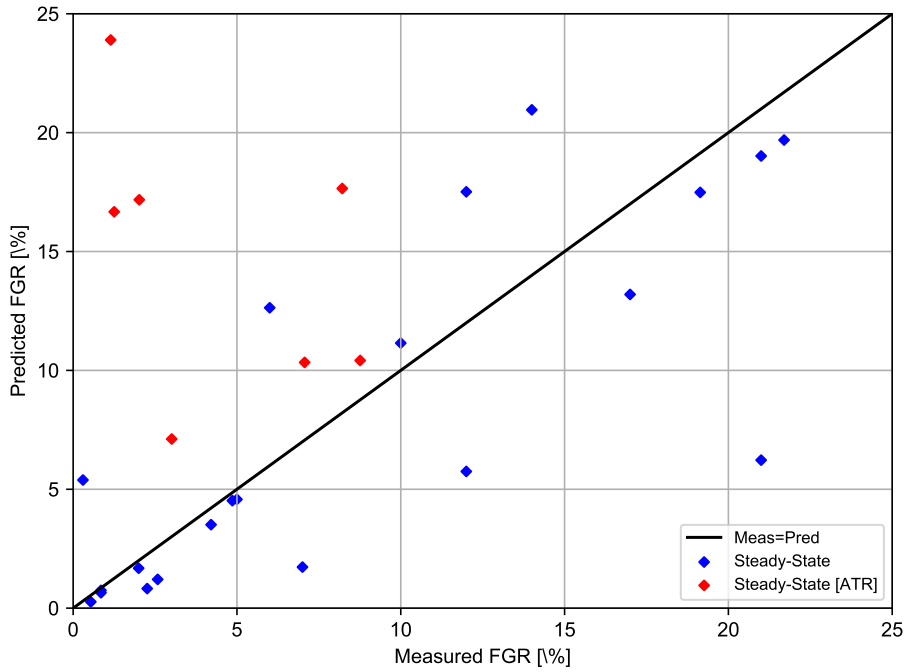

Figure 4-3. Comparison of FAST predictions to measured FGR data for the MOX steady-state assessment cases

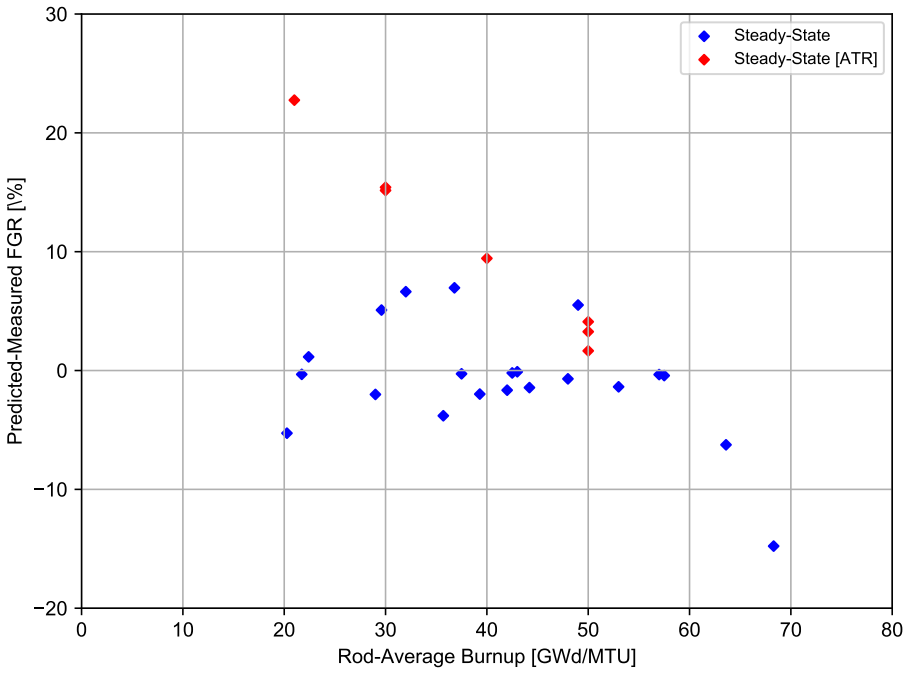

Figure 4-4. Predicted minus measured FGR versus rod-average burnup for the MOX steady-state assessment cases

The steady-state MOX cases with measured and predicted FGRs are shown in Table 4-2. The standard deviation for the steady-state predictions is 6.8% FGR. It is noted that some of these MOX rods are from the Advanced Test Reactor (ATR) at Idaho National Laboratory and are subject to large radial flux profiles. Because of this, it is difficult to estimate the rod-average power. If the ATR rods are removed from the calculation of standard deviation, a standard deviation of 4.4% absolute FGR is calculated. These figures demonstrate that FAST provides a best-estimate calculation of fission gas over a wide range of gas release levels up to a rod-average burnup of 62 [GWd/MTU]. There are a few cases at higher burnup, but these cases indicated that FAST may begin to underpredict FGR at burnup levels beyond 62 [GWd/MTU] (Figure 4-4).

Table 4-2. Steady-state MOX FGR assessment cases

Rod	Rod-Average Burnup [GWd/MTU]	Measured FGR [%]	FAST-1.0.1 Predicted FGR [%]
IFA-651.1r1	22.41	10*	11.13
IFA-651.1r3	21.73	2*	1.68
IFA-651.1r6	20.27	7*	1.88
ATR PII C2 P5	21.00	1.146	22.19
ATR PIII C3 P6	30.00	1.253	15.96
ATR PIII C10 P13	30.00	2.019	16.98
ATR PIV C4 P7	40.00	8.214	18.69
ATR PIV C5 P8	50.00	3.009	7.12
ATR PIV C6 P9	50.00	7.066	10.11
ATR PIV C12 P15	50.00	8.761	9.87
Gravelines N06	48.00	4.210	3.50
Gravelines N12	57.00	4.860	4.48
Gravelines P16	53.00	2.580	1.21
IFA-629.1	29.00	21.700	19.13
IFA-606 Phase 2	49.00	12.000	17.00
IFA 633.1r6	32.00	6.000	12.66
M504 H8	37.50	0.540	0.26
M504 I2	43.00	0.850	0.75
M504 K9	42.50	0.850	0.65
M504 M9	44.20	2.260	0.82
IFA-597.4/.5/.6/.7r10	35.70	17.000	13.17
IFA-597.4/.5/.6/.7r11	36.80	14.000	20.95
IFA-629.3r5	68.30	21.000	6.28
IFA-629.3r6	63.60	12.000	5.73
E09 Rods Inner	29.60	0.200	5.66

Table 4-2. Steady-state MOX FGR assessment cases (continued)

Rod	Rod-Average Burnup [GWd/MTU]	Measured FGR [%]	FAST-1.0.1 Predicted FGR [%]
E09 Rods Inner	29.60	0.400	5.66
E09 Rods Intermediate	39.30	21.000	19.05
E09 Rods Intermediate	39.30	21.000	19.05
E09 Rods Outer	42.00	19.500	17.86
E09 Rods Outer	42.00	18.200	17.86
E09 Rods Outer	42.00	19.500	17.86
E09 Rods Outer	42.00	18.900	17.86
E09 Rods Outer	42.00	19.600	17.86
M308 Segment 2	57.50	5.000	4.24

* End-of-Life FGR estimated from rod pressure data (larger error than data from puncture)

4.1.3 UO_2-Gd_2O_3 Steady-State FGR Predictions

The four steady-state UO_2-Gd_2O_3 cases with measured and predicted FGRs are shown in Table 4-3. The standard deviation for these four predictions is 0.3% absolute FGR. Based on this comparison, it appears that the modified Massih model employed by FAST to describe FGR for UO_2 fuels can provide reasonable predictions for FGR from UO_2-Gd_2O_3 fuel. It is noted that the burnup range is limited (34-40 [GWd/MTU]) and the gas release values are small. Therefore, it cannot be fully confirmed that this conclusion will hold for high burnup. However, this observation is consistent with previous studies conducted by [Delorme et al., 2012] and [Arana et al., 2012]. Delorme studied an irradiated M5^{TM}-clad fuel rod containing UO_2 doped with 8 wt% Gd. The rod average burnup was 39.2 [GWd/MTU] and exhibited 0.51% FGR. Although an enhanced high burnup structure was observed and attributed to the chemical effect of Gd additions, the FGR data was consistent with UO_2 rods irradiated to similar levels of burnup, although the measured FGR values are very low. Arana characterized the FGR from fuel rods subjected to high duty conditions in Vadenllos II as part of a High Burnup Program (PAQ). Gd-doped rods containing 2 and 8 wt% Gd were irradiated to ~50 and 55 [MWd/kgU] under high power and high burnup conditions, respectively. The FGR data from these rods were consistent with the FGR data measured from UO_2 pellets under similar power levels.

Table 4-3. Steady-State UO_2-Gd_2O_3 FGR Assessment Cases

Rod	Rod-Average Burnup [GWd/MTU]	Measured FGR [%]	FAST-1.0.1 Predicted FGR [%]
GAIN 301	38.8	0.23	0.53

Table 4-3. Steady-State UO_2-Gd_2O_3 FGR Assessment Cases (continued)

Rod	Rod-Average Burnup [GWd/MTU]	Measured FGR [%]	FAST-1.0.1 Predicted FGR [%]
GAIN 302	37.9	0.19	0.37
GAIN 701	38.9	0.98	0.71
GAIN 701	38.9	0.66	0.30

4.2 Assessment of Power-Ramped FGR Predictions

4.2.1 UO_2 Power-Ramped FGR Predictions

Figure 4-5 shows the predicted FGR as a function of measured FGR for the power-ramped UO_2 rods.

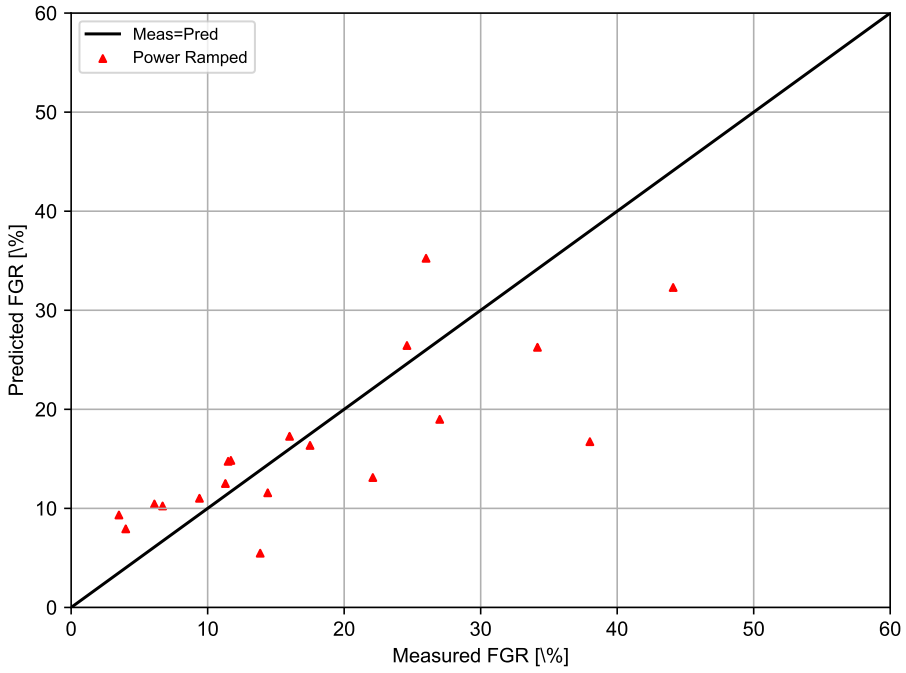

Figure 4-5. Comparison of FAST predictions to measured FGR data for the UO_2 power-ramped assessment cases

Figure 4-6 shows the predicted minus measured FGR as a function of burnup for the power-ramped UO_2 rods.

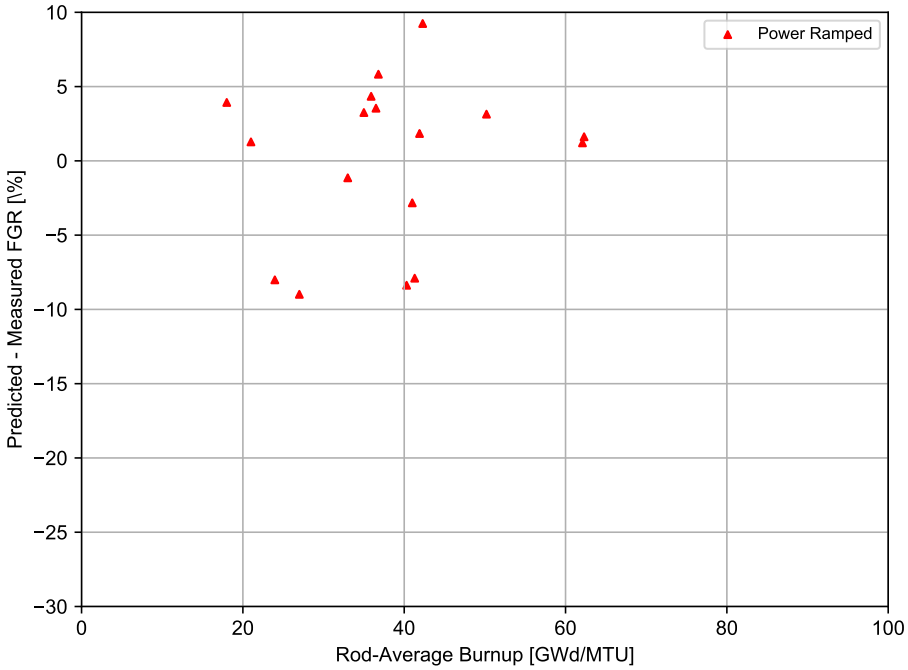

Figure 4-6. Predicted minus measured FGR Versus rod-average burnup for the UO_2 power-ramped assessment cases

The power-ramped UO_2 cases with measured and predicted FGRs are shown in Table 4-4. These comparisons show that the code provides a good prediction of the transient FGR data except for the two High Burnup Effects Program (HBEP) rods, D200 and D226, which are underpredicted by 21% and 12% release, respectively. The fuel in both of these rods is considered atypical of today's fuel used in commercial rods because it is prone to significant fuel densification ($>$ 2.5% theoretical density (TD)), unlike the less densification prone (stable) fuel ($<$ 1.5% TD) of current fuel designs. In addition, there is evidence that fuel with significant densification releases more fission gas than current stable fuel. The standard deviation for the power-ramped predictions without D200 and D226 is 5.4% absolute FGR. These figures demonstrate that FAST provides a best-estimate calculation of fission gas over a wide range of gas release levels up to a rod-average burnup of 62 [GWd/MTU].

Table 4-4. Power-ramped UO_2 FGR assessment cases

Rod	Rod-Average Burnup [GWd/MTU]	Measured FGR [%]	FAST-1.0.1 Predicted FGR [%]
HBEP D200	25.00	38.00	16.23
HBEP D226	44.00	44.10	31.62
pk6-2	36.80	3.50	9.19
pk6-3	36.50	6.70	10.11
pk6-S	35.90	6.10	10.15
Inter Ramp Rod 16	21.00	16.00	14.84

Table 4-4. Power-ramped UO_2 FGR assessment cases (continued)

Rod	Rod-Average Burnup [GWd/MTU]	Measured FGR [%]	FAST-1.0.1 Predicted FGR [%]
Inter Ramp Rod 18	18.00	4.00	6.48
RISØ f14-6.in	27.00	22.10	13.97
RISØ f7-3.in	35.00	11.50	13.88
RISØ f9-3.in	33.00	17.50	17.24
RISØ ge2	41.90	24.60	25.64
RISØ ge4	23.96	27.00	18.31
RISØ ge6	42.29	26.00	33.64
RISØ ge7	41.00	14.40	10.88
B&W Studsvik R1	62.30	9.40	11.83
B&W Studsvik R3	62.10	11.30	13.16
RISØ AN1	41.30	34.16	25.54
RISØ AN8	40.30	13.85	5.47
regate	50.20	11.70	11.35

Normal operational transients typically last between 4 and 12 hours, while AOO power transients last less than 30 minutes. Because both of these types of transients can lead to FGR, the NRC requires that both be included in the rod internal pressure analyses to demonstrate that they meet the no cladding liftoff criterion for establishing a rod pressure limit. In general, the short hold time AOO transient results in the lower FGR. However, the burst release typically seen in transients on the order of less than 30 minutes appears to be increasing with increasing burnups, particularly above 62 [GWd/MTU], such that the code may be underpredicting release for short time period transients at high burnup. Therefore, future code verification will examine FGR data with power ramps of short duration.

4.2.2 MOX Power-Ramped FGR Predictions

Figure 4-7 shows the predicted FGR as a function of measured FGR for the power-ramped MOX rods.

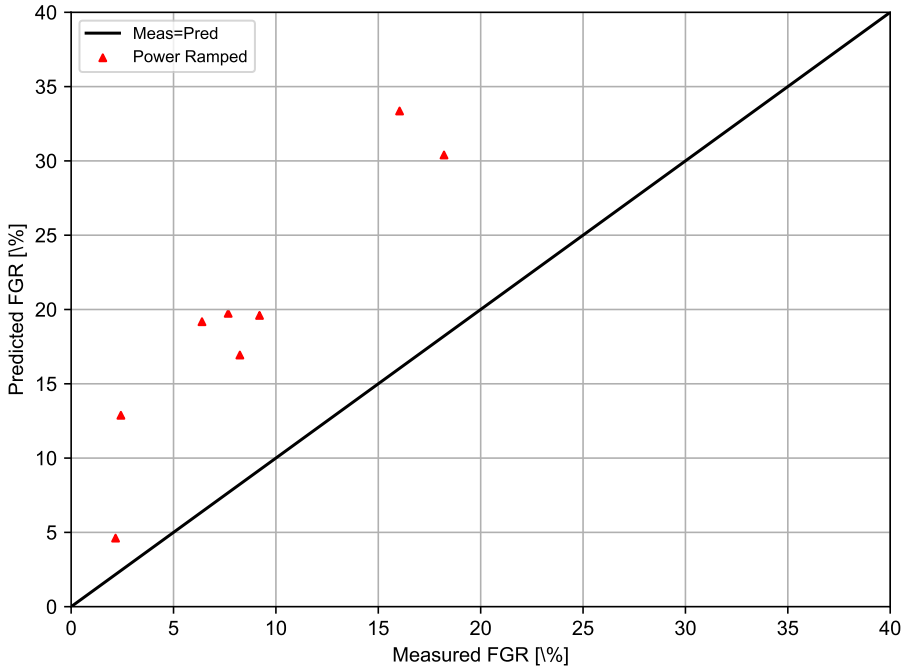

Figure 4-7. Comparison of FAST predictions to measured FGR data for the MOX power-ramped assessment cases

Figure 4-8 shows the predicted minus measured FGR as a function of burnup for the power-ramped MOX rods.

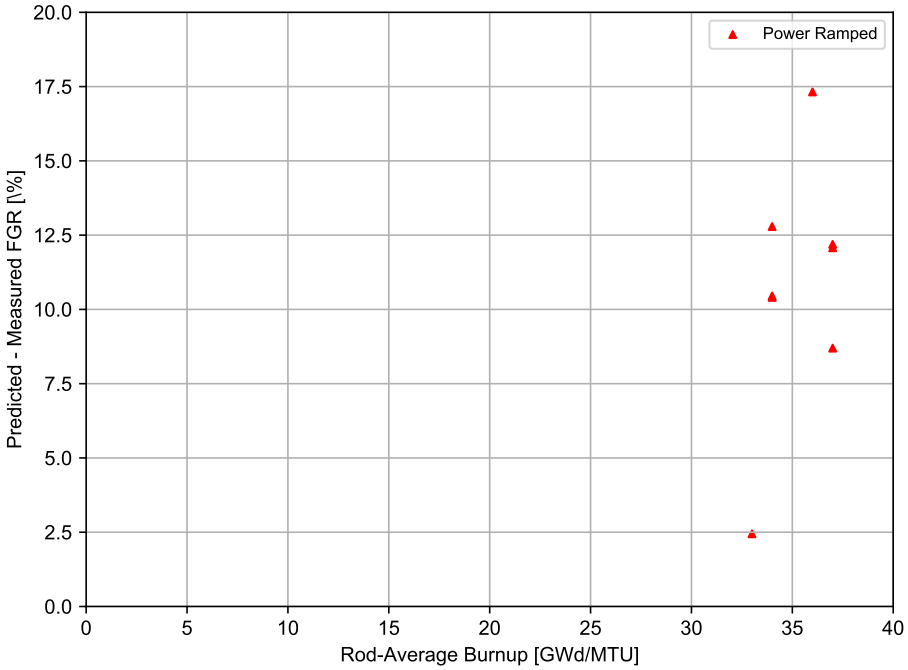

Figure 4-8. Predicted minus measured FGR Versus rod-average burnup for the MOX power-ramped assessment cases

The power-ramped MOX cases with measured and predicted FGRs are shown in Table 4-5. The standard deviation for the steady-state predictions is 11.6% absolute FGR and the average deviation (bias) is 10.3% absolute FGR. These figures demonstrate that FAST tends to overpredict the gas release measurement for power-ramped MOX rods. However, it is noted that a limited number of power-ramped rods from only one experimental program are represented here. In addition, it is conservative to overpredict FGR during a power ramp.

Table 4-5. Power-ramped MOX FGR assessment cases

Rod	**Rrod-average burnup** [GWd/MTU]	**Measured FGR** [%]	**FAST-1.0.1 Predicted FGR** [%]
M501 HR-1	37	7.67	19.55
M501 HR-2	37	8.24	16.92
M501 HR-3	37	18.21	29.87
M501 HR-4	36	16.04	31.63
M501 MR-1	34	2.43	12.32
M501 MR-2	34	9.20	19.40
M501 MR-3	34	6.39	18.43
M501 MR-4	33	2.17	5.00

This page intentionally blank.

5.0 Internal Rod Void Volume Assessment

5.1 Fuel Rod Void Volume

An accurate prediction of the internal void volume of a fuel rod is important in the calculation of the internal rod pressures along with the FGR prediction. The change in the fuel rod void volume with burnup is primarily due to the combined effects of cladding creep, fuel swelling, and axial cladding growth. Nine well characterized fuel rods were selected to assess the capability of FAST to accurately calculate fuel rod void volumes for high burnup. The cases selected include eight full-length rods (rod TSQ002 from ANO-2, rod 15309 from Oconee and rods 2AH3-D15, 2AH3-D12, 0AH5-E14, 07R2D5, AL06-D6, and AD23-D5 from Ringhals 2 and 3) and three short (44 [in] long) rods (36-I-8, 111-I-5, and 24-I-6) that were irradiated in the BR-3 reactor. The Ringhals 3 rods were clad in Optimized ZIRLO™; the Ringhals 2 rods were clad in M5™; the remaining rods were clad with standard Zircaloy-4. All are PWR rods. The burnup levels achieved on these rods range from 33.3 to 62.95 [GWd/MTU]. It would be desirable to include more commercial fuel rods in this assessment, but to date no more fuel rods with reported power histories and measured void volumes have been found.

Table 5-1 presents the measured and FAST-calculated void volume at both BOL and EOL for the eleven fuel rods. The calculations were made at 25 [°C] (77 [°F]) and atmospheric pressure, which should be reasonably close to the temperature at which the data were collected. A range of values for void volume is provided for Oconee rod 15309 because this is the range of void volumes measured from 16 sibling fuel rods from the same assembly–including the representative rod 15309. All 16 rods have very similar EOL burnups and similar power histories. Therefore, the void volume range includes representative uncertainty in the fabricated void volumes, measured rod power histories, and burnup.

Table 5-1. Measured and calculated void volume for eleven high burnup fuels rods

Reactor	Rod	Burnup [GWd/MTU]	BOL Measured [in^3]	BOL Calculated [in^3]	EOL Measured [in^3]	EOL Calculated [in^3]
BR-3	36-I-8	61.5	NA	0.6395	0.5080	0.656
BR-3	111-I-5	48.6	NA	0.6420	0.5160	0.583
BR-3	24-I-6	60.1	NA	0.6401	0.4910	0.594
ANO-2	TSQ002	53.0	1.55	1.5278	1.0876	1.126
Oconee	15309	49.5 to 49.9	2.14	2.1190	1.600 - 1.700	1.546
Ringhals 3	2AH3-D15	34.1	NA	1.2283	0.9460	0.917
Ringhals 3	2AH3-D12	33.3	NA	1.2763	0.9460	0.943
Ringhals 3	0AH5-E14	57.82	NA	1.2826	0.7930	0.960
Ringhals 2	07R2D5	62.0	NA	1.6913	1.0800	1.240
Ringhals 2	AL06-D6	27.97	NA	1.4867	1.2200	1.180
Ringhals 2	AD23-D5	62.95	NA	1.4440	1.0800	0.988

FAST does a good job of calculating the integral fuel rod void volumes, particularly for the commercial reactor rods where as-fabricated void volumes were provided. The three BR-3 test rods are overpredicted by about 20 % on average, but this may be due to an overestimation in the as-fabricated void volumes.

6.0 Cladding Corrosion Assessment

Seven well characterized fuel rods were selected to demonstrate the capability of FAST to accurately calculate fuel rod waterside oxidation for high burnup. The cases selected include seven full-length rods (rod TSQ002 from ANO-2; rod 15309 from Oconee; rod A1 from bundle MTB99; rod H8/36-6 from TVO-1; and rods A06, A12, and N05 from Vandellos II). The set includes both PWR and BWR fuel rods that are standard Zircaloy-4, ZIRLO®, or M5™ in PWRs and Zircaloy-2 in BWRs. (These are the cladding alloys currently modeled in FAST.) The rod-average burnup levels achieved on these rods range from 45 to 53 $[\mathrm{GWd/MTU}]$. The corrosion and hydrogen pickup models in FAST have been compared to significantly more separate effects data [Geelhood and Beyer, 2008] [Geelhood and Beyer, 2011] to demonstrate good predictions, but these cases are those with reported power histories and end-of-life measured oxide thickness.

FAST calculated peak oxide layer thicknesses are bracketed by the choice of crud layer thickness for the PWR rods and are in good agreement for the two BWR rods. The purpose of these code-data comparisons is to demonstrate similar predictions as with standalone versions of the corrosion/hydriding models. The BWR peak corrosion values are fairly well matched by the FAST predictions, and these predictions are not as sensitive to the crud layer input because of the relatively lower heat fluxes and lower operating temperatures.

The conclusion is that the modeling of waterside oxidation is sufficient in FAST for best-estimate analyses. Using integral effect and separate effect data the following standard deviations for each alloy has been calculated or estimated as shown in [Geelhood and Beyer, 2008].

- Zircaloy-2: $\sigma = 7.6\,[\mu\mathrm{m}]$
- Zircaloy-4: $\sigma = 15.3\,[\mu\mathrm{m}]$
- ZIRLO®: $\sigma = 15\,[\mu\mathrm{m}]$
- M5™: $\sigma = 5\,[\mu\mathrm{m}]$

6.1 BWR Cladding Corrosion

The only alloy currently used in the United States for BWR conditions is Zircaloy-2. The following assessment shows the FAST predictions of cladding corrosion for two commercial rods with Zircaloy-2.

6.1.1 Zircaloy-2 Corrosion

Table 6-1 shows the measured and FAST calculated peak oxide layer thickness for the two selected high burnup BWR rods.

Table 6-1. Peak oxide measured and calculated for two high burnup BWR fuel rods

Reactor	Rod	Burnup [GWd/MTU]	Measured [μm]	Calculated [μm]
Monticello	MTB99 rod A1	45.0	25	29
TVO-1	H8/36-6	51.4	28	22

These comparisons indicate satisfactory capability of FAST to predict peak cladding waterside oxidation under BWR conditions.

6.2 PWR Cladding Corrosion

The alloys currently used in the United States for PWR conditions are Zircaloy-4, ZIRLO®, Optimized ZIRLO™ and M5™. The following assessment shows the FAST predictions of cladding corrosion for two commercial rods with Zircaloy-4, two commercial rods with ZIRLO®, and one commercial rod with M5™.

6.2.1 Zircaloy-4 Corrosion

Figures 6-1 and 6-2 show the measured and predicted corrosion layer thicknesses as a function of axial position along the rod for the two PWR rods with Zircaloy-4 cladding.

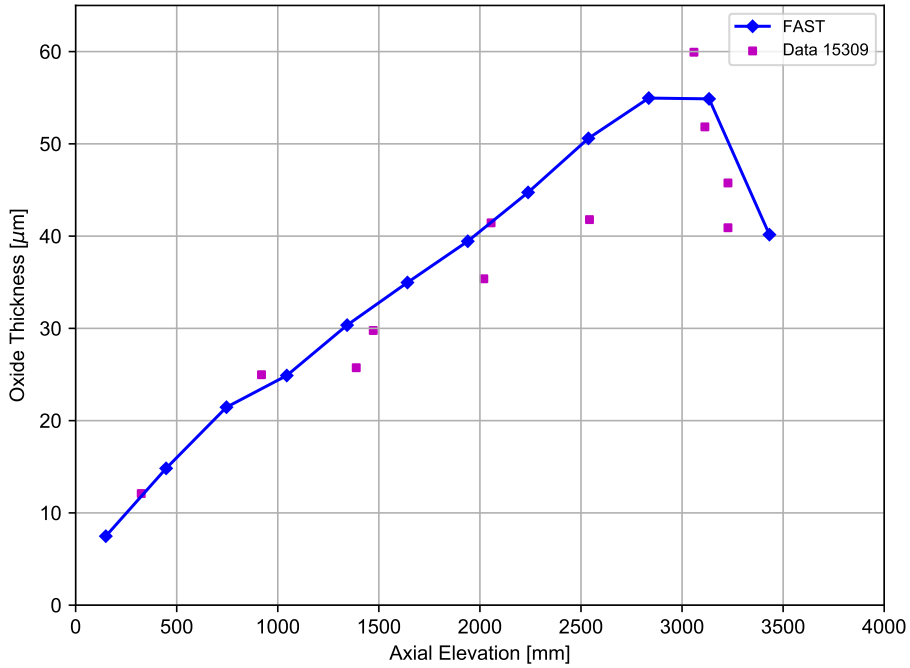

Figure 6-1. Measured and predicted corrosion layer thickness as a function of axial position for Oconee 5-cycle PWR Zircaloy-4 Rod 15309, 49.5 [GWd/MTU] (rod-average)

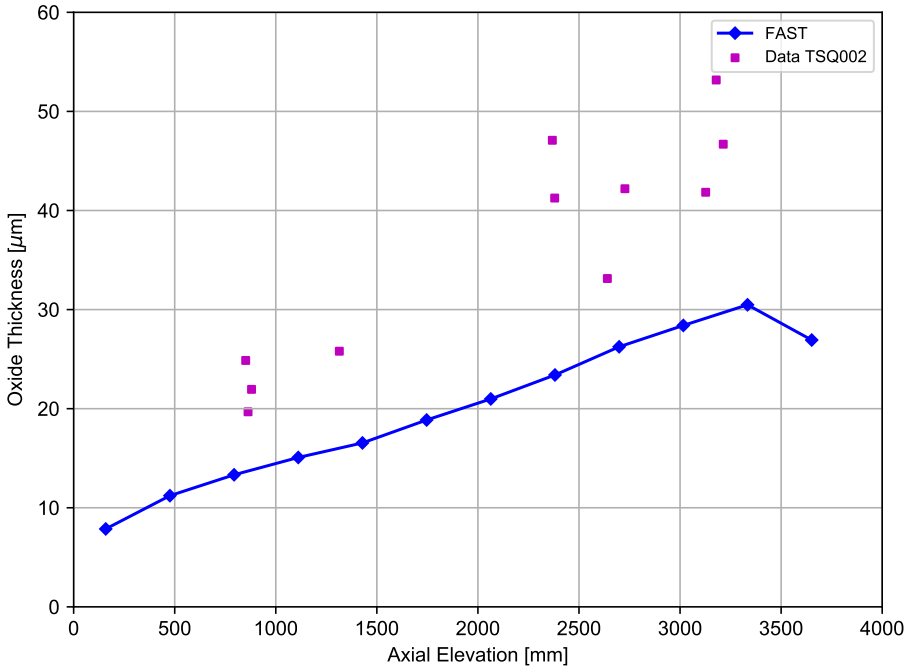

Figure 6-2. Measured and predicted corrosion layer thickness as a function of axial position for ANO-2 5-cycle PWR Zircaloy-4 Rod TSQ002, 53 [GWd/MTU] (rod-average)

These comparisons indicate satisfactory capability of FAST to predict peak cladding waterside oxidation of Zircaloy-4 under PWR conditions.

6.2.2 ZIRLO® Corrosion

Figures 6-3 and 6-4 show the measured and predicted corrosion layer thicknesses as a function of axial position along the rod for the two PWR rods with ZIRLO® cladding.

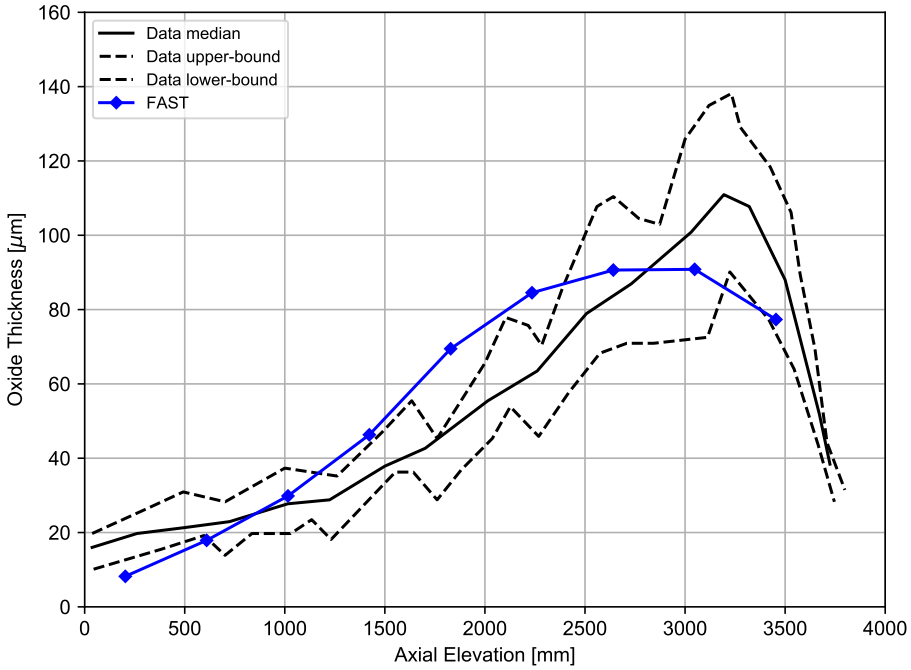

Figure 6-3. Measured and predicted corrosion layer thickness as a function of axial position for Gravelines 5-Cycle PWR ZIRLO® Rod A06, 65.9 [GWd/MTU] (rod-average)

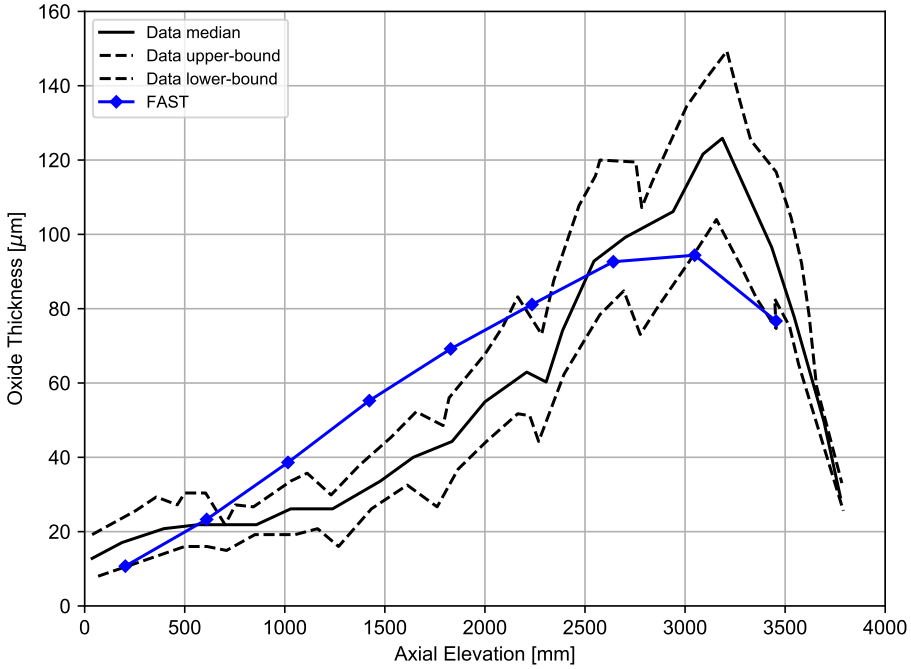

Figure 6-4. Measured and predicted corrosion layer thickness as a function of axial position for Gravelines 5-Cycle PWR ZIRLO® Rod A12, 66.4 [GWd/MTU] (rod-average)

These comparisons indicate satisfactory capability of FAST to predict peak cladding waterside

oxidation of ZIRLO® under PWR conditions.

6.2.3 M5™ Corrosion

Figure 6-5 shows the measured and predicted corrosion layer thicknesses as a function of axial position along the rod for the PWR rod with M5™ cladding.

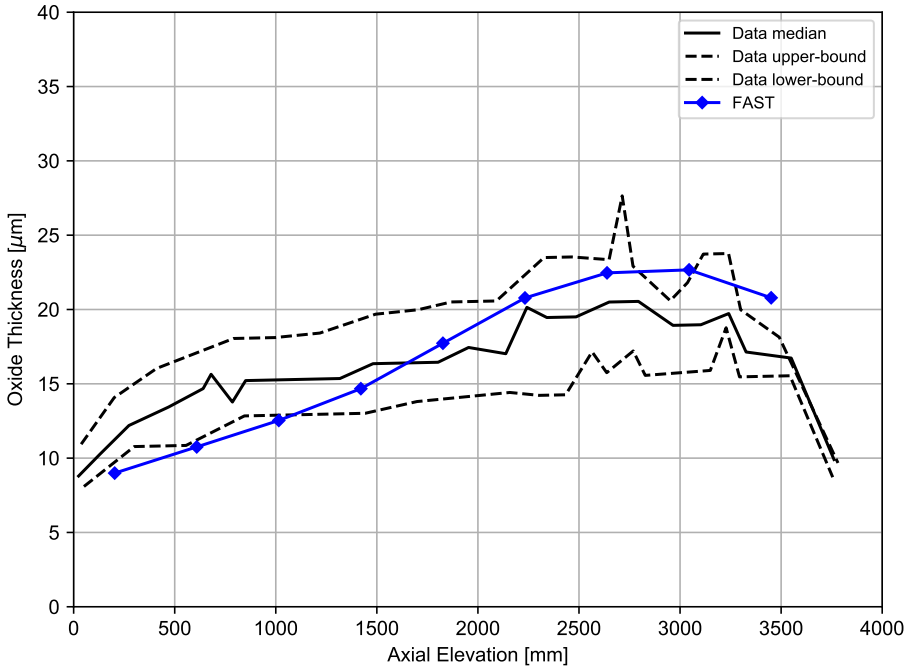

Figure 6-5. Measured and predicted corrosion layer thickness as a function of axial position for Gravelines 5-Cycle PWR M5™ Rod N05, 68.1 [GWd/MTU] (rod-average)

This comparison indicates satisfactory capability of FAST to predict peak cladding waterside oxidation of M5™ under PWR conditions.

This page intentionally blank.

7.0 Cladding Hoop Strain During Power Ramps

7.1 Assessment Cases

The ability of FAST to predict permanent hoop strain during power ramps was originally assessed against a database consisting of 29 power-ramped rods at burnup levels between 18 and 76 [GWd/MTU] to ramp terminal levels between 30 and 52 [kW/m]. Some of these rods were held at the ramp terminal level for a significant period of time ($>$ 4 [h]) while others were held for a very short period of time (between 1 and 30 [s]). The measured and predicted rod-average permanent hoop strains are shown in Figures 7-1 and 7-2. These figures show that in general FAST overpredicts the measured hoop strain. It was found that FAST overpredicts cladding permanent strain by 0.11% (on average) with significant variation between predicted and measured.

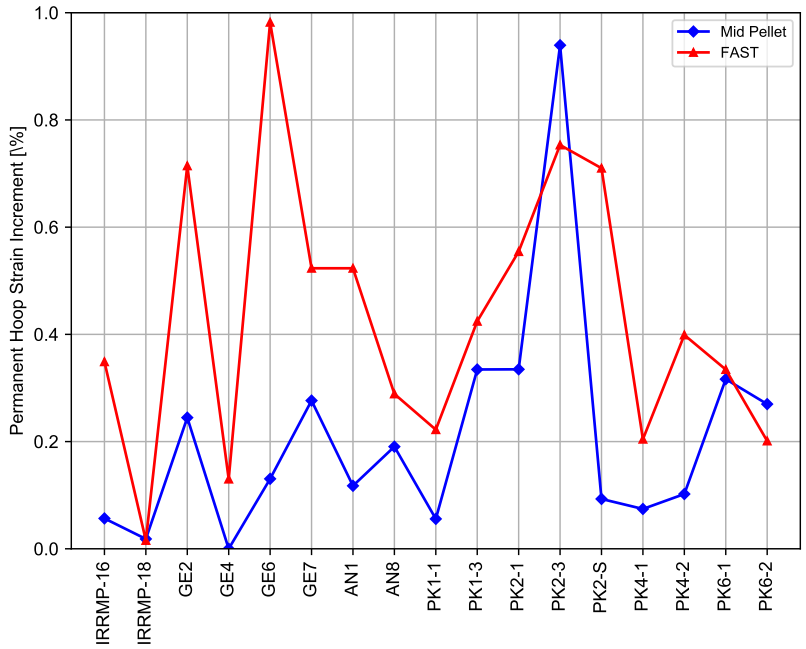

Figure 7-1. Measured and predicted rod-average permanent hoop strain for first half of the assessment database

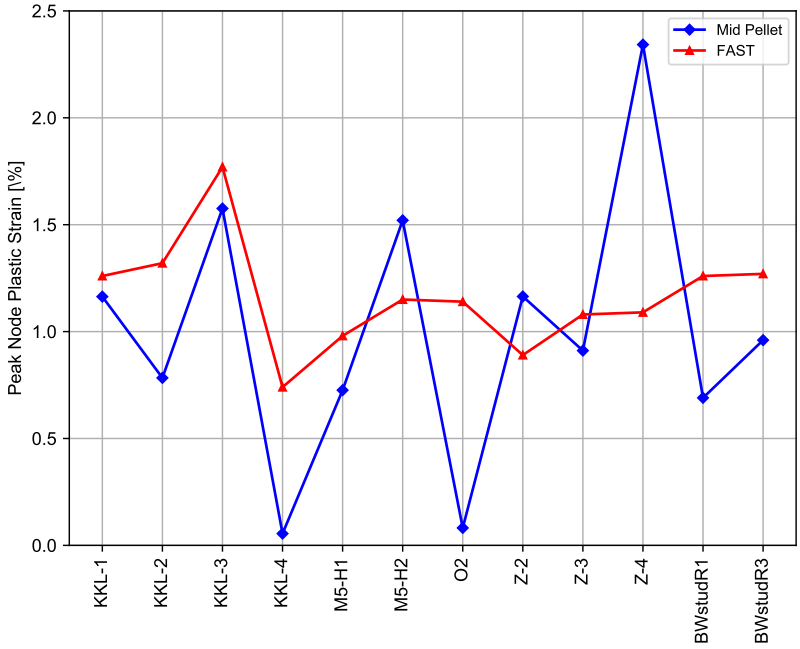

Figure 7-2. Measured and predicted peak node permanent hoop strain for second half of the assessment database

This overprediction is consistent with the fact that FAST uses a rigid pellet assumption. This means that the pellet is assumed to be significantly stronger than the cladding such that it will not deform, other than the code-assumed accommodation of 50% of the relocation, when it comes in contact with the cladding.

7.2 Comparisons vs. Ramp Terminal Level

Figure 7-3 shows the predicted minus measured permanent hoop strain for all the assessment cases as a function of ramp terminal power level. There does not appear to be any bias in the predictions with increase ramp terminal power level. However, it does appear that the ramps with short hold times are all overpredicted more than the SCIP ramps with long hold times.

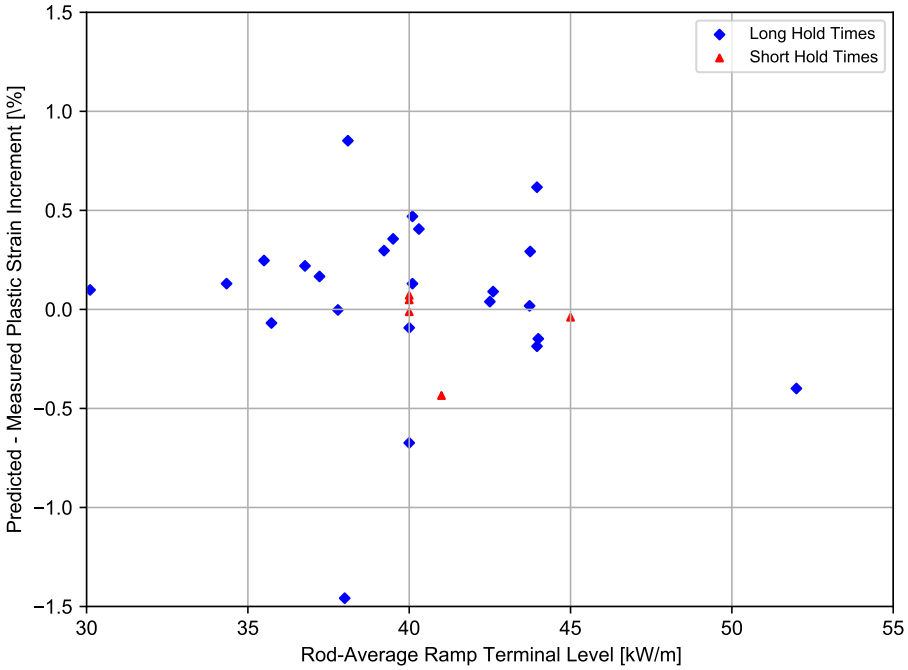

Figure 7-3. Predicted minus measured permanent hoop strain as a function of ramp terminal power level

7.3 Comparisons vs. Burnup

Figure 7-4 shows the predicted minus measured permanent hoop strain for all the assessment cases as a function of burnup. FAST generally provides a good prediction or slight over-prediction of permanent hoop strain up to 76 [GWd/MTU].

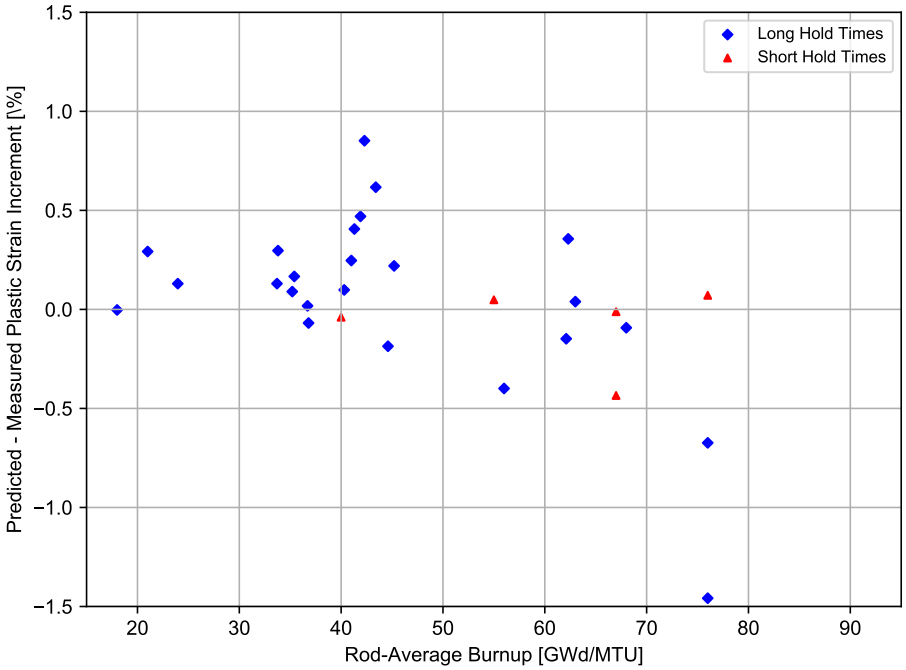

Figure 7-4. Predicted minus measured permanent hoop strain as a function of burnup

The FAST predictions for the ramp test data appear to be predicted well up to 62 [GWd/MTU]. There is more scatter in the predictions for power ramps above 62 [GWd/MTU] but other than one ramp test that is significantly underpredicted they also seem to be predicted well.

8.0 Conclusions

The FAST steady-state fuel performance code has been assessed against a set of pre-selected data from 137 well characterized fuel rods. The data used for the assessment consisted of measurements of thermal (fuel temperature), FGR, rod internal void volume, and cladding corrosion. The fuel rods represent a range of design parameters, including different fuel rod diameters, lengths, gap sizes, and fill-gas compositions and a wide range of operating conditions with peak LHGRs varying from 8 to 18 [kW/ft], rod-average burnups from 0 to 99 [GWd/MTU], and FGRs ranging from less than 1% to greater than 50% . The estimates of code thermal and FGR predictive error are based on code comparisons to both the benchmark and independent data sets.

- Thermal: Comparisons were made for BOL UO_2 temperature measurements and UO_2, MOX, and UO_2-Gd_2O_3 temperature measurements as a function of burnup. For the UO_2 BOL temperature measurements, the FAST predictions were within a standard error of 4.6% of measured values and no average bias. For the UO_2 temperature measurements as a function of burnup, the FAST predictions were within a standard error of 4.7% of the measured values. Only IFA-677 rod 2 was underpredicted by up to 150 [K] (11% relative) at BOL. For the MOX temperature measurements as a function of burnup, the FAST predictions were within a standard error of 4.8% of the measured values and much closer in most cases. Only IFA-633.1 was overpredicted by up to 150 [K] (13% relative) at EOL. This overprediction may be due to the code overpredicting the FGR leading to higher fuel ratures. For the UO_2-Gd_2O_3 temperature measurements as a function of burnup, the FAST predictions were within a standard error of 4.8% of the measured values and much closer in most cases.

  Typically, a standard error of 3 to 4% is the uncertainty in temperature due to power level uncertainty.

  Overall, FAST gives reasonable predictions (standard error of less than 5%) of fuel centerline temperature for fuel rods with UO_2, MOX, and UO_2-Gd_2O_3 fuel.

- Fission Gas Release: Comparisons were made for the UO_2, MOX, and UO_2-Gd_2O_3 FGR measurements for rods with widely varying power levels and burnups. The UO_2 FGR model was assessed for steady-state conditions and power-ramped rods. For the UO_2 cases, a standard deviation of 2.6% FGR (absolute) was calculated for the steady-state rods and a standard deviation of 5.4% FGR (absolute) was calculated for the power-ramped rods when two rods with non-prototypical pellets were removed. These standard deviations are considered reasonable. Although there is little data above 62 [GWd/MTU], it appears that FAST may underpredict UO_2 fuel above this burnup level.

  For the MOX cases, a standard deviation of 4.4% FGR (absolute) was calculated for the steady-state rods when the ATR rods with large power uncertainty were removed, and a standard deviation of 11.6% FGR (absolute) was calculated for the limited number of power-ramped rods that all came from one experimental program. The steady-state standard deviation is considered reasonable. The power-ramped rods were all overpredicted, which is conservative for rod internal pressure and temperature calculations. However, a larger database of MOX power-ramped cases is needed to further assess if this overprediction is due to a code deficiency. Although there is little data above 62 [GWd/MTU], it appears that FAST may underpredict MOX fuel above this burnup level.

A limited assessment of UO_2-Gd_2O_3 data showed good agreement between measurements and predictions using the UO_2 FGR model in FAST. Based on these comparisons and observations by other researchers it was concluded that the FGR from these rods should be conservatively bounded with the UO_2 FGR model.

Overall, FAST gives reasonable predictions (within 5% FGR absolute) of fuel centerline temperature for fuel rods with UO_2, MOX, and UO_2-Gd_2O_3 fuel.

- Internal Void Volume: Comparisons were made to data from four commercial reactor and three test reactor fuel rods. The code predicted the two commercial rods well but overpredicted the BR□3 test rod data by approximately 25% (relative) on average.

- Cladding Corrosion: Comparisons were made to data from two commercial BWR rods with Zircaloy-2 cladding, two commercial PWR rods with Zircaloy-4 cladding, two commercial PWR rods with ZIRLO® cladding, and one commercial PWR rod with M5™ cladding. The oxide corrosion predictions were very good and tend to bracket the data. Using integral effect and separate effect data, the following standard deviations for each alloy have been calculated or estimated.
  - Zircaloy-2: $\sigma = 7.6\,[\mu\text{m}]$
  - Zircaloy-4: $\sigma = 15.3\,[\mu\text{m}]$
  - ZIRLO®: $\sigma = 15\,[\mu\text{m}]$
  - M5™: $\sigma = 5\,[\mu\text{m}]$

- Cladding Hoop Strain: The original hoop strain assessment cases that were available up to a burnup of around 45 $[\text{GWd}/\text{MTU}]$ demonstrated that, on average, FAST slightly overpredicts cladding hoop strain by 0.1% strain. FAST overpredicted all the short hold times cases. Despite this overprediction, FAST provides reasonable hoop strain predictions up to 62 $[\text{GWd}/\text{MTU}]$.

9.0 References

[Arana et al., 2012] Arana I, C Munoz-Reja, and F Culbebras. 2012. "Post-Irradiation Examination of High Burnup Fuel Rods from Vandellos II." In TopFuel Reactor Fuel Performance. Manchester, United Kingdom. European Nuclear Society.

[Bagger et al., 1978] Bagger C, H Carlson, and P Knudsen. 1978. Details of Design Irradiation and fission Gas Release for the Danish UO2-Zr Irradiation Test 022. RISØ-M-2152, Risø National Laboratory, Roskilde, Denmark.

[Balfour, 1982] Balfour M. 1982. BR-3 High Burnup Fuel Rod Hot Cell Program, Final Report, Vol. 1. WCAP-10238, D0E/ET/34073-1, Westinghouse Electric Corporation, Pittsburgh, PA.

[Balfour et al., 1982] Balfour M, W Chubb, and R Boyle. 1982. BR-3 High Burnup Fuel Rod Hot Cell Program Vol. 2: Data Summary. WCAP-10238, DOE/ET/34073-2, Westinghouse Electric Corporation, Pittsburgh, PA.

[Barner et al., 1990] Barner J, M Cunningham, M Freshley, and D Lanning. 1990. High Burn up Effects Program Summary Report. DOE/NE/3406-1, HBEP-61, Battelle, Pacific Northwest Laboratories, Richland, WA.

[Baumgartner, 1984] Baumgartner J. 1984. BWR Fuel Bundle Extended Burnup Program Technical Progress Report, January 1983 to December 1983. DOE/ET/34031-17, GEAP-30643, General Electric Company, San Jose, CA.

[Beguin, 1999] Beguin S. 1999. The Lift-Off Experiment with MOX Fuel Rod in IFA-610.2 Initial Results. HWR-603, OECD Halden Reactor Project, Halden, Norway.

[Blair and Wright, 2004] Blair P and J Wright. 2004. The IFM/MOX Comparative Test, IFA-651.1: Results after Four Cycles of Irradiation. HWR-763, OECD Halden Reactor Project, Halden, Norway.

[Boulanger et al., 2004] Boulanger D, M Lippens, L Mertens, J Basselier, and B Lance. 2004. "High Burnup PWR and BWR MOX Fuel Performance: A Review of BELGONUCLEAIRE Recent Experimental Programs." In International Meeting on LWR Fuel Performance. Orlando, FL. American Nuclear Society.

[Bradley et al., 1981] Bradley E, M Cunningham, D Lanning, and R Williford. 1981. Data Report for the Instrumented Fuel Assembly IFA-513. NUREG/CR-1838, PNL-3637, Pacific Northwest Laboratory, Richland, WA.

[Chantoin et al., 1997] Chantoin P, E Sartori, and J Turnbull. 1997. "The Compilation of a Public Domain Database on Nuclear Fuel Performance for the Purpose of Code Development and Validation." In International Topical Meeting on LWR Fuel Performance, pp. 515–522. Portland, OR. Americal Nuclear Society.

[Claudel and Huet, 2001] Claudel J and F Huet. 2001. Results from the Burnup Accumulation Test with High Exposure (63 MWd/kgHM) Model Fuel (IFA-648). HWR-651, OECD Halden Reactor Project, Halden, Norway.

[Cook et al., 2003] Cook P, B Christiansen, G Dassel, E Matthews, I Robinson, R Stratton, C Walker, and R Weston. 2003. "Performance of BNFL MOX Fuel." In TopFuel 2003 Conference. Würzburg, Germany. Kerntechnische Gesellschaft e.V.

[Cook et al., 2004] Cook P, E Matthews, M Barker, R Foster, A Donaldson, C Ott, D Papaioannou, and C Walker. 2004. "Post-Irradiation Examination and Testing of BNFL SBR MOX Fuel." In International Meeting on LWR Fuel Performance. Orlando, FL. American Nuclear Society.

[Cook et al., 2000] Cook P, R Stratton, and C Walker. 2000. "Post Irradation Examination of BNFL MOX Fuel." In International Topical Meeting on Light Water Reactor Fuel Performance. Park City, UT. American Nuclear Society.

[CSN and ENUSA, 2002] CSN and ENUSA. 2002. Characteristics of the ENUSA Rods Irradiated in the Vandellos II Reactor up to 68 GWd/t and Planned to be Used in the CABRI International Programme. CABRI International Programme. CABRI Water Loop, 2002/34.

[de Meulemeester et al., 1973] de Meulemeester E, N Hoppe, G de Contenson, and M Watteau. 1973. "Review of Work Carried out by BELGONUCLEAIRE and CEA on the Improvement and Verification of the COMETHE Computer Code with the Aid of In-Pile Experimental Results." In BNES International Conference on Nuclear Fuel Performance, number ECS-EEC-73-595. London, United Kingdom.

[Delorme et al., 2012] Delorme R, C Valot, L Fayaette, I Pujol X.and Aubrun, J Lamontagne, , T Blay, , B Pasquet, P Bienvenu, I Roure, C Pozo, G Carlot, C Sabathier, P Martin, G Trillon, V Auret, and S Bouffard. 2012. "Study of Fission Gas Behaviour and Fuel Restructuration in Irradited (U,Gd)O_2 Fuel." In TopFuel Reactor Fuel Performance. Manchester, United Kingdom. European Nuclear Society.

[Djurle, 1985] Djurle S. 1985. Final Report of the Super-Ramp Project. DOE/ET/34032-1, U.S. Department of Energy, Washington, D.C.

[Forsberg and Massih, 1985] Forsberg K and A Massih. 1985. "Diffusion theory of fission gas migration in irradiated nuclear fuel UO_2." Journal of Nuclear Materials 135(2–3):140–148.

[Fujii and Claudel, 2001] Fujii H and J Claudel. 2001. The Lift-Off Experiments, IFA-610.3 (UO_2), and IFA-610.4 (MOX) Evaluation of In-Pile Measurement Data. HWR-650, OECD Halden Reactor Project, Halden, Norway.

[Geelhood and Beyer, 2008] Geelhood K and C Beyer. 2008. "Corrosion and Hydrogen Pickup Modeling in Zirconium Based Alloys." In Water Reactor Fuel Performance Meeting. Seoul, Korea. Korean Nuclear Society.

[Geelhood and Beyer, 2011] Geelhood K and C Beyer. 2011. "Hydrogen Pickup Models for Zircaloy-2, Zircaloy-4, M5™, and ZIRLO™." In Water Reactor Fuel Performance Meeting. Chengdu, China.

[Geelhood et al., 2021a] Geelhood K, W Luscher, L Kyriazidis, C Goodson, and J Corson. 2021a. MatLib-1.0: Nuclear Material Properties Library. PNNL-31158, Pacific Northwest National Laboratory, Richland, WA.

[Geelhood et al., 2021b] Geelhood K, D Richmond, D Colameco, W Luscher, L Kyriazidis, C Goodson, and J Corson. 2021b. FAST-1.0.1: A Computer Code for Thermal-Mechanical Nuclear Fuel Analysis under Steady-state and Transients. PNNL-31160, Pacific Northwest National Laboratory, Richland, WA.

[Hirai et al., 1995] Hirai M, J Davies, and R Williamson. 1995. "Diffusivities of fission gas species in UO_2 and $(U,Gd)O_2$ nuclear fuels during irradiation." Journal of Nuclear Materials 226(1–2):238–251.

[Hodge et al., 2003] Hodge S, L Ott, and F Griffin. 2003. Implications of the PIE Results for the 40-Gwd/MT-Withdrawal Mox Capsules. ORNL/MD/LTR-241, Volume 2, Oak Ridge National Laboratory, Oak Ridge, TN.

[Hodge et al., 2002] Hodge S, L Ott, F Griffin, and C Luttrell. 2002. Implications of the PIE Results for the 30-Gwd/MT-Withdrawal Mox Capsules. ORNL/MD/LTR-212, Vol. 2, Rev. 1, Oak Ridge National Laboratory, Oak Ridge, TN.

[Hoffmann and Kraus, 1984] Hoffmann H and N Kraus. 1984. Fabrication and Characterization Data of BN2 UO_2-Gd_2O_3 Fuel Rod. GN 84/10, Belgonucleaire, Bruxelles, Belgium.

[Janvier et al., 1967] Janvier JC, B de Bernaday de Sigoyer, and R Delmas. 1967. Irradiation of Uranium Oxide in Strong Cladding Effect of Initial Diametral Gap on Overall Behavior. Commiserat a l'Energie Atomic, Paris, France. Program CC-7, 1st and 2nd Sections, CEA-R-3358.

[Jošek, 2008a] Jošek R. 2008a. The High Initial Rating Test IFA-677.1: Final Report on In-Pile Results. HWR-872, OECD Halden Reactor Project, Halden, Norway.

[Jošek, 2008b] Jošek R. 2008b. LOCA Testing at Halden: The BWR Experiment IFA-650.7. HWR-906, OECD Halden Reactor Project, Halden, Norway.

[Kallstrom, 2005] Kallstrom R. 2005. SCIP, Task 0; Ramp Test Results, Final Report. N-05/154: STUDSVIK-SCIP-42, Studsvik Nuclear AB, Sweden.

[Klecha, 2006] Klecha L. 2006. Comparative Integral Irradiation Test on Gadolinia Fuel (IFA-681). HWR-832, OECD Halden Reactor Project, Halden, Norway.

[Knudsen et al., 1983] Knudsen P, C Bagger, H Carlsen, I Misfeldt, and M Mogensen. 1983. Risø Fission Gas Release Project Final Report. DOE/ET/34033-1, U.S. Department of Energy, Washington, D.C.

[Koike, 2004] Koike H. 2004. The MOX Fuel Behaviour Test IFA-597.4/.5/.6/.7; Summary of In-Pile Fuel Temperature and Gas Release Data. HWR-729, OECD Halden Reactor Project, Halden, Norway.

[Lanning, 1986] Lanning D. 1986. Irradiation History and Final Post-Irradiation Data for IFA-432. NUREG/CR-4717, PNL-5977, Pacific Northwest Laboratory, Richland, WA.

[Lanning et al., 1987] Lanning D, M Cunningham, J Barner, and E Bradley. 1987. Qualification of Fission Gas Release Data from Task 2 Rods. HBEP 25, Final Report, Pacific Northwest Laboratory, Richland, WA.

[Lysell and Birath, 1979] Lysell G and S Birath. 1979. Hot Cell Post-Irradiation Examination of Inter-Ramp Fuel Rods. STIR-51, Studsvik AB Atomenergi, Studsvik, Sweden.

[Manley et al., 1989] Manley A, P Kennedy, aRI Scogings B.C., and J Thompson. 1989. Post Irradiation Examination of Three Rods Comprising Task 3 of the GAIN Programme. GN 89/50, United Kingdom Atomic Energy Authority, Windscale Laboratory, United Kingdom.

[Matsson and Turnbull, 1998] Matsson I and J Turnbull. 1998. The integral fuel rod behaviour test IFA-597.3: Analysis of the measurements. HWR-543, OECD Halden Reactor Project, Halden, Norway.

[Mertens and Lippens, 2001] Mertens L and M Lippens. 2001. "Study of Fission Gas Release on High Burnup MOX Fuel." In TopFuel Reactor Fuel Performance. Stockholm, Sweden. European Nuclear Society.

[Mertens et al., 1998] Mertens L, M Lippens, and J Alvis. 1998. The FIGARO Programme: The Behaviour of Irradiated MOX Fuel Tested in the IFA-606 Experiment, Description of Results and Comparison with COMETHE Calculation. HPR 349/30, OECD Halden Reactor Project, Halden, Norway.

[Mogard et al., 1979] Mogard H, U Bergenlid, S Djurle, J Gyllander, E Larsson, G Lysell, K Ronnberg G. Saltvedt, and H Tomani. 1979. Final Report of the Inter-Ramp Project. STIR-53, Studsvik AB Atomenergi, Studsvik, Sweden.

[Morris et al., 2000] Morris R, C Baldwin, S Hodge, L Ott, C Malone, and N Packan. 2000. MOX Average Power Intermediate PIE: 21 GWd/MT Final Report. ORNL/MD/LTR-199, Oak Ridge National Laboratory, Oak Ridge, TN.

[Morris et al., 2001] Morris R, C Baldwin, S Hodge, and N Packan. 2001. MOX Average Power 30 GWd/MT PIE: Final Report. ORNL/MD/LTR-212, Volume 1, Oak Ridge National Laboratory, Oak Ridge, TN.

[Morris et al., 2005] Morris R, C Baldwin, and N Packan. 2005. MOX Test Fuel 50 GWd/MT PIE: Capsule 5 Quick Look. ORNL/MD/LTR-272, Oak Ridge National Laboratory, Oak Ridge, TN.

[Newman, 1986] Newman L. 1986. The Hot Cell Examination of Oconee 1 Fuel Rods After Five Cycles of Irradiation. DOE/ET/34212-50, Babcock and Wilcox Company, Lynchburg, VA.

[Notley et al., 1967] Notley M, R DesHais, and J MacEwan. 1967. Measurements of the Fission Product Gas Pressures Developed in UO_2 Fuel Elements During Operation. AECL-2662, Atomic Energy of Canada, Ltd., Chalk River, ON.

[Notley and MacEwan, 1965] Notley M and J MacEwan. 1965. The Effect of UO_2 Density on Fission Product Gas Release and Sheath Expansion. AECL-2230, Atomic Energy of Canada, Ltd., Chalk River, ON.

[Ozawa, 2004] Ozawa T. 2004. "Performance of ATR MOX Fuel Assemblies Irradiated to 40 GWd/t." In International Meeting on LWR Fuel Performance. Orlando, FL. American Nuclear Society.

[Petiprez, 2002] Petiprez B. 2002. Ramp Tests with Two High Burnup MOX Fuel Rods in IFA-629.3. HWR-714, OECD Halden Reactor Project, Halden, Norway.

[Reindl et al., 1991] Reindl J, G Bart, A Erne, R Hofer, A Hermann, R Restani, and H Zwuicky. 1991. Destructive Examinations on the BN2, Ge5, and NF17 Fuel Rods 9, 10, 11, 23, 24, and 33 of the GAIN Programme. GN 91/60, Paul Scherrer Institut, Switzerland.

[Rø and Rossiter, 2005] Rø E and G Rossiter. 2005. The SBR MOX and UO_2 Comparison Test in Gas Flow Rig IFA-633: An Update of Results. HWR-0823, OECD Halden Reactor Project, Halden, Norway.

[Schrire, 2018] Schrire D. 2018. Selected Vattenfall hot cell PIE data for benchmarking of FRAPCON. Vattenfall Nuclear Fuel AB, Sweden.

[Segura and Bernaudat, 2002] Segura J and C Bernaudat. 2002. Fuel Characterization Data and Power History of the Rod which is to be tested in the CARI-WL CIPO-2 Test. CABRI International Programme. CABRI Water Loop 2002/27.

[Smith et al., 1994] Smith G, R Pirek, H Freeburn, and D Schrire. 1994. The Evaluation and Demonstration of Methods for Improved Nuclear Fuel Utilization. DOE/ET-34-013-15, Combustion Engineering, Windsor, CT.

[Struzik, 2004] Struzik C. 2004. REGATE L10, fission gas release and cladding diameter of UO_2 rod during and after a transient at Bu = 47 MWd/kg. NEA-1696/01, Commissariat à l'Energie Atomique, Cadarache, France.

[Thérache, 2005] Thérache B. 2005. The High Initial Rating Test, IFA-677.1: Results after First Cycle of Irradiation. HWR-819, OECD Halden Reactor Project, Halden, Norway.

[Turnbull, 2001] Turnbull J. 2001. "Concluding Report on Three PWR Rods Irradiated to 90 MWd/kg UO_2 in IFA-519.9: Analysis of Measurements Obtained In-pile and by PIE." In EHPG-Meeting, number HWR-668. Lillehammer, Norway.

[Turnbull and White, 2002] Turnbull J and R White. 2002. The Thermal Performance of the Gas Flow Rigs: A Review of Experiments and Their Analyses. HWR-715, OECD Halden Reactor Project, Halden, Norway.

[Tverberg et al., 2005] Tverberg T, B Volkov, and JC Kim. 2005. Final Report on the UO_2-Gd_2O_3 fuel performance test in IFA-636. HWR-817, OECD Halden Reactor Project, Halden, Norway.

[Tvergerg and Amaya, 2001] Tvergerg T and M Amaya. 2001. Study of Thermal Behaviour of UO_2 and $(U,Gd)O_2$ to High Burnup (IFA-515). HWR-671, OECD Halden Reactor Project, Halden, Norway.

[Wesley et al., 1994] Wesley D, K Mori, and S Inoue. 1994. "Mark BEB Ramp Testing Program." In International Topical Meeting on Light Water Reactor Fuel Performance, p. 343. West Palm Beach, FL.

[White, 1999] White R. 1999. The Re-Irradiation of MIMAS MOX Fuel in IFA-629.1. HWR-586, OECD Halden Reactor Project, Halden, Norway.

[White et al., 2001] White R, S Fisher, P Cook, R Stratton, C Walker, and I Palmer. 2001. "Measurement and analysis of fission gas release from BNFL's SBR MOX fuel." 288(1):43–56.

[Wiesenack, 1992] Wiesenack W. 1992. "Experimental Techniques and Results Related to High Burn-Up Investigations at the OECD Halden Reactor Project." In Technical Committee Meeting, number IAEA-TECDOC-697, pp. 118–123. Pembroke, ON.

[Wright, 2004] Wright J. 2004. The SBR MOX and UO_2 Comparison Test in Gas Flow Rig IFA-633: Results after Seven Cycles of Irradiation. HWR-764, OECD Halden Reactor Project, Halden, Norway.

Appendix A – Description of Assessment Cases

A.1 Steady-State Assessment Cases

A.1.1 Halden IFA-432 Rods

The IFA-432 test [Lanning, 1986] was irradiated under a research program on fuel rod steady-state performance sponsored by the NRC from 1974 to 1986. The IFA-432 test assembly was a heavily instrumented, six-rod assembly irradiated in the Halden heavy boiling water reactor (HBWR) from 1975 to 1984. The purpose was to test the long-term steady-state performance of BWR-6 type fuel rods, operated at power levels that were at the upper bound for full-length commercial fuel rods. The fuel pellets were fabricated at Pacific Northwest National Laboratory (PNNL) and shipped to Halden; final rod and assembly fabrication was completed at the Halden site. Destructive examinations of selected rods were carried out at Harwell Laboratories, UK.

The assembly included six instrumented rods and three replaceable non-instrumented spares. Each instrumented fuel rod had a centerline thermocouple in both the top and the bottom end of the fuel column and a pressure transducer to monitor rod internal pressure. The assembly instrumentation included six vanadium self-powered neutron detectors (SPNDs) and one cobalt neutron detector, together with rod elongation sensors at each rod position, coolant thermocouples at the top and bottom of the assembly, and a coolant flow meter (turbine).

The test rods were designed to simulate BWR-6 rod cladding type and radial dimensions, with variations in fuel-cladding gap sizes, fuel types, and fill gas compositions. The fuel rod length was much shorter than full-length ($\sim$144 [in]) commercial reactor rods to fit well within the short length of the Halden reactor core. Fuel rod overall length was 25 [in], with an active fuel column length of 22.8 [in]. The overall void volume was held to 0.5 [in^3] (by selection of a $\sim$1 [in] plenum length at the upper end); this was done to approximate the ratio between fuel volume and void volume found in full-length rods. The cladding for all rods was Zircaloy-2.

Rods 1, 2, and 3 all had typical high-density (95% TD) stable sintered UO_2 fuel pellets and helium fill gas at 1 [atm] pressure; slight differences in the pellet diameters created variations in fuel-cladding gap size among the rods. Data taken from rod 1 upper and lower thermocouple, rod 2 lower thermocouple, and rod 3 upper and lower thermocouple during the first ramp to power were used in the BOL temperature assessment. Data from the rod 1 lower thermocouple and the rod 3 lower thermocouple were used in the temperature assessment as a function of burnup. It should be noted that much of the helium fill gas was lost from some of these rods during irradiation due to leakage past the thermocouple penetration through the end caps.

A.1.2 Halden IFA-513 Rods

The IFA-513 test fuel assembly [Bradley et al., 1981] was irradiated in the Halden reactor from November 1978 to mid-1981 under a continuation of an NRC program to test the performance of BWR-6 type fuel and the effects of fission gas contamination of the helium fill gas.

Rods 1 and 6 both had typical high density (95% TD) stable sintered UO_2 fuel pellets. Rod 1 had helium fill gas at 1 [atm] while rod 6 had 23% xenon and 77% helium fill gas at 1 [atm]. Data taken from rod 1 upper and lower thermocouple and rod 6 upper and lower thermocouple during the first

ramp to power were used in the BOL temperature assessment. Data from the rod 1 upper and lower thermocouple and the rod 6 upper and lower thermocouple were used in the temperature assessment as a function of burnup.

A.1.3 Halden IFA-633 Rods

The IFA-633 test assembly consisted of six instrumented rods (three short binderless route (SBR) MOX fuel rods and three UO_2 rods) irradiated from BOL through a burnup of 31 [GWd/MTM]. Rod 6 [Wright, 2004] was the only MOX rod instrumented with both a fuel centerline thermocouple and a pressure transducer such that temperature and FGR measurements can be compared. Rods 1, 3, and 5 [Rø and Rossiter, 2005] were UO_2 rods instrumented with centerline thermocouples and were used to assess the FAST predictions of temperature as a function of LHGR at BOL. This test assembly experienced a power ramp at a burnup of approximately 20 [GWd/MTM] to achieve fission gas bubble interlinkage. The MOX fuel was fabricated with the SBR process with a grain size of 7.5 [microns] and was typical of commercial fuel.

Rod 6 was used to assess the FAST temperature predictions for MOX as a function of burnup and the MOX FGR predictions. Rods 1, 3, and 5 were used to assess the FAST temperature predictions for UO_2 as a function of LHGR at BOL.

A.1.4 Halden IFA-677.1 Rods

The high initial rating test, IFA-677.1 [Thérache, 2005] [Jošek, 2008b], was loaded in the Halden reactor in December 2004 and had completed six cycles of irradiation under HBWR conditions as of September 2007, achieving a rig average burnup of 30 [GWd/MTU]. The single cluster contained six rods supplied by Westinghouse, Framatome ANP, and Global Nuclear Fuel (GNF), all fitted with pressure transducers, fuel centerline thermocouples in both ends, and fuel stack elongation detectors, and with a cladding extensometer for one of the rods. The experiment was aimed at investigating the performance of modern fuels subjected to high initial rating with respect to thermal behavior, dimensional changes (densification and swelling), FGR, and PCMI.

Rod 2 (Framatome ANP), rod 3 (GNF), rod 4 (GNF), and rod 6 (Westinghouse) were all used to assess the BOL UO_2 temperature predictions of FAST as a function of LHGR. In addition, rod 2 was used to assess the UO_2 temperature predictions as a function of burnup up to 32 [GWd/MTU].

A.1.5 Halden IFA-562 Rod

The Halden Ultra High Burnup (HUHB) test fuel assembly (IFA-562) [Wiesenack, 1992] was initiated by the Halden reactor project to demonstrate the effect of burnup on fuel thermal conductivity. The HUHB configuration of the assembly consisted of six rods, four of which were instrumented with centerline expansion thermometers and two with pressure transducers. The rods were under irradiation in the Halden reactor from September 1989 to 1997. Documented data for fuel center temperatures and linear heat ratings are available to a rod-average burnup of 76 [MWd/MTU].

Four rods (rods 15, 16, 17, and 18) contained “expansion centerline thermometers.” These are tungsten (1.8% ZrO) rods that run the full length of the rod on the inside of the pellets and guage the average center temperature of each rod via thermal expansion of the rod detected by resistance change. Two rods (rods 13 and 14) each contained a pressure transducer for measuring

rod internal pressure. The assembly instrumentation included four SPNDs, three of which were located coplanar at the top of the assembly and one near the bottom to define the thermal neutron flux distribution within the assembly.

The behavior of LHGR and measured temperatures were very similar for all four rods with temperature sensors. One rod (number 18) was selected for comparison to FAST predictions.

A.1.6 Halden IFA-597.3 Rod

The fuel segments for the high-burnup integral rod behavior test IFA-597 [Matsson and Turnbull, 1998] were refabricated from fuel rod 33-25065, which was irradiated in the Ringhals 1 BWR in Sweden, for approximately 12 years. The irradiation of this rod and its sibling rod 33-25046 was performed in two stages. During the first irradiation, 1980 to 1986, the rods were part of Ringhals assembly 6477 and an approximate rod-average burnup of 35 [GWd/MTU] was reached. The rods were then placed into fuel assembly 9902 for a second period of irradiation from 1986 to 1992 in Ringhals 1. The locations of fuel rods 33-25065 and 33-25046 in this assembly were positions 9902/D5 and 9902/E4, respectively. A final rod-averaged burnup of 59 [GWd/MTU] was achieved. The burnup at the location of the Halden refabricated segments was estimated as 67 [GWd/MTU].

Rods 8 and 9 were loaded into positions 2 and 5 in IFA-597.2 (second loading) and irradiated in Halden for some 20 days in July 1995. After a few power ramps, rod 9 failed and the assembly was withdrawn. During this time, useful data were generated on centerline temperature as a function of power.

Rod 9 was removed and replaced by rod 7. The assembly was returned to the reactor as IFA-597.3 (third loading); the irradiation started in January 1997 and continued to May of that year having accrued a further $\sim$2 [GWd/MTU]. Data obtained included centerline temperature as a function of power and burnup, (rod 8), FGR estimated from the increase in rod internal pressure transducer (rod 8), and clad elongation (rod 7).

The assembly was discharged and transported to Kjeller for PIE. FGRs of 12.6% and 15.8% were measured from puncturing and gas extraction from rods 7 and 8, respectively.

Rod 8 was used to assess the UO_2 temperature and FGR predictions of FAST.

A.1.7 Halden IFA-515.10 Rods

IFA-515.10 [Tvergerg and Amaya, 2001] contained hollow rods with centerline thermocouples irradiated up to a burnup of greater than 80 [GWd/MTU]. Two of the rods contain UO_2 and two of the rods contain 8% gadolinia. However, the gadolinium used in these rods is composed of ^{160}Gd, which is a non-neutron absorbing isotope. In this way, the effect of the thermal conductivity degradation due to gadolinia can be separated from the power reduction that is typically seen in fuel containing gadolinia. For these rods, a special version of FAST was used that does not use the power profiles for neutron-absorbing gadolinia.

Rods A1 and A2 are sibling rods of UO_2 and urania-gadolinia (UO_2-Gd_2O_3), respectively, and experience very similar power histories. This is also true for rods B1 and B2. Halden has reported

that the thermocouples failed in rods A1, A2, and B2 at the burnup indicated on Figures 3-12, 37(b), 38(b).

After this point, the temperature data are no longer valid.

These four rods were used to assess the FAST temperature predictions for UO_2 and UO_2-Gd_2O_3 fuel as a function of burnup.

A.1.8 Halden IFA-681 Rods

IFA-681 [Klecha, 2006] consists of six rods that had been irradiated for four cycles, or 340 days, as of 2006. Ongoing irradiation is currently underway in the Halden reactor. The input files for the UO_2 rods (rods 1 and 5) have been extended for six cycles to 507 days. All six of these rods were modeled using FAST. Three of these rods contain solid pellets with hollow pellets at the top end and are equipped with centerline thermocouples in the top pellets. These three rods have UO_2 (rod 1), 2% Gd_2O_3 (rod 2), and 8% Gd_2O_3 (rod 3) pellets.

The other three rods contain all hollow pellets and are equipped with expansion thermometers. These three rods also have UO_2 (rod 5), 2% Gd_2O_3 (rod 4), and 8% Gd_2O_3 (rod 6) pellets, with rod 6 being filled with 50% argon and 50% helium.

For rod 3, there are some overpredictions (50 to 120 $[^\circ C]$) in the third and fourth cycles. This may be due to error in the temperature measurement or the estimation of the rod power level. This seems likely because the power level during these cycles is reported to increase from about 21 $[kW/m]$ to about 25 $[kW/m]$, while the temperature is reported to remain constant at about 850 $[^\circ C]$. It also seems strange for the power level in this rod to increase during these cycles while the power level in the other rods is constant during these cycles.

These six rods were used to assess the FAST temperature predictions for UO_2 and UO_2-Gd_2O_3 fuel as a function of burnup.

A.1.9 Halden IFA-558 Rods

IFA-558 [Turnbull and White, 2002] was an assembly commissioned by Central Electricity Generating Board (later Nuclear Electric) to investigate the effect of hydrostatic restraint on the onset of grain boundary interlinkage, and hence, FGR. The assembly comprised six identical, short BWR type rods, each fitted with a pressure transducer and upper and lower fuel centerline thermocouples. The rods contained 7% enriched hollow pellets supplied by British Nuclear Fuels, Ltd. (BNFL) with a 200 $[\mu m]$ cold diametral fuel-to-clad gap. In this way, PCMI effects were minimized, which would otherwise have introduced unwanted uncertainty in the hydrostatic pressure in the fuel pellets.

The assembly was loaded in February 1986 and continued operation successfully until discharge at $\sim$40 $[GWd/MTU]$ in March 1992. The fuel rods were subsequently sent to AEA Technology for PIE.

During startup, the rods were filled with helium gas at 2 $[bar]$ pressure. Once the temperatures had stabilized at the prescribed normal operating powers, the pressures of four rods were altered in pairs in such a way as to minimize the spread of temperatures. Subsequently, rods 1 and 2 were

operated at the maximum internal pressure of 40 [bar], rods 5 and 6 operated at 20 [bar], while rods 3 and 4 remained at 2 [bar]. These pressures were maintained during all gas flow measurements and were only reduced at cold shutdown for safety reasons. The spread in fuel centerline temperatures during operation at around 35 [kW/m] for rods 2 through 6 was less than 60 [°C], but rod 1 was consistently some 50 [°C] higher.

Radioactive FGR was measured frequently, particularly in rod 3, and the measurements were used to monitor the onset of grain boundary interlinkage. In addition, all gas swept out of the rods was retained in separate cold traps to measure the activity of ^{85}Kr, which was used to estimate the cumulative release of stable fission gas. This FGR data demonstrated that rod internal pressures up to 40 [bar] had little effect on FGR.

Rod 6 was used to assess the UO_2 temperature predictions of FAST.

A.1.10 Halden IFA-629.1 Rods

The IFA-629.1 [White, 1999] test involved two MOX test rods (rods 1 and 2), but only rod 2 was punctured for FGR measurement such that only this rod will be used for FGR comparison. Both rods are used for the temperature comparison as a function of burnup. The MOX fuel was fabricated using the MIMAS-AUC process by Belgonucleaire (BN). The mother rod for the IFA-629.1 test rods was a full-length PWR MOX rod irradiated for two cycles in the Saint-Laurent PWR, France, with rods 1 and 2 cut as segments from the full-length rod and refabricated into short segments. The rod 2 segment had a burnup of 29 [GWd/MTM] following commercial irradiation, which was extended to 40 [GWd/MTM] during the Halden irradiation. The maximum LHGRs in Halden were significant, at 35 to 40 [kW/m].

These two rods were used to assess the FAST temperature predictions for MOX as a function of burnup. Rod 2 was used to assess the FAST MOX FGR predictions.

A.1.11 Halden IFA-610 Rods

One segment from four-cycle PWR MOX EdF rod N016 (which was base-irradiated for four cycles in the French Gravelines-4 reactors to a burnup of approximately 55 [MWd/kgM]) was re-fabricated and instrumented for use in the sequential IFA-610.2,4 cladding liftoff experiments [Beguin, 1999] [Fujii and Claudel, 2001]. The rod was tested under simulated PWR conditions in a pressurized water loop within the Halden reactor. The rod was connected to a gas supply system, and temperature measurements were made in both helium and argon fill gases at varying pressures. Fuel temperature data from helium gas fill periods were used to assess the FAST temperature predictions.

The rod was base-irradiated at nominal LHGRs for ~ 1500 days. The final burnup for the segment was 54.5 [MWd/kgM]. The rod was instrumented with a fuel center thermocouple and a rod elongation sensor. Internal gas pressure was varied throughout the ~ 100 day IFA-610.2 test to investigate the threshold for cladding liftoff. The LHGR level during the IFA-610.2 test was steady at about 14 to 15 [kW/m], and LHGR at the thermocouple was about 13.5 to 14 [kW/m].

In IFA-610.4, the LHGRs were similar at the beginning and drifted downward to 12.5 and 12.0 [kW/m] for rod-average and thermocouple location, respectively [Fujii and Claudel, 2001]. The test dura-

tion was similar to that of IFA-610.2 (100 days); however, after 50 days, questions of potential thermocouple degradation were raised, and code data comparison was only conducted over the first 50 days of the test.

These two experiments were used to assess the FAST temperature predictions for MOX as a function of burnup.

A.1.12 Halden IFA-648.1 Rods

The IFA-648.1 irradiation [Claudel and Huet, 2001] was simply a burnup extension at low LHGR for two refabricated instrumented segments from Gravelines-4 four-cycle PWR MOX rods, one segment each from rods N12 and P16. The irradiation was carried on at low LHGR under simulated PWR conditions in a pressurized water loop within the Halden reactor. The rods were then power-ramped in the follow-on IFA-629.3 test to investigate FGR and rod elongation behavior.

The other rods were base-irradiated at nominal LHGRs for $\sim$1200 days. The final burnup for the rods N12 and P16 were 57 and 53 [MWd/kgM], respectively. The two rods were instrumented differently upon refabrication. Rod 1 carried a fuel center thermocouple and a rod elongation sensor. Rod 2 carried a fuel center thermocouple and a pressure transducer. The LHGRs were kept deliberately low to accumulate more burnup without inducing FGR.

These two rods were used to assess the FAST temperature predictions for MOX as a function of burnup.

A.1.13 Halden IFA-629.3 Rods

Following base irradiation in a commercial PWR and further irradiation in Halden, two rods were further irradiated from 62 [GWd/MTU] to 68 to 72 [GWd/MTU]. The MOX fuel was fabricated using the MIMAS (micronized master blend) process. The documentation does not mention whether the UO_2 was fabricated using the ammonium diuranate (ADU) or ammonium uranyl carbonate (AUC) process, but it is likely that the AUC process was used because the fuel was fabricated in the early 1990s. The MOX rods in IFA-629.3 [Petiprez, 2002] were irradiated for four cycles in the Gravelines-4 PWR; after this period, two experimental rods were refabricated from the full-length rods, refilled with helium, and loaded in the IFA 648.1 rig to accumulate more burnup at low powers and no additional gas release. Following irradiation in IFA-648.1, rod 6 was punctured and refilled with helium and the two rods were irradiated in IFA-629.3. These rods were irradiated up to a final burnup of 68 and 72 [GWd/MTM] and discharged for PIE. The measured gas release values for these rods have been obtained by puncture meas

These two rods were used to assess the FAST temperature predictions for MOX as a function of burnup and the MOX FGR predictions.

A.1.14 Halden IFA-606 Rod

The IFA-606 test assembly [Mertens et al., 1998] [Mertens and Lippens, 2001] consisted of four refabricated rod segments from a full-length PWR MOX rod irradiated in the Beznau-1 reactor, Switzerland, at nominal LHGRs to a burnup of 50 [MWd/kgM]. The MOX fuel was fabricated using the MIMAS-AUC process by BN. Two test rods were instrumented with a fuel thermocouple and a

pressure transducer, and irradiated under Halden conditions for approximately 30 days at elevated LHGR in “Phase 2” of the test, to determine FGR behavior. The code-data comparisons presented are for only rod 2 that measured FGR by rod puncture, with a 12.5 micron grain size.

The fuel rod segment was instrumented with a pressure transducer and a fuel centerline thermocouple. The rod was base-irradiated at nominal LHGRs for $\sim$1500 days. The rod segment reached a burnup of 49.5 [GWd/MTM] during commercial operation, with additional 30 days of irradiation in Halden for a total burnup of 50.6 [GWd/MTM].

This rod was used to assess the FAST temperature predictions for MOX as a function of burnup and the MOX FGR predictions.

A.1.15 Halden IFA-636 Rods

IFA-636 [Tverberg et al., 2005] contained both hollow pellets with centerline thermocouples and solid pellets irradiated up to a burnup of 25 [GWd/MTU]. FAST was used to model two of the rods from this assembly. These rods contained 8 % gadolinia of the type typically used in power reactors. Centerline temperature data from IFA-636 rod 2 (hollow pellets) was used to compare to FAST predictions.

Centerline temperature from IFA-636 rod 4 (solid rod) was estimated by Halden based on measurements from IFA-636 rod 2. These estimates were used to compare to FAST predictions. These estimates may have more error than those for rod 2 due to both power uncertainties and uncertainties in estimating rod 4 temperature from rod 2 data.

These two rods were used to assess the FAST temperature predictions for UO_2-Gd_2O_3 fuel as a function of burnup.

A.1.16 BR-3 Rods

The DOE sponsored high-burnup irradiation of five well-characterized PWR-type test rods [Balfour, 1982] [Balfour et al., 1982] in the BR-3 reactor, located in Mol, Belgium, to demonstrate the feasibility of extending commercial fuel rod burnup and thereby help to minimize radioactive waste disposal. These rods were fabricated by Westinghouse Corporation, whose staff also oversaw the PIEs. The PIE on the rods was carried out in the BR-2 hot cell facility at the Mol site. The rods were of basic PWR radial dimensions. Goal peak burnups exceeded 70 [GWd/MTU].

The test rods were designed to simulate Westinghouse PWR (15×15) rod cladding type and radial dimensions, with variations in fuel enrichment and rod position providing variations in power history. The fuel rod length was much shorter than the full-length ($\sim$144 [in]) commercial reactor rods and fit well within the short length of the BR-3 reactor core. The fuel rod overall length was 44 [in] with an active fuel column length of 38.4 [in].

Six rods were selected for comparison with FAST FGR predictions: 24-I-6, 36-I-8, 111-I-5, 28-I-6, 30-I-8, and 332. Three of these rods were also selected for comparison with FAST void volume predictions: 24-I-6, 36-I-8, and 111-I-5.

A.1.17 Zorita Rod

Four fuel assemblies were initially irradiated in Zroita cycles 1 and 2. A total of 41 of the fuel rods in each assembly were removable, and 16 of these rods per assembly had high enrichment (4.08 to 6.6 wt% ^{235}U) to achieve high linear power levels and burnups. One of these rods, rod 332 [Balfour et al., 1982], with high enrichment that was irradiated up to 57 [GWd/MTU], was selected as an FGR assessment case for FAST.

A.1.18 BNFL BR-3 Rods

Battelle, Pacific Northwest Laboratories administered the international group-sponsored High Burnup Effects Program (HBEP), which continued from 1978 to 1990. The objective of the HBEP was to determine the effects of extended burnup on fuel rod performance, especially FGR. A variety of test rods and commercial power reactor rods were irradiated and examined under the HBEP, including two PWR assemblies (366 and 373) [Lanning et al., 1987] [Barner et al., 1990] containing PWR-type test rods irradiated in a single assembly in the BR-3 test reactor in Mol, Belgium. Both of these assemblies experience high power, and the rods showed significant FGR.

One rod from each assembly (rod DE from 373 and rod 5-DH from 366) was selected to be part of the UO_2 FGR assessment cases for FAST.

A.1.19 DR-3 Rods

Test 022 comprised three UO_2-Zr test fuel pins which were irradiated in the DR-3 reactor at Risø, Denmark, at 7.2 [MPa] (70 [atm]) system pressure [Bagger et al., 1978]. A burnup of approximately 42 [GWd/MTU] was accumulated at heat loads in the range of 35 to 53 [kW/m]. Fission gas analysis for two of the pins (PA29-4 and M2-2C) showed that the releases were 49 and 36% .

The three almost identical test fuel pins had 12.6 [mm] sintered UO_2 pellets of 2.28% enrichment in 128 [mm] long stacks. The cladding was cold-worked and stress-relieved Zircaloy-2 tubing of approximately 0.55 [mm] wall thickness which had been autoclaved on both sides. The diametral pellet-clad clearance was 0.24 [mm], and the pins were backfilled with 0.1 [MPa] (1 [atm]) helium.

These two rods were used to assess the FAST UO_2 FGR predictions.

A.1.20 NRX Rods

Several sets of UO_2 fuel rods were irradiated in a pressurized water loop in the NRX reactor in Chalk River, Canada [de Meulemeester et al., 1973] [Notley et al., 1967]. The goal of these tests was to measure the gas pressures inside the rods, with the following objectives:

- To determine the effects of fuel density on gas pressure and FGR.
- To determine the effects of element power output variations on gas pressure and FGR.
- To obtain data to test the predictions of a model for calculating the variation of gas pressure with power output.

After irradiation, the rods were dimensioned and punctured for fission gas analysis. Samples from the rods were also analyzed for chemical burnup. Five of these rods were selected as UO_2 FGR assessment cases for FAST because they provide FGR data at low burnups (<11 [GWd/MTU]) while the other FGR assessment data were at burnups greater than 20 [GWd/MTU]. Rods CBR, CBY, and CBP were irradiated together to 2.7 [GWd/MTU] in 85 days. Rod LFF was irradiated to 3.3 [GWd/MTU] in 108 [days]. Rod EPL-4 was irradiated to 10.4 [GWd/MTU] in 100 days.

A.1.21 EL-3 Rods

Sixteen cartridges, each containing two rods, were irradiated in the EL-3 reactor, France, for a varying number of cycles to achieve burnups from 3 to 12 [GWd/MTU]. The aspects of the rods studied in this project were:

- Macroscopic appearances: crack network, material movement, and dimensional changes
- Microscopic appearances: recrystallization, pore redistribution, and new phases
- Migration of fission products: stable gases released by the fuel and distribution of solid fission products

Each cartridge was constructed of Zircaloy-2 and consisted of two separate stages, each containing a stack of UO_2 fuel 123 [mm] high at each end, and in the central joint, space was provided for cobalt flux indicators. Each stage contained a chromel-alumel thermocouple located in the center of the stack. The cartridges were then filled with helium.

After irradiation, the rods were dimensioned and punctured for fission gas analysis. Gamma scans were done as well as a radiochemical analysis. The rods 4110-AE2 and 4110-BE2 [Janvier et al., 1967] were used to assess the UO_2 FGR predictions of FAST.

Both rods 4110-AE2 and 4110-BE2 contained fuel pellets with an as-fabricated density of 10.52 [g/cm^3]. AE2 ran at a power of 17.6 [kW/ft] while BE2 ran at a power of 17.8 [kW/ft]. Rods 4110-AE2 and 4110-BE2 were maintained throughout life at constant average LHGRs of 17.6 and 17.8 [kW/ft], respectively. Both ran with a flat axial power profile. The input LHGRs were a flat 17.6 and 17.8 [kW/ft], with a few steps to get up to power.

These two rods were used to assess the FAST UO_2 FGR predictions at burnups less than 15 [GWd/MTU].

A.1.22 FUMEX 6f and 6s Rods

Two rods were base-irradiated in the Halden HBWR at low power to 55 [GWd/MTU]. Each of these rods was then refabricated to include pressure transducers and run at higher power while the pressure was being monitored. These rods, FUMEX 6s and FUMEX 6f [Chantoin et al., 1997] were included as FAST UO_2 FGR assessment cases.

A.1.23 Halden IFA-429 Rod

The IFA-429 test fuel assembly [Turnbull, 2001] was initiated by NRC-Research and designed and fabricated by Idaho National Laboratory (with fuel pellet fabrication by PNNL) to demonstrate the

effect of burnup, power level, and fuel grain size on fuel thermal behavior and FGR. The assembly consisted of 18 original short rods, arranged in three clusters of 6 rods each, and 15 noninstrumented spare and replacement rods. Rod DH is a replacement rod that was re□instrumented with a pressure transducer after it had attained about 30 [GWd/MTU] burnup at relatively low LHGR; the rod was then irradiated in IFA-519 at much higher and variable LHGR as part of a load-follow test, and eventually attained a peak burnup of 99 [GWd/MTU]. The FGR for this rod was obtained by puncture during PIE. It should be noted that the puncture data provided much higher release values than were estimated from the pressure transducer measurements because the rod pressures had exceeded the measurement capabilities of the pressure transducer.

A.1.24 Arkansas Nuclear One Unit 2 PWR Rod

DOE sponsored a program with ABB Combustion Engineering and Energy Operations, Inc. to improve the use of PWR fuel. The scope of this project was to develop more efficient fuel management concepts and an increase in the burnup of discharged fuel.

Two 16×16 lead test assemblies were irradiated in the Arkansas Nuclear One-Unit 2 reactor (ANO-2). This is a PWR that operates at 2815 [MWt]. One of the assemblies, D039, was irradiated for three cycles and achieved a burnup of 33 [GWd/MTU]. The other assembly, number D040, was irradiated for five cycles and achieved a burnup of 52 [GWd/MTU].

Rod TSQ002 [Smith et al., 1994], irradiated in assembly D040, was of standard CE 16×16 design and contained solid UO_2. Assembly D040 was irradiated from 1979 to 1988 in ANO-2, cycles two through six. It accumulated 52 [GWd/MTU] assembly-average burnup. Rod TSQ002 accumulated an end-of-life (EOL) rod-average burnup of 56.1 [GWd/MTU]. The rod-average LHGR varied from 2.75 to 6.95 [kW/ft], with the higher values near BOL.

This rod was used to assess the FAST UO_2 FGR predictions, the EOL void volume predictions and the Zircaloy-4 corrosion predictions.

A.1.25 Oconee PWR Rod

DOE sponsored a long-term, multi-organizational program on the performance of LWR fuel rods during operation to extend burnups. As part of that program, Babcock and Wilcox (B&W) 15×15-type PWR fuel assemblies were irradiated to 3, 4, and 5 cycles in the Oconee PWR, operated by Duke Power Company. One assembly, 1D45, completed five cycles of irradiation in June 1983, having achieved an assembly average burnup of 50 [GWd/MTU] during 1553 effective full-power days.

Several rods from the assembly were nondestructively and destructively examined in the B&W hot cells. This document summarizes the design and operating parameters for one rod, number 15309 [Newman, 1986]. Fuel density and microstructure, rod growth, cladding oxidation/hydriding, and diametral strain data are available for this rod together with FGR measurement via rod puncture and plenum gas analysis. The FGR for this low-powered rod was $< 1\%$; but the cladding oxidation, growth, and diametral strain were significant.

The rods were standard 15×15 full-length PWR rods. The rod initially had a rod-average LHGR of 7 to 8 [kW/ft]; however, this decreased to $\sim$4 [kW/ft] by EOL. The axial power profile flattened

early and remained relatively flat throughout life.

This rod was used to assess the FAST UO_2 FGR predictions, the EOL void volume predictions and the Zircaloy-4 corrosion predictions.

A.1.26 Halden IFA-651 Rods

The IFA-651.1 rig [Blair and Wright, 2004] contained six fuel rod segments. Three of these rod segments contained inert matrix fuel and three rod segments contained MOX fuel. The MOX rods (rods 1, 3, and 6) were modeled with FAST. Rod 1 MOX fuel was fabricated using an SBR that results in a relatively homogenous distribution of the PuO_2 compared to MOX fabricated using the MIMAS process. Rods 3 and 6 were fabricated at Paul Scherrer Institute using a two-stage attrition milling process developed by the Korean Atomic Energy Research Institute. Micrographs provided appear to demonstrate that this process provides a homogenous distribution of PuO_2 similar to that observed in the SBR process.

These rods were irradiated for four cycles in the Halden reactor to a rod-average burnup between 20 and 23 [GWd/MTM]. PIE showed that the fuel in rods 1 and 6 had an in-reactor densification of 2% , while the fuel in rod 3 had an in-reactor densification of 1% . These values have been entered into the code as input parameters. The measured gas release values used for model verification have been estimated from pressure measurements and are subject to greater uncertainty than measurements made by rod puncture.

These three rods were used to assess the FAST temperature predictions for MOX as a function of burnup and the MOX FGR predictions.

A.1.27 Advanced Test Reactor WG-MOX Rods

Oak Ridge National Laboratory has reported base-irradiation LHGR histories and post-irradiation FGR for seven fuel pins irradiated in the ATR [Morris et al., 2000] [Morris et al., 2001] [Morris et al., 2005] [Hodge et al., 2002] [Hodge et al., 2003]. These pins were irradiated in stainless steel capsules. Several pins were withdrawn for PIE after Phases II, III, and IV, after the pins had accumulated 21, 30, and 40 to 50 [GWd/MTM], respectively. The fuel used in these pins was fabricated using weapons-grade (WG) plutonium with a process similar to MIMAS. Fuel produced from WG plutonium differs from commercial MOX fuel in two ways. First, the WG MOX has greater amounts of ^{239}Pu, and second, WG MOX contains small amounts of gallium.

The measured gas release values for these rods have been obtained by puncture measurement.

These three rods were used to assess the FAST MOX FGR predictions.

A.1.28 Gravelines-4 PWR Rods

The Halden Project has reported base-irradiation LHGR histories and post-irradiation (rod puncture) FGR for three full-length PWR MOX rods from Gravelines-4 reactor, France, which were subsequently sectioned to produce test rods for various instrumented tests [Beguin, 1999] [Fujii and Claudel, 2001] [Claudel and Huet, 2001] [Petiprez, 2002]. These commercial rods did not

experience LHGRs in excess of 25 [kW/m] or temperatures in excess of 1500 [K], resulting in measured FGR below 5% .

These three full-length commercial rods were used to assess the FAST MOX FGR predictions.

A.1.29 Beznau-1 M504 Rods

The M504 program [Cook et al., 2003] [Cook et al., 2004] consisted of four MOX rods irradiated in assembly M504 for four cycles in the Beznau-1 PWR reactor. The MOX fuel was fabricated using the SBR process, which results in a relatively homogenous distribution of the PuO_2. These rods were irradiated up to a burnup between 37 and 43 [GWd/MTM]. The measured gas release values are relatively low and have been obtained from puncture measurements that have less uncertainty than those estimated from pressure measurements.

These four rods were used to assess the FAST MOX FGR predictions.

A.1.30 Beznau-1 M308 Rod

In the M308 program [Boulanger et al., 2004], segmented MOX rods were irradiated in the Beznau reactor up to peak burnups of 55 to 60 [GWd/MTM]. The MOX fuel was fabricated using the MIMAS–AUC process by BN, which results in larger PuO_2 particle sizes than the SBR process. Sufficient detail on the power history and measured FGR was provided for Segment 2, such that this segment was modeled using FAST. Only the cladding inner and outer diameters were provided for this segment; however, since these values were identical to the cladding inner and outer diameters for a Westinghouse 15×15 fuel rod, it was assumed the rest of the rod dimensions were the same as for a Westinghouse 15×15 fuel rod.

This rod was used to assess the FAST MOX FGR predictions

A.1.31 Halden IFA-597.4/.5/.6/.7 Rods

IFA-597.4, 5, 6, and 7 [Koike, 2004] contained two MOX rods, containing fuel that was fabricated with the MIMAS-ADU process. Rod 10 contained mostly solid pellets, with a few hollow pellets at the top of the stack to accommodate the fuel centerline thermocouple. Rod 11 contained all hollow pellets. These rods were irradiated for four cycles in the Halden reactor to a burnup between 35 and 37 [GWd/MTM]. The power history at the thermocouple position was provided for both rod 10 and rod 11. To determine the rod-average LHGR, for rod 10, the power history was increased by the ratio of average power to power at the top of the rod, and the ratio of the volume of a solid pellet to the volume of a hollow pellet. For rod 11, the power history was increased by only the ratio of average power to power at the top of the rod. For these pellets, the out-of-pile re-sintering tests of 24 hours at 1700 [°C] showed a density increase of 0.46% . However, based on in-pile free volume and pressure measurements, it was determined that the maximum densification was 0.8% for rod 10 and 1.4% for rod 11. These measured values were used in the FAST input files.

The measured gas release values used for the FAST assessment have been estimated from pressure measurements and are subject to greater uncertainty than measurements made by rod puncture.

These two rods were used to assess the FAST temperature predictions for MOX as a function of burnup and the MOX FGR predictions.

A.1.32 FUGEN Rods

The MOX fuel assembly, E09 [Ozawa, 2004], was irradiated for 10 cycles in the Japanese advanced thermal reactor, Fugen. This assembly reached the highest assembly average burnup of 38 $[\mathrm{GWd/MTM}]$. The rods in this assembly were arranged in a circular pattern consisting of three concentric rings. The power history was approximately the same for all rods in a given ring. However, the power histories given for each ring did not provide the rod-average burnup that was measured in the pellets via gamma scanning. This discrepancy is most likely due to uncertainty in the linear heat rates that were provided. To model these cases, the power histories that were supplied were increased by a factor so the burnup calculated using these histories would be equivalent to the measured burnup.

The pellet stack consisted of pellets with varying plutonium concentration in different axial regions. The top and bottom areas contained more plutonium than the central region. Since it is not possible to specify the plutonium concentration at various axial regions along the pellet stack in FAST, two cases were run. In the first case, the plutonium concentration for the middle section was used for the entire rod, and in the second case, the plutonium concentration for the top and bottom sections was used for the entire rod. This allowed the effect of plutonium concentration on FGR to be seen. Plutonium concentration had very little impact on the predicted FGR ($< 5\%$ relative).

The measured gas release values for these rods have been obtained by puncture measurement on several rods from each ring.

These three rods were used to assess the FAST MOX FGR predictions.

A.1.33 Monticello BWR Rod

A DOE program was completed in 1985 in which nine 8×8 fuel assemblies in the Monticello BWR were taken to high burnup (up to 45.6 $[\mathrm{MWd/MTM}]$ assembly average), and the rods were periodically examined nondestructively and sampled for destructive examinations [Baumgartner, 1984]. Four of the assemblies went for the “full term” from cycle 3 through cycle 9 from May 1974 to September 1982.

All of these rods have fully annealed Zircaloy-2 cladding. One of these rods, rod A1 from assembly MTB99 was used in the Zircaloy-2 corrosion assessment for FAST.

A.1.34 TVO-1 BWR Rod

Battelle, Pacific Northwest Laboratories administered the international group-sponsored HBEP, which continued from 1978 to 1990. The objectives of the HBEP were to determine the effects of extended burnup on fuel rod performance, especially FGR. A variety of test rods and commercial power reactor rods were irradiated and examined under the HBEP, including nine full-length 5- and 6-cycle rods from the TVO-1 BWR in Finland [Barner et al., 1990]. One of these rods was used to assess the corrosion performance of FAST for Zircaloy-2: rod number H8/36-6 from 5-cycle fuel assembly 6116.

The rod occupied position H8, which was the control blade corner position. The rod-averasge burnup at EOL was 44.6 [GWd/MTU], with a peak value (confirmed by chemical burnup analysis) of 50.9 [GWd/MTU]. The rod-average LHGR varied between 12 and 24 [kW/m] (3.3 to 7.6 [kW/ft]), but large variations in the peak-to-average LHGR ratio occurred due to control blade movements.

A.1.35 Vandellos PWR ZIRLO® Rods

A joint Spanish and Japanese effort irradiated a large number of full-length fuel rods for five cycles in the Spanish PWR Vandellos 2 (CSN, ENUSA 2002). The rods were clad with ZIRLO® and Mitsubishi Developed Alloy (MDA). Two of the ZIRLO® rods (A06 and A12) have been modeled with FAST to assess the performance of the ZIRLO® corrosion model to high burnup.

A.1.36 Gravelines-5 PWR M5™ Rod

One high-burnup rod was taken from the French reactor Gravelines-5 and refabricated for the RIA test CIP0-1, performed in the CABRI reactor, France [Segura and Bernaudat, 2002]. This rod, N05, was clad with M5™. Before refabrication, rod N05 was examined and the oxide layer thickness was measured. This full-length commercial rod has been modeled with FAST to assess the performance of the M5™ corrosion model to high burnup.

A.1.37 GAIN UO_2-Gd_2O_3 Rods

The GAIN Programme, which was an international program lead by Belgonucleaire, irradiated four rods with two different doping concentrations. Rods 301 and 302 were doped with 3wt% Gd while rods 701 and 702 were doped with 7wt% Gd. All four rods were irradiated in BR3 for four cycles, but rod 701 was removed for transient tests between cycles in BR2 [Hoffmann and Kraus, 1984] [Manley et al., 1989] [Reindl et al., 1991]. FGR measurements were obtained from each rod.

A.2 Power-Ramp Assessment Cases

A.2.1 Ramped HBEP Obrigheim/Petten Rods

The HBEP was an international, group-sponsored program administrated by Battelle Pacific Northwest Laboratory from 1979 to 1989 [Barner et al., 1990]. The objective was to investigate the impact of extended burnup on fuel rod performance, especially FGR. A total of 81 rods of both BWR and PWR types were irradiated and examined under the program, with rod-average burnups ranging up to 69 [GWd/MTU] and peak pellet burnups up to 83 [GWd/MTU].

Under Task 2 of the program, full-length segmented rods were irradiated in commercial power reactors and then subjected to power ramps in test reactors. The rod segments comprised “rodlets” that were individual short-length fuel rods, mated end-to-end to form the full-length rods. Following irradiation to a variety of burnup levels, the rods were disassembled into the individual rodlets, and the rodlets were ramp-tested in test reactors. The peak LHGRs in these ramps ranged from 35 to 50 [kW/m], and hold times ranged from 48 to 196 hours. The FGR during bumping was a function of the peak LHGRs and ranged from 10 to 45% . The pre-bump LHGRs ranged from 15 to 35 [kW/m], as confirmed by calibrated nondestructive ^{85}Kr activity determinations for the plenum gas, and the pre-bump FGRs were generally low (1 to 5%).

Two PWR-type ramped rodlets were chosen for comparison to FAST predictions. Both were fabricated by Kraftwerk Union (KWU), irradiated in the same fuel assembly in the Obrigheim PWR, Germany, and then power-ramped to approximately the same peak LHGR (41 to 43 [kW/m]) in the JRC-Petten test reactor, the Netherlands. Rodlet D200 attained 25 [GWd/MTU] burnup in one reactor cycle at LHGRs of 25(2) [kW/m]. Rodlet D226 attained 45 [GWd/MTU] by further irradiation in the same assembly for two more cycles, with LHGR generally decreasing with time from 25 [kW/m] at BOL to ~17 [kW/m] during the final cycle. The fuel in these rods resulted in high fuel densification $< 2.5\%$ TD and high open porosity that is atypical of today's fuel. Comparisons of the FGR data from these power-ramped rods to other power-ramped data with lower densification and open porosity fuel typical of today's fuel suggests that these FGR data are higher than observed from today's fuel. As a result, the FAST code tended to underpredict this data, which is not surprising.

The post-bump FGR is greater for the higher-burnup rodlet D226 than for rodlet D200 (44 vs. 38%), despite D226 having a smaller as-fabricated fuel cladding gap. The pre-ramp FGRs, based on ^{85}Kr activity in the plenums, were very similar: 4.2 and 6.6% , respectively. Therefore, the net FGR during ramping is greater for rodlet D226, and this was attributed to burnup effects. This rodlet pair thus provides a test of the burnup effects inherent in FAST.

A.2.2 Super-Ramp Rods

The Super-Ramp Project was an international, group-sponsored program involving base-irradiation of segmented full-length BWR and PWR rods in various power reactors, followed by ramp-testing of the rod segments in the Studsvik R-2 test reactor in Sweden [Djurle, 1985]. The project's purpose was to establish the failure threshold for rods of varying types and burnup, and some rod segments did fail during high-power ramp testing. Rod segments that did not fail, however, gave data on FGR and cladding permanent hoop strain during EOL power transients.

Three rod segments were selected as FGR assessment cases and nine rod segments were selected as cladding hoop strain assessment cases. These were all non-failed PWR rod segments, which had been base-irradiated in the Obrigheim PWR for three cycles up to a burnup of 34 to 37 [GWd/MTU]. The segments were then ramp-tested in the Studsvik reactor to ramp terminal levels as high as 43 [kW/m]. The FGRs and residual cladding hoop strain were measured following the ramp test.

The segmented PWR rods were designed in basic conformance with KWU's 15×15 PWR fuel design. The general design specifications are given in Table A15.1. The fuel segment length was short, 39 [cm] overall and 31.5 [cm] active fuel length, to match well within the ~1 [m] active length of the Studsvik reactor core. The diametral fuel-cladding gap was 145 [microns] (5.7 [mils]). The fuel pellet density is 95% TD, and the standard KWU densification test is only 2.2 hours at 1700 [°C] rather than the 24 hour densification test at 1700 [°C] required by the NRC as a measure of maximum densification. Therefore, the quoted maximum densification for this fuel "none" may be low, and it may be as great as 1% TD–the latter figure is used as FAST input.

A.2.3 Inter-Ramp Rods

The Studsvik Inter-Ramp Project objective was to investigate the mechanical failure threshold for BWR 8×8 type fuel rods. Short rodlets with standard BWR 8×8 dimensions and components were

fabricated by ABB/Atom specifically for the project and were base-irradiated to ∼20 [GWd/MTU] at low LHGRs before EOL ramping at rapid rate to high LHGRs to probe for cladding failure. Hold times at the ramp terminal (LHGR) level were 24 hours for non-failed rods. For the non-failed rods, post-ramp FGR was determined by rod puncture.

Two of the non-failed, ramp-tested Inter-Ramp rods, numbers 16 and 18 [Mogard et al., 1979] [Lysell and Birath, 1979], were selected for FGR and cladding permanent hoop strain assessment.

Twenty short 21 [in] rodlets were fabricated for the test, with nominal 8×8 BWR fuel rod characteristics, and there were some departures from these characteristics. Rods 16 and 18 were both "nominal rods" with 6 [mil] diametral gaps, 1 [atm] helium fill, and 95% TD solid, dished fuel pellets. The rods were irradiated in approximate BWR coolant conditions in pressurized loops within the Studsvik reactor. Rods 16 and 18 operated for ~ 550 days at LHGRs ranging from 20 to 40 [kW/m] and achieved burnups of 21 and 18 [GWd/MTU], respectively.

Rods 16 and 18 were then preconditioned for 24 hours at 29 and 25 [kW/m], respectively, and then ramped at a rate of ∼70 [W/m] per second to terminal levels (maximum peak LHGR values) of 48 and 41 [kW/m], respectively, where they were each held for 24 hours, during which the coolant was monitored for added radioactivity (indicating rod failure). Neither rod failed. Therefore, puncture and FGR determinations were feasible, and were performed.

A.2.4 Ramped Halden/DR-2 Rods

The RisøFission Gas Release Project was an international, group-sponsored program administrated by RisøLaboratories, from 1980 to 1981. The objective was to investigate the impact of extended burnup and EOL power ramping on FGR in BWR-type fuel rods. This was done by performing power-bumping tests in the DR-2 reactor (Denmark) on 9 of the 14 rods irradiated in test fuel assembly IFA-148. This assembly was operated in the Halden reactor, Norway, from 1968 to 1979. The power ramps featured 24-hour hold periods at the peak power level, with the peak power level varied among the tests. These tests were supplemented by nondestructive examinations before and after the bumping irradiations, rod puncturing/gas analysis on all tested rods, and detailed destructive examinations on selected rods.

Three of the bumped rods were selected as FAST FGR assessment cases: rods F7-3, F9-3, and F14-6 [Knudsen et al., 1983], which had rod-average burnups of 35, 33, and 27 [GWd/MTU], respectively. The analyses of plenum gas ^{85}Kr activity before and after bumping were performed, and these were calibrated against the post-bump rod puncture results to yield an estimate of the net FGR caused by the power bumping. Thus, these cases provide the opportunity to assess the transient power induced short-term FGR predictions of the FAST FGR model.

The IFA-148 assembly contained a total of 14 short BWR-type test rodlets, with 7 rods each in two clusters (upper and lower clusters). The fuel pellets were 5% enriched sintered urania, with some variations in density and grain size. These two assessment cases, the nominal grain size and the fuel pellet densities, are equal (13 to 16 [micron] grain size and density of 93.4% TD, with a 0.6% increase upon resinter). The rods were initially filled with 1 [atm] helium fill gas.

A.2.5 Risø-3 Ramped Rods

The RisøNational Laboratory in Denmark has carried out three irradiation programs of slow ramp and hold tests, so called “bump tests,” to investigate FGR and fuel microstructural changes. The third and final project, which took place between 1986 and 1990, bump-tested fuel re-instrumented with both pressure transducers and fuel centerline thermocouples.

The innovative technique used for refabrication involved freezing the fuel rod to hold the fuel fragments in position before cutting and drilling away the center part of the solid pellets to accommodate the new thermocouple.

The fuel used in the project was from IFA-161 irradiated in the Halden BWR to 52 [GWd/MTU], GE BWR fuel irradiated in Quad Cities 1 and Millstone 1 from 23 to 45 [GWd/MTU], and ANF PWR fuel irradiated in Biblis A (Germany) to 43 [GWd/MTU]. All these rods were subsequently ramped in the DR-3 reactor.

Four of the GE BWR rods (GE2, GE4, GE6, and GE7) [Chantoin et al., 1997] and two of the ANF rods (AN1 and AN8) [Chantoin et al., 1997] were selected to assess the FAST predictions of UO_2 FGR and cladding hoop strain.

A.2.6 B&W Rods Ramped at Studsvik

Three well-characterized 1.10 [m] long rodlets that had been irradiated to burnups slightly greater than 62 [GWd/MTU] in ANO-1 were ramp tested in the Studsvik R2 experimental reactor [Wesley et al., 1994]. Peak power levels of 39.5, 42.0, and 44.0 [kW/m] and a 12 hour hold time were selected for these tests. No failures were experienced during testing and no incipient cracks were detected in the cladding during the post-ramp examinations. The FGR after the ramp was measured. Two of these rods (rods 1 and 3) were used in the assessment of the FAST UO_2 FGR predictions.

A.2.7 Regate Rod

This Regate experiment [Struzik, 2004] deals with the study of FGR and fuel swelling during power transient at medium burnup. The rod was base-irradiated in the Gravelines-5 PWR and then re-irradiated in the test reactor SILOE in Grenoble, France. Since the rod was initially a segmented rod, the refabrication process prior to loading in the test is minor. In particular, the rod was not purged of its fission gases following refabrication.

The segmented rod consisted of UO_2 fuel with 4.5% enrichment. It was irradiated up to 47 [GWd/MTU]. In the SILOE reactor, the rod was given a conditioning power step of 195 [W/cm] for 48 hours and then was ramped at 10 [W/cm]/min and held at 385 [W/cm] for 90 minutes. This rod is particularly valuable for examining FGR for power ramps of short time duration because the other power ramped UO_2 rods used for FAST assessment were for hold times of 4) hours or greater.

This rod was used as part of the FAST UO_2 FGR assessment.

A.2.8 Beznau-1 M501 Rods

Two MOX rods were irradiated for three cycles in the Beznau-1 PWR up to a rod-average burnup between 34 and 37 [GWd/MTM]. The MOX fuel was fabricated using SBR that results in a relatively homogenous distribution of the PuO_2. One of these rods had a high plutonium enrichment (5.54 wt%) and one had a medium plutonium enrichment (3.72 wt%). After this, eight rodlets were refabricated from these two rods. Rodlets HR-1 to HR-4 [White et al., 2001] [Cook et al., 2000] [Cook et al., 2003] [Cook et al., 2004] were refabricated from the high-enrichment rod, number 4463, and rodlets MR-1 to MR-4 [White et al., 2001] [Cook et al., 2000] [Cook et al., 2003] [Cook et al., 2004] were refabricated from the medium enrichment rod, number 7612. These rodlets were ramp tested in the Petten high flux reactor. The ramp consisted of a 60 hour hold time at a preconditioning level followed by a ramp to a higher level with a hold of 12 hours for all the rodlets except MR-4, which was only held at the higher level for 20 minutes. It should be noted that the preconditioning and ramp power levels listed in the documents are the peak node powers. These values have been divided by the peak-to-average ratio to determine the rod-average power levels for these ramp tests.

These eight rodlets were used to assess the FAST MOX FGR predictions.

A.2.9 Studsvik Cladding Integrity Project Ramped Rods

The Studsvik Cladding Integrity Program (SCIP) has subjected 10 test rods to power ramp testing [Kallstrom, 2005]. Each test rod was subjected to a designated type of ramp test, which included staircase, short hold, long hold, and two-step power ramp tests. Each test rod was fabricated from a rodlet sectioned from a previously irradiated father rod.

Four ramp test rods were made by refabricating rodlets from BWR father rods that had been irradiated in Kernkraftwerk, Leibstadt. These test rods were labeled KKL-1, KKL-2, KKL-3, and KKL-4 and were irradiated to approximately 63, 67, 56, and 40 [MWd/mtU] average rodlet burnup, respectively. Before ramp testing, each rod was conditioned for a designated period of time and LHGR. The first ramp test, KKL-1, was aimed at defining the ramp terminal level where rod failure would occur. The rod was subjected to a staircase ramp, and after six steps of 5 [kW/m] with a 1 hour hold time between steps, the rodlet failed after 40 minutes at an LHGR of 42 [kW/m]. To determine if the failure, which was caused by an outside-in crack, was dependent on burnup, a similar test was performed on KKL-3. A staircase ramp consisting of eight steps at 5 [kW/m] with a 1 hour hold time between steps was performed up to 52 [kW/m]. After holding for 12 hours at 52 [kW/m], no failure was observed in KKL-3. Ramp tests of the other two rods, KKL-2 and KKL-4, were aimed at studying the geometric changes during a power transient and their dependence on burnup. The rods, KKL-2 and KKL-4, were held at 41 and 45 [kW/m] for 30 and 5 seconds, respectively. Neither KKL-2 or KKL-4 failed during ramp testing.

Two ramp test rods, M5-H1 and M5-H2, were fabricated from the same father rod, which had been irradiated in Ringhals 4 PWR and used to study the influence of holding time on geometric changes. The rods, M5-H1 and M5-H2, had been irradiated to a rodlet-average burnup of 67 and 68 [MWd/kgU], respectively, and conditioned for a designated period of time and LHGR prior to ramp testing. During the short hold and long hold ramp tests, holding times of 5 seconds and 12 hours were used on M5-H1 and M5-H2, respectively, at an LHGR of 40 [kW/m]. Neither rod failed

during the ramp test.

Ramp testing was performed on rod O2 (55 [MWd/kgU] burnup) to study geometric changes and PCI. Rod O2 had been previously irradiated in the BWR Oskarshamn 2 to an average rodlet burnup of 55 [MWd/kgU]. A short hold ramp test was performed by holding rod O2 at an LHGR of 45 [kW/m] for 30 seconds. Rod O2 did not fail during the ramp test.

Ramp test rods Z-2, Z-3, and Z-4 had each been irradiated to 76 [MWd/kgU]. Rods Z-3 and Z-4 were irradiated in the PWR North Anna while rod Z-2 was irradiated in the PWR Vandellos. Rod Z-3 was intended to study the hydrogen embrittlement by ramping the rod to an LHGR of 40 [kW/m] for a 5 second hold. However, failure occurred at an LHGR of 39 [kW/M], which prevented the short hold ramp test from being completed. Rods Z-2 and Z-4 were intended to study delayed hydrogen cracking (DHC), and were subjected to two-step power ramp tests. Rod Z-2 was initially ramped to an LHGR of 35 [kW/m] and held for 6 hours before being ramped to an LHGR of 40 [kW/m] and held for an additional 6 hours. Rod Z-4 was initially ramped to 33 [kW/m] and held for 6 hours before being ramped to 38 [kW/m] and held for an additional 6 hours. The rods, Z-2 and Z-4, did not fail during the two-step power ramp.

These 10 rods were used to assess the FAST predictions of cladding hoop strain.

Pacific Northwest National Laboratory

902 Battelle Boulevard
P.O. Box 999
Richland, WA 99352
1-888-375-PNNL (7675)

www.pnnl.gov